



# **Asphalt Research Consortium**

## **Quarterly Technical Progress Report July 1 – September 30, 2008**

October 2008

Prepared for  
Federal Highway Administration  
Contract No. DTFH61-07-H-00009

By  
Western Research Institute  
Texas A&M University  
University of Wisconsin-Madison  
University of Nevada-Reno  
Advanced Asphalt Technologies

[www.westernresearch.org](http://www.westernresearch.org)  
[www.ARC.unr.edu](http://www.ARC.unr.edu)

# TABLE OF CONTENTS

INTRODUCTION .....	1
GENERAL CONSORTIUM ACTIVITIES .....	3
PROGRAM AREA: MOISTURE DAMAGE.....	5
Category M1: Adhesion.....	5
Category M2: Cohesion.....	10
Category M3: Aggregate Surface .....	21
Category M4: Modeling.....	29
Category M5: Moisture Damage Prediction System .....	32
Appendix A: Development of a Coupled Micromechanical Moisture Damage Model.....	35
Appendix B: A Coupled Mechanical-Moisture-Induced Damage Model for Asphaltic Mixes .....	40
PROGRAM AREA: FATIGUE.....	47
Category F1: Material and Mixture Properties .....	47
Category F2: Test Method Development.....	65
Category F3: Modeling.....	80
Appendix C: Slides Presented at the Reno ETG Meeting .....	91
PROGRAM AREA: ENGINEERED MATERIALS.....	103
Category E1: Modeling.....	103
Category E2: Design Guidance.....	125
PROGRAM AREA: VEHICLE-PAVEMENT INTERACTION.....	143
Category VP1: Workshop.....	143
Category VP2: Design Guidance.....	143
Category VP3: Modeling.....	150
PROGRAM AREA: VALIDATION.....	157
Category V1: Field Validation.....	157
Category V2: Accelerated Pavement Testing.....	158
Category V3: R&D Validation .....	159
PROGRAM AREA: TECHNOLOGY DEVELOPMENT.....	169
PROGRAM AREA: TECHNOLOGY TRANSFER.....	171
Category TT1: Outreach and Databases .....	171





## **INTRODUCTION**

This document is the Quarterly Report for the period of July 1 to September 30, 2008 for the Federal Highway Administration (FHWA) Contract DTFH61-07-H-00009, the Asphalt Research Consortium (ARC). The Consortium is coordinated by Western Research Institute with partners Texas A&M University, the University of Wisconsin-Madison, the University of Nevada Reno, and Advanced Asphalt Technologies.

The Quarterly Report is grouped into seven areas, Moisture Damage, Fatigue, Engineered Paving Materials, Vehicle-Pavement Interaction, Validation, Technology Development, and Technology Transfer. The format of the report is based upon the Research Work Plan that is grouped by Work Element and Subtask.

This Quarterly Report summarizes the work accomplishments, data, and analysis for the various Work Elements and Subtasks. This report is being presented in a summary form in response to a request from the FHWA Agreement Officer's Technical Representatives (AOTR's) Dr. Jack Youtcheff and Mr. Eric Weaver. Reviewers may want to reference the Year 2 Work Plans in order to obtain background information on specific areas of research. The more detailed information about the research such as approaches to test method development, data collection, and analysis will be reported in research publications as part of the deliverables. An updated version of the Year 2 Work Plan with additional information that was requested by the reviewers of the Year 2 Work Plan is being prepared and will be posted on the ARC website, [www.arc.unr.edu](http://www.arc.unr.edu), in the Fall of 2008.

The Year 1 and Year 2 Work Plans, quarterly reports, and other related documents and information about the Asphalt Research Consortium can be found at the ARC website, [www.arc.unr.edu](http://www.arc.unr.edu).

## **SUPPORT OF FHWA AND DOT STRATEGIC GOALS**

The Asphalt Research Consortium research is responsive to the needs of asphalt engineers and technologists, state DOT's, and supports the FHWA Strategic Goals and the Asphalt Pavement Road Map. More specifically, the research reported here supports the Strategic Goals of safety, mobility, and environmental stewardship. By addressing the causes of pavement failure and thus determining methods to improve asphalt pavement durability and longevity, this research will provide the motoring public with increased safety and mobility. The research directed at improved use of recycled asphalt pavement (RAP), warm mix asphalt, and cold mix asphalt supports the Strategic Goal of environmental stewardship.



## **GENERAL CONSORTIUM ACTIVITIES**

### **PROGRESS THIS QUARTER**

During the last quarter, Western Research Institute (WRI) hosted the 45<sup>th</sup> Annual Petersen Asphalt Research Conference and the 8<sup>th</sup> Annual Pavement Performance Prediction (P<sup>3</sup>) Symposium on July 14 – 18. Several Consortium members made presentations during the two meetings. During the week of the meetings, the Consortium members met with Co-AOTR's Dr. Jack Youtcheff and Mr. Eric Weaver to discuss the progress on the approval of the Year 2 Work Plan, and additional information needed for the Year 2 Work Plan.

Consortium members attended the Binder and Mix and Construction ETG meetings in Reno, Nevada that occurred on September 16 – 18. Dr. Hussain Bahia presented an update on the ARC binder fatigue research and Dr. Dallas Little presented an update on the ARC research in the moisture damage and fatigue program areas.

### **WORK PLANNED FOR NEXT QUARTER**

Consortium members will attend the RAP ETG meeting in Phoenix on October 28 and 29, 2008. Following the RAP ETG, the Consortium members will meet with Co-AOTR's Dr. Jack Youtcheff and Mr. Eric Weaver to discuss preparation of the Year 3 Work Plan and associated documents.





## **PROGRAM AREA: MOISTURE DAMAGE**

### **CATEGORY M1: ADHESION**

#### **Work Element M1a: Affinity of Asphalt to Aggregate (UWM)**

##### Work Done This Quarter

During this quarter, the materials for this work plan were selected to fit the previously approved testing matrix. The base binders chosen for testing in this work plan were:

- FH, a PG 64-22 neat binder with a high content of asphaltenes (16.25% as determined per ASTM D4124-01).
- CRM, a PG 58-28 neat binder with a low content of asphaltenes (9.06% as determined per ASTM D4124-01).

Polymer-modified binders were prepared using the above two materials as base binders. The chosen polymer modifiers were those described in the approved testing matrix. Granite and limestone rock disks were prepared for the modified Dynamic Shear Rheometer (DSR) tests. Moisture-damage tests were conducted following the testing matrix. The focus this quarter was on comparing the results using two rock disks versus one rock and one metal surface. This work is important to evaluate whether a metal cone-plate can be used with a rock disk to ensure uniformity of stress distribution within a sample.

##### Significant Results

A summary of the testing results during this quarter are shown in figure M1a.1.

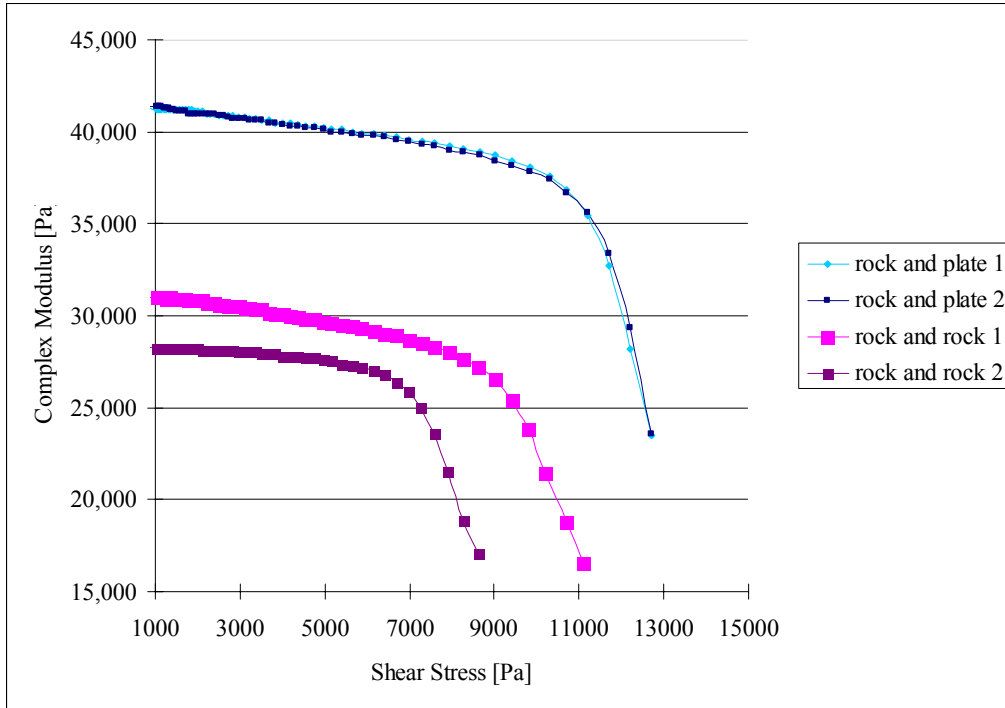


Figure M1a.1. Graph. Stress sweep testing results at 46 °C for the CRM neat binder in dry conditions, with granite rock disks.

Figure M1a.1 shows a comparison between tests conducted on an asphalt sample between two granite rock disks versus one granite disk and one steel plate. The geometry used is a 25 mm parallel plate DSR geometry with a testing gap of 1.000 mm. It is clear that the results are more repeatable by using only one rock disk instead of two. Another significant advantage of using one rock disk instead of two is the ability to run twice the number of tests using the same number of rock disks. Even though the absolute values recorded in the tests are different between two rock disks versus one rock and one steel plate, the material ranking is similar.

Since these tests are run primarily for comparison and ranking purposes, the team recommends performing all testing using just one rock disk instead of two. This method of testing will also allow the team to better correlate results from the modified DSR test with the modified Pneumatic Adhesion Tensile Testing Instrument (PATTI) test results or the DSR run tack test.

These findings are verified on polymer-modified binders, as shown in figure M1a.2.

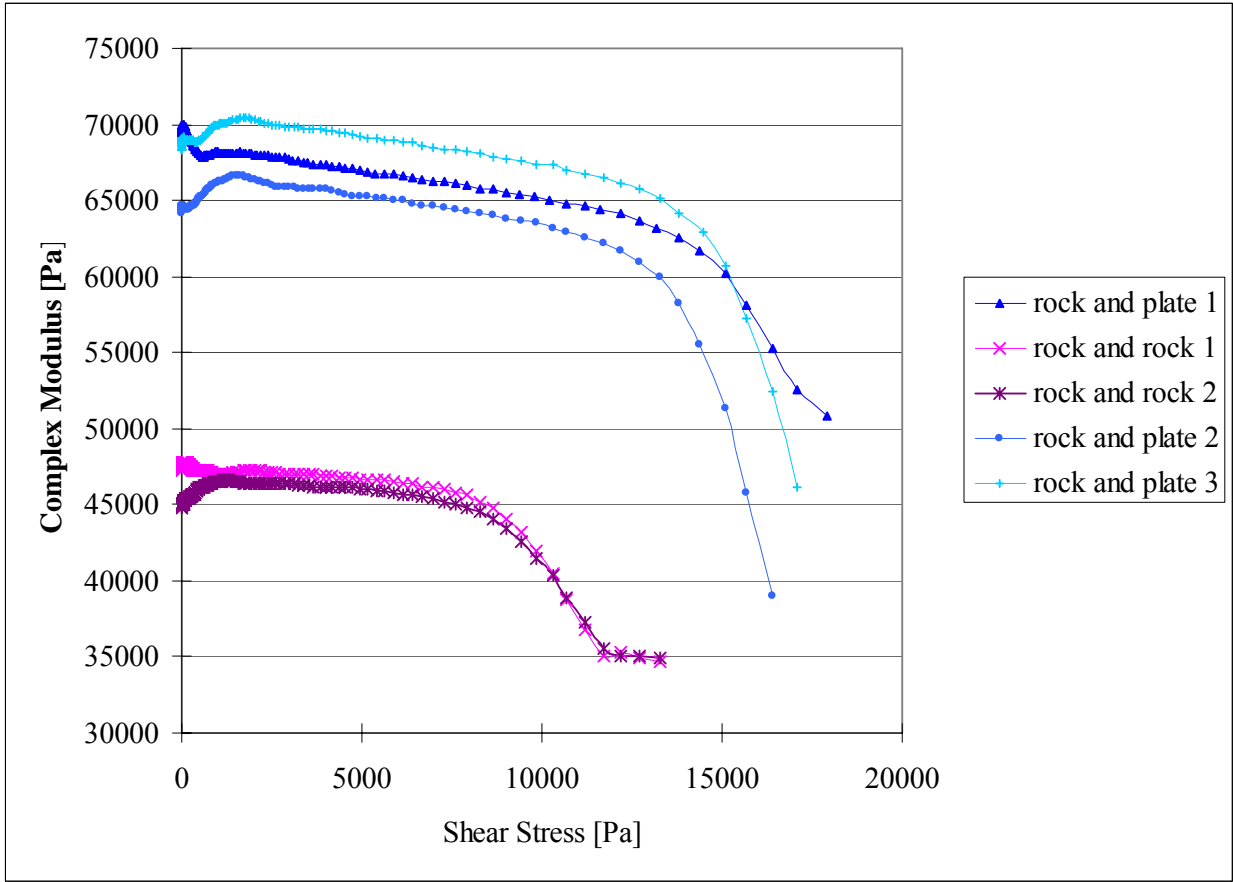


Figure M1a.2. Graph. Stress sweep testing results at 46 °C for the CRM modified with 2% wt linear styrene-butadiene-styrene (LSBS) binder, in dry conditions, with granite rock disks.

Significant Problems, Issues and Potential Impact on Progress

Due to an unforeseen family event that affected a staff member who plays a key role in this work plan, the presentation scheduled for this quarter was postponed to the next quarter. No other major impacts on the work plan’s progress are expected.

Work Planned Next Quarter

In Q4 2008, the team will continue to run tests using the modified DSR procedure. The team will also continue work on evaluating the moisture damage of asphalt mixtures as described in the work plan and will work on correlating the binder test results with the results obtained on mixes.

## **Work Element M1b: Work of Adhesion Based on Surface Energy**

### ***Subtask M1b-1: Surface Free Energy and Micro-Calorimeter Based Measurements for Work of Adhesion (TAMU)***

#### Work Done This Quarter

No activity was planned for this quarter.

#### Significant Results

None.

#### Significant Problems, Issues and Potential Impact on Progress

None.

#### Work Planned Next Quarter

Work on this subtask is planned for the last quarter.

### ***Subtask M1b-2: Work of Adhesion at Nano-Scale using AFM (WRI)***

#### Work Done This Quarter

The detailed work plan, submitted as part of the Year 2 Work Plan, was approved during the past quarter.

#### Significant Results

None.

#### Significant Problems, Issues and Potential Impact on Progress

None.

#### Work Planned Next Quarter

In the next quarter, items listed in **Sub-Subtask M1b-2.1** will be started. This will include acquiring sample materials, beginning oxidation conditioning of asphalts and identifying supplies and equipment that will be need for the project. A literature search will also be initiated.

### ***Subtask M1b-3: Identify Mechanisms of Competition Between Water and Organic Molecules for Aggregate Surface (TAMU)***

#### Work Done This Quarter

This subtask is investigating the mechanisms responsible for adhesion and debonding of model organic compounds (representing functional groups in asphalt binder) to minerals and representative aggregates. We are measuring the heat of reactions of the chemical mechanisms using a dual-mode flow adsorption calorimeter. Differences in molar heats of reaction of different organics bonding to the same absorbent are indicative of differences in the bonding strength of each absorbate with the absorbent of interest.

Work during this quarter focused on the continued development of the instrument. In particular, we integrated an ultraviolet-visible spectrophotometer with the dual-mode flow adsorption calorimeter to provide continuous monitoring of the solution concentration of the organics compounds.

In addition, we established the reproducibility and accuracy of the calorimeter by repeated measurements of the molar heats of reactions of benzoic acid adsorption and desorption to silica at pH 3 during flow-through experiments.

#### Significant Results

There are no significant results for this quarter as we focused on aggregate characterizations.

#### Significant Problems, Issues and Potential Impact on Progress

There are no significant issues.

#### Work Planned Next Quarter

We plan on initiating flow through experiments to measure the molar heat of reaction of the adhesion of model organic compounds that represent asphalt to minerals and aggregates, as well as the molar heats of reactions of water adsorption to organic-coated minerals and aggregates.

Adhesion will be modeled in the flow-through calorimeter by organic sorption from nonaqueous phase solvents. Experimental variables include the chemistry of the model organic, single model organics versus mixtures of model organics, ionic salt content of the nonaqueous phase solvent, and the surface chemistry of the mineral or aggregate.

Competition of water and the model organics for the mineral or aggregate surfaces will be characterized through flow-through experiments that introduce small amounts of water to the systems created during the adhesion studies above.

### **Work Element M1c: Quantifying Moisture Damage Using DMA (TAMU)**

#### Work Done This Quarter

No activity was planned for this quarter.

#### Significant Results

None.

#### Significant Problems, Issues and Potential Impact on Progress

None.

#### Work Planned Next Quarter

Work on this task will start in year 3 of the project.

### **CATEGORY M2: COHESION**

#### **Work Element M2a: Work of Cohesion Based on Surface Energy**

##### *Subtask M2a-1: Methods to Determine Surface Free Energy of Saturated Asphalt Binders (TAMU)*

#### Work Done This Quarter

No activity was planned for this quarter.

#### Significant Results

None.

#### Significant Problems, Issues and Potential Impact on Progress

None.

#### Work Planned Next Quarter

Work on this task is anticipated to start in year 4 of the project.

## ***Subtask M2a-2: Work of Cohesion Measured at Nano-Scale using AFM (WRI)***

### Work Done This Quarter

The detailed work plan, submitted as part of the Year 2 Work Plan, was approved during the past quarter.

### Significant Results

None.

### Significant Problems, Issues and Potential Impact on Progress

None.

### Work Planned Next Quarter

In the next quarter, items listed in **Sub-Subtask M2a-2.1** will be started. This will include acquiring sample materials and identifying supplies and equipment that will be need for the project. A literature search will also be initiated.

## **Work Element M2b: Impact of Moisture Diffusion in Asphalt Mixtures**

### ***Subtask M2b-1: Measurements of Diffusion in Asphalt Mixtures (TAMU)***

#### Work Done This Quarter

One of the aspects that researchers have tried to address in the past few weeks is the ability to interchange FTIR cells while the test is in progress. Diffusion of water even through very thin films of asphalt binders is a slow process. Achieving moisture saturation in the thin film can take up to a few days. However, it is not efficient to use the FTIR spectroscope for the entire duration of the test with only one specimen. Researchers are currently trying to determine whether or not multiple specimens can be tested using the FTIR simultaneously. During these tests, the FTIR cell (along with the binder coating and water retaining cell) is removed from the spectrometer after recording the spectra for a few minutes. Following this step, the cell is again placed in the spectrometer at pre-specified times and for specified durations to record the spectra. This process will allows preparation of several cells and testing these simultaneously using the spectrometer. Researchers are currently comparing the diffusion rates obtained following this procedure with the diffusion rates obtained by using a single cell continuously placed in the spectrometer for the entire duration of the test.

Another objective of this research was to determine the influence of hysteresis in moisture gradient on the diffusivity through binder films. To this end, researchers have conducted preliminary tests to establish a protocol for obtaining these measurements. In these preliminary tests, the binder film was exposed to moisture until it closely approached saturation. Upon

reaching approximately 80% saturation, the water in the cell was removed and the exposed film surface was then subjected to a dry boundary condition. This reversed the direction of movement of moisture. The rate at which moisture diffused out from the binder was also determined using spectral measurements. After drying the film selected durations of time, the film surface was again exposed to moisture and the rate of diffusion was determined as before. This test is currently in progress and researchers are interested in comparing the diffusivity of moisture through the original film and through the same film after it has been exposed to one wet-dry cycle.

#### Significant Results

None.

#### Significant Problems, Issues and Potential Impact on Progress

None.

#### Work Planned Next Quarter

Measurements using the FTIR to determine the diffusivity of water through asphalt binders will be continued through the next quarter. Emphasis in the next quarter will be to, establish the repeatability of the test method; evaluate sensitivity of the test method to changes in film thickness and type of binder; complete development of the method described above to test multiple specimens at the same time using a single FTIR; and conduct preliminary analysis of the data.

#### ***Subtask M2b-2: Kinetics of Debonding at the Binder-Aggregate Interface (TAMU)***

#### Work Done This Quarter

Most of the work accomplished under subtask M2b-1 also directly relates to this subtask. The most significant difference in this subtask is that a portion of the binder-ATR window interface will be purposefully exposed to be in direct contact with the water. This will allow the water to diffuse through the film as well as propagate along the binder-ATR window interface.

#### Significant Results

None.

#### Significant Problems, Issues and Potential Impact on Progress

None.

#### Work Planned Next Quarter

Researchers plan to continue work with emphasis on M2b-1 before addressing the specifics of this subtask.



## Work Element M2c: Measuring Thin Film Cohesion and Adhesion Using the PATTI Test and the DSR (UWM)

### Work Done This Quarter

This quarter, evaluation of the modified Pneumatic Adhesion Tensile Testing Instrument (PATTI) device and the testing procedure was performed. Following the previously approved testing matrix, both modified and unmodified binders were subjected to the modified PATTI test. The research team focused its efforts on refining the test procedure and the equipment design.

### Significant Results

The team conducted initial testing in cooperation with the University of Wisconsin–Madison’s cost share partners from the University of Stellenbosch, South Africa. A brief summary of the testing results obtained during this quarter is presented in table M2c.1.

Table M2c.1. Summary of pullout test results.

<b>T = 0 s</b>						
Binder	Trial	Max Pullout Tension Recorded Value (kPa)	Max Pullout Tension LabView Value (kPa)	Initial Pressure t = 0 s (kPa)	Zeroed Value LabView - Initial (kPa)	Difference Zeroed Value - Recorded Value (kPa)
CRS-2	1	3384.73	7340.17	4069.90	3270.27	114.46
CRS-2	2	3025.00	6980.43	3955.43	3025.00	0.00
LMCRS-2	1	2125.68	6081.11	4069.90	2011.22	114.46
LMCRS-2	2	1978.51	5933.95	4004.49	1929.46	49.05
<b>T = 0.001 s</b>						
Binder	Trial	Max Pullout Tension Recorded Value (kPa)	Max Pullout Tension LabView Value (kPa)	Initial Pressure t = 0.001 s (kPa)	Zeroed Value LabView - Initial (kPa)	Difference Zeroed Value - Recorded Value (kPa)
CRS-2	1	3384.73	7340.17	3971.79	3368.38	16.35
CRS-2	2	3025.00	6980.43	4053.55	2926.89	98.11
LMCRS-2	1	2125.68	6081.11	3988.14	2092.97	32.71
LMCRS-2	2	1978.51	5933.95	4069.90	1864.05	114.46
<b>T = 0.002 s</b>						
Binder	Trial	Max Pullout Tension Recorded Value (kPa)	Max Pullout Tension LabView Value (kPa)	Initial Pressure t = 0.002 s (kPa)	Zeroed Value LabView - Initial (kPa)	Difference Zeroed Value - Recorded Value (kPa)
CRS-2	1	3384.73	7340.17	4053.55	3286.62	98.11
CRS-2	2	3025.00	6980.43	3971.79	3008.64	16.36
LMCRS-2	1	2125.68	6081.11	4053.55	2027.57	98.11
LMCRS-2	2	1978.51	5933.95	3971.79	1962.16	16.35

A number of tests were run on the modified PATTI device to evaluate the effect of pressure rates on different binders (neat, Elvaloy-modified and styrene-butadiene-styrene [SBS]-modified); different surfaces (glass, granite and limestone); and different bonding temperatures. One of the greatest concerns while developing these tests was to evaluate the relative compliance obtained at different pullout pressure rates as set on the PATTI pressure control panel. Figure M2c.1 summarizes these results and shows that binder stiffness does not have an effect on the pressure rates. The overall compliance of the system controls the pressure rate, and the stiffness of the binder has little or no influence.

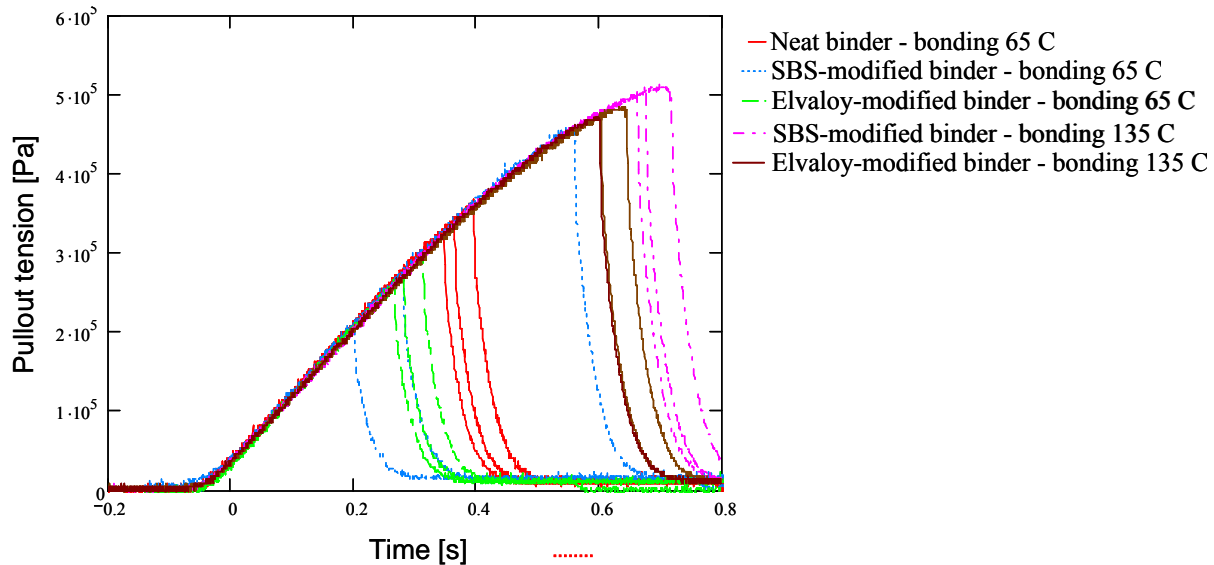
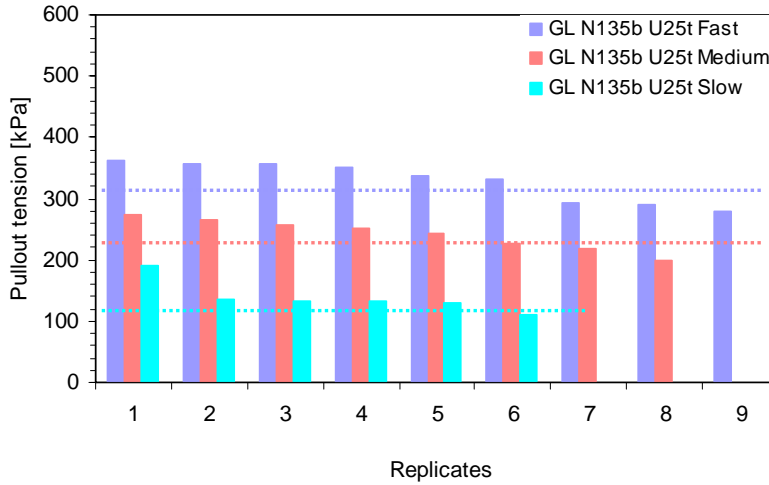


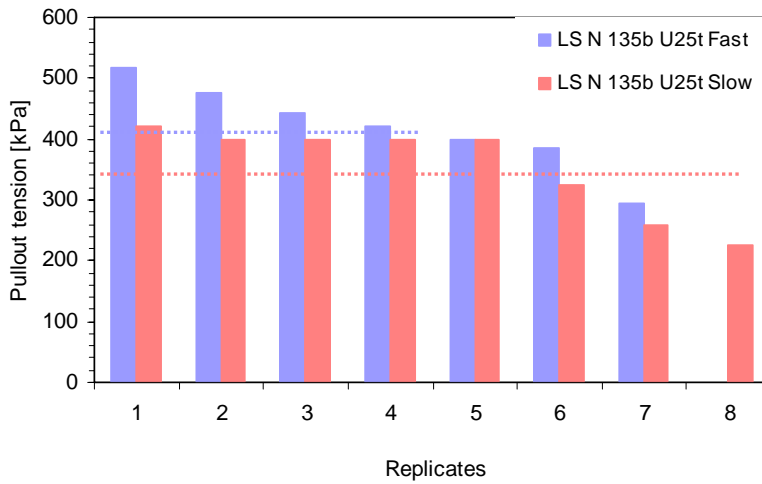
Figure M2c.1. Graph. Evaluation of the effect of binder stiffness on compliance and pressure rates. The applied pressure rate was set constant at 891 kPa/s. There is no difference in line pressure rates as a function of the binder type or binding temperatures.

Testing continued to evaluate the effect of pressure rates on each of the different testing parameter combinations. Figure M2c.2 shows the effect of pressure rate for different neat binders on glass, limestone and granite surfaces prepared at 135 °C bonding temperatures. Figure M2c.3 summarizes these results by showing a plot of the measured pullout tensions for different pullout rates on each of the three surfaces. There is a clear trend: Pullout tensions increase with increasing pressure rates. However, the standard deviation is large, particularly in the case of the limestone surface. One of the reasons for this large standard deviation is that the limestone rock tested was a poor quality aggregate, and in some cases the specimen failed at the rock rather than at the interface (adhesive failure) or within the binder itself (cohesive failure). Figure M2c.4 illustrates the problem found in the failure in limestone aggregate. Similar effects were seen in other binder and binding temperature responses.



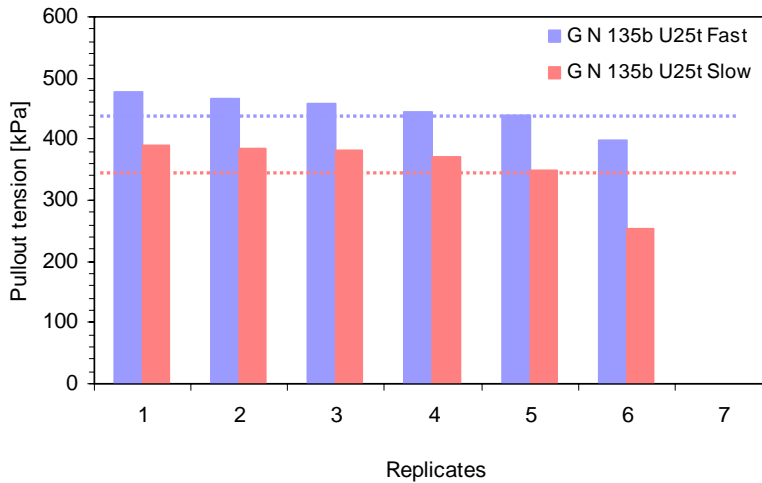
Rates:  
 Fast: 1800 kPa/s  
 Medium: 700 kPa/s  
 Slow: 100 kPa/s

(a)



Rates:  
 Fast: 2036 kPa/s  
 Slow: 1529 kPa/s

(b)



Rates:  
 Fast: 2036 kPa/s  
 Slow: 883 kPa/s

(c)

Figure M2c.2. Graphs. Effect of pressure rates on pullout tensions for (a) glass, (b) limestone and (c) granite.

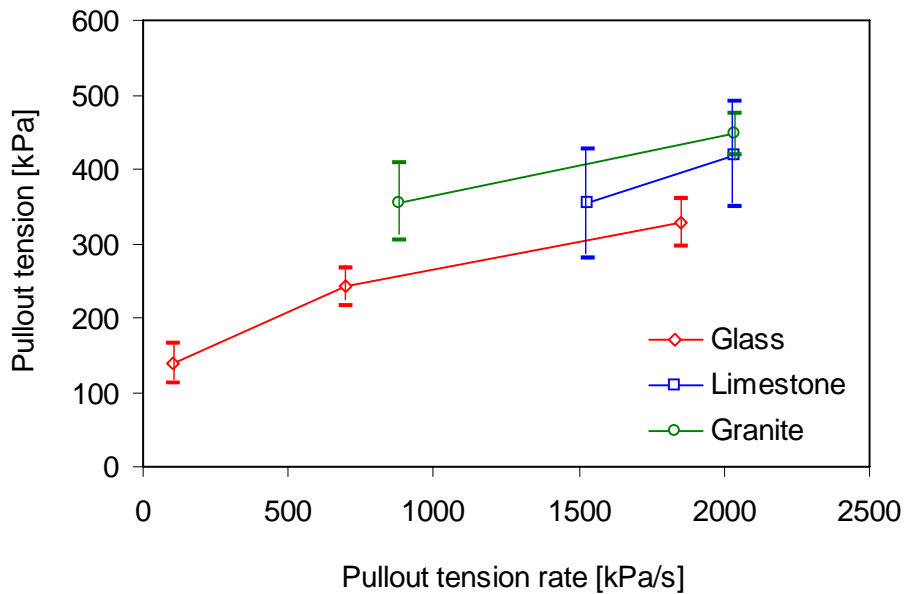


Figure M2c.3. Graph. Summary of the effect of pullout pressure on pullout tension for different surfaces: glass, limestone and granite. Neat binder bonded at 135 °C was used.



Figure M2c.4. Photographs. Example of pullout test failure at the rock. The Vienna rock source will not be used in future testing.

Another important observation is that these results combine both the effects of cohesive and adhesive failure at the binder-aggregate system; this was documented using digital photography. Because the binder is expected to show the most uniform response, purely cohesive failures would not have produced the different failure responses evidenced.

### Binder Type Effect

The effect of binder type on pullout tension was tested by changing the type of binder while keeping the same mineral surface, binding temperature and pullout pressure rates. Typical results are summarized in figure M2c.5. These results show that in glass and granite surfaces, the SBS-modified binder (Flint Hills PG 70-22 3% LSBS: base asphalt modified with 3% by weight linear SBS triblock copolymer) results in pullout tensions that are statistically greater than the pullout tension in the neat binder. However, there is no statistical difference in the pullout tension results in the limestone specimens for the two different types of binders. These results seem to show the importance of affinity between binders and aggregates. Furthermore, the observed failure surfaces appear to reflect a contribution of the aggregate type to the response as well as both adhesive and cohesive behavior.

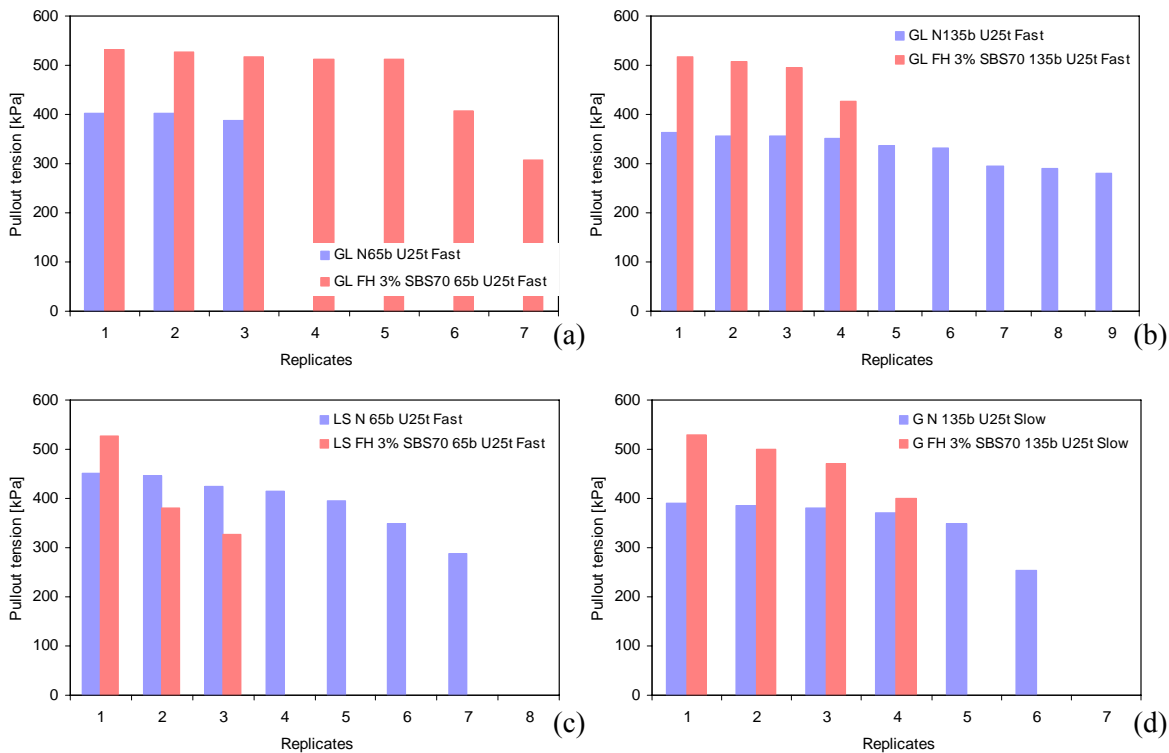


Figure M2c.5. Graphs. Effect of binder on the pullout tension response (neat versus SBS-modified binder): (a) glass surfaces tested at fast pressure rates and 65 °C bonding temperature, (b) glass surfaces tested at fast pressure rates and 135 °C bonding temperature, (c) limestone surfaces tested at fast pressure rates and 65 °C bonding temperature, and (d) granite surfaces tested at slow pressure rates and 135 °C bonding temperature. (GL = glass plate; LS = limestone aggregate; G = granite aggregate.)

### Mineral Surface Type Effect

The affinity of a binder to different surfaces was evaluated by measuring the maximum pullout tension versus systems prepared with neat binder on glass, limestone and granite surfaces. Figure M2c.6 presents a summary of the test results. A very interesting observation from these results is that the mineral surface clearly influences the pullout tension results. Granite and limestone surfaces show greater pullout tension values than glass surfaces. This is an unexpected result as the smooth-surfaced glass plate would be expected to show higher pullout tension results. It appears also that the observed effect is more important when the bonding temperature is greater (135 °C versus 65 °C).

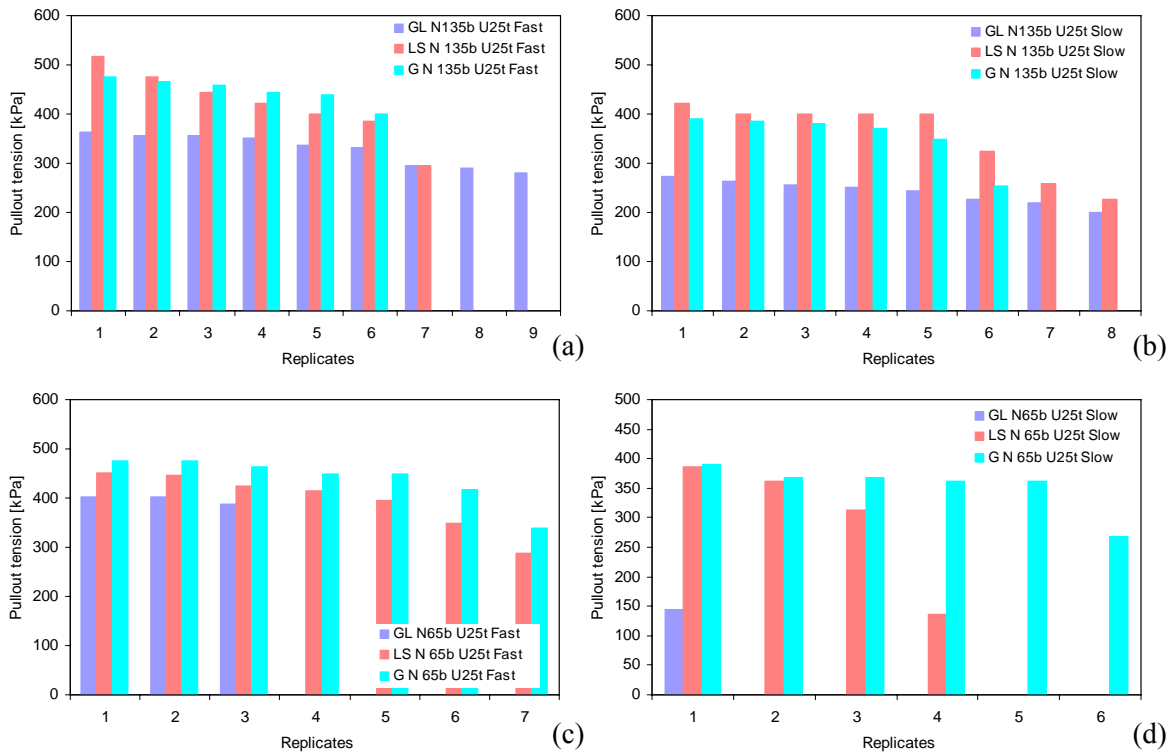


Figure M2c.6. Graphs. Effect of mineral surfaces on the pullout tension response of neat binder: (a) fast loading rates and 135 °C bonding temperature, (b) slow loading rates and 135 °C bonding temperature, (c) fast loading rates and 65 °C bonding temperature, and (d) slow loading rates and 65 °C bonding temperature. (GL = glass plate; LS = limestone aggregate; G = granite aggregate.)

### Binding Temperature Effects

To evaluate the effect of binding temperatures on the pullout tension response, tests were run on glass, limestone and granite surfaces using neat binder bonded at different temperatures and tested using similar, but not identical, pressure rates. The results are summarized in figure M2c.7. These results do not appear to show any statistical difference between the two bonding temperatures.

Because the pullout tests are very sensitive to minor changes in pressure rates, a set of tests was run while the PATTI pressure control regulator was set at slow pressure rate and kept constant during this parametric study. Individual results are presented in figure M2c.8 as pressure history plots while the summary of the maximum pullout pressure test results are presented in figure M2c.9. The results suggest that the effect of bonding temperature is only important in the case of modified binders, whereas neat binder does not seem to be controlled by the binding temperature. These results may have a significant effect on the way specimens are prepared.

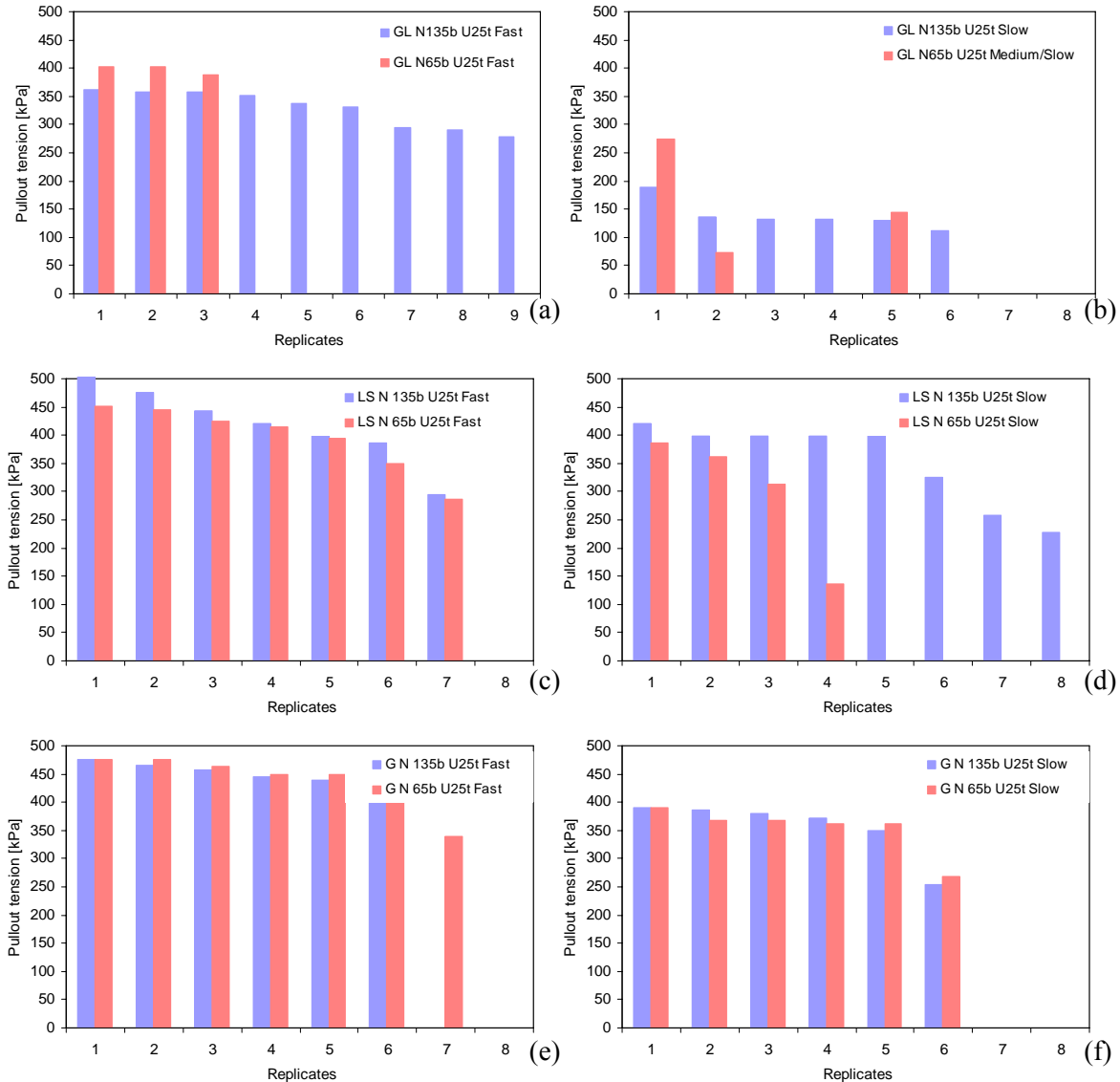


Figure M2c.7. Graphs. Effect of bonding on the pullout tension response of neat binder: (a) glass surface at fast pressure loading rates, (b) glass surface at slow pressure loading rates, (c) limestone surface at fast loading rates, (d) limestone surface at slow pressure loading rates, (e) granite surface at fast pressure loading rates and (f) granite surface at slow loading rates. (GL = glass plate; LS = limestone aggregate; G = granite aggregate.)

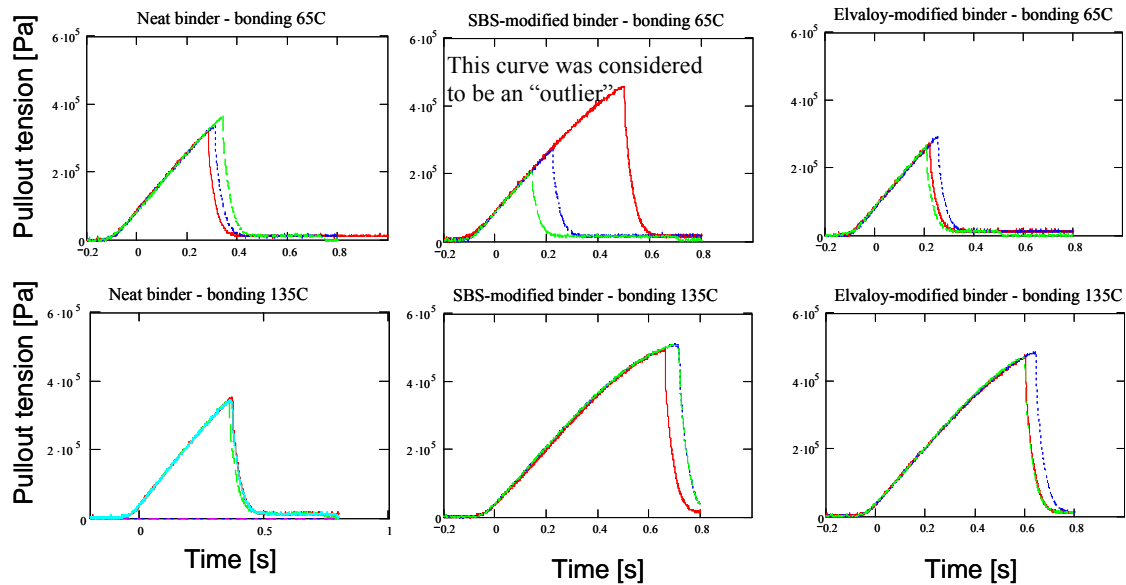


Figure M2c.8. Graphs. Pullout history curves for neat, SBS-modified and Elvaloy-modified binder on glass surfaces. The top row presents results for specimens prepared at 65 °C while the bottom row presents results for specimens prepared at 135 °C. All specimens were tested at pressure rates of 891 kPa/s.

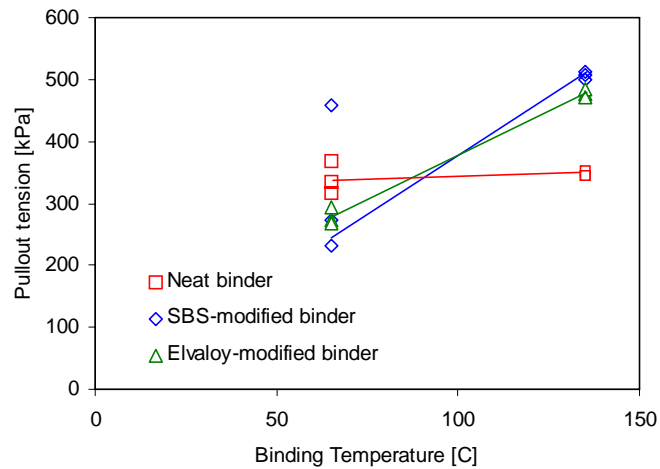


Figure M2c.9. Graph. Summary pullout tension test results for neat, SBS-modified and Elvaloy-modified binder on glass surfaces. All specimens were tested at pressure rates of 891 kPa/s.

### Significant Problems, Issues and Potential Impact on Progress

None.



## Work Planned Next Quarter

The work planned for the next quarter is detailed below, by topic.

- *Surface roughness.* The research team will possibly measure surface roughness with a laser profilometer or British Pendulum.
- *Application temperature.* Stub temperature will be held constant with a digital hot plate prior to application to the test sample. Four factors will be considered: aggregate temperature (warm and cold) and emulsion temperature (warm and cold).
- *Bitumen source.* The research team will use the bitumen materials described in the approved experimental matrix.
- *Aggregate source.* The aggregate to be used will be limestone and granite with possibly a third local aggregate. The research team will consider curing times of 2, 6, 24, and 30 hours.
- *Stone moisture.* The research team will consider wet and dry moisture factors.
- *Rate of loading.* The research team will establish a benchmark loading rate and control the loading rate by modifying the existing setup with a solenoid valve flow controller.
- *Film thickness.* Modification of pullout stubs will allow for better control of film thickness. The research team will continue to test both PATTI stub configurations.
- *Relevant test method.* Equipment for the PATTI test and the PosiTest by DeFelsko will be used.

## **CATEGORY M3: AGGREGATE SURFACE**

### **Work Element M3a: Aggregate Surface Characterization (TAMU)**

#### Work Done This Quarter

Current understanding of the aggregate and bitumen properties that control and shape surface energy is limited, which in turn limits our ability to *a priori* predict surface energy of any given aggregate-asphalt combination. The work in this work element is organized around the (1) characterization of the chemical composition of the surfaces of reference minerals and aggregates through electron beam spectroscopes, including electron microprobe, backscatter electrons and electron-dispersive spectroscopy (EDS), and (2) the characterization of the surface energies of reference minerals and aggregates through the universal sorption device and microcalorimetry. The results from these tasks will support the development of a predictive model of aggregate surface energies based upon the surface energies of the minerals that compose the aggregate.

Tasks completed this quarter include additional chemical and mineralogical analysis for the following aggregates: Lithonia granite (RA), basalt (RK), and Gulf Coast Gravel (RL). In

addition, mineralogical samples were obtained for kaolinite, montmorillonite and chlorite. Specific accomplishments are highlighted in the tables below.

Surface energy measurements for quartz, microcline, calcite, labradorite, biotite, and olivine have been collected using the universal sorption device. The components of surface energy were calculated on replicates of the samples.

Sample preparation and aggregate surface characterization tasks completed this quarter are shown in table M3a.1.

Table M3a.1. Status of tasks associated with mineralogical and chemical characterization of aggregates.

<b>SHRP</b>	<b>Name</b>	<b>08 Qtr</b>	<b>Thin Section Prep Status</b>	<b>Microprobe Analysis Status</b>
<b>RA</b>	Lithonia Granite	1	1 aggr sample prepared, 2 more in progress	1 set of X-ray maps, 1 set of BSE images, 1 preliminary set of WDS quant analyses
		2	2 more aggregate samples prepared	2 sets of X-ray maps, BSE images are not needed because of grain size
<b>RC</b>	Limestone (higher absorption)	1	2 aggr samples prepared	1 set of X-ray maps, 1 set of BSE images, 1 preliminary set of WDS quant analyses
		2	-	No additional analyses
<b>RD</b>	Limestone (low absorp.)	1	4 aggr samples prepared,	4 sets of X-ray maps, 1 set of BSE images, 1 preliminary set of WDS quant analyses
		2	-	No additional analyses
<b>RK</b>	Basalt	1	2 aggr samples prepared, 1 more in progress	2 sets of X-ray maps, 1 set of BSE images, 1 preliminary set of WDS quant analyses
		2	1 sample in progress	3 additional sets of X-ray maps, 13 set of BSE images, 1 set of WDS quant analyses for pyroxene, olivine, amphibole
<b>RL</b>	Gulf Coast Gravel	1	5 aggr samples prepared, 9 more in progress	4 sets of X-ray maps, 1 set of BSE images, 1 preliminary set of WDS quant analyses
		2	9 more in progress	9 sets of X-ray maps

Sample preparation and mineral surface characterization tasks completed this quarter are shown in the table M3a.2.

Table M3a.2. Status of tasks associated with mineralogical and chemical characterization of mineral components of aggregates.

Mineral	Group	08 Qtr	(1) Acquisition Status (2) Microprobe Mount Status	Microprobe Analysis Status
Quartz	Silica Mineral	1	(1) > 200 grams acquired (Arkansas, RNG specimen) (2) Polished microprobe mount in preparation	In progress
		2	In progress	In progress
Microcline	Alkali Feldspar	1	(1) > 160 grams acquired (G&G collection, B0434) (2) Preliminary polished mount prepared	Preliminary homogeneity and quantitative chemical analysis acquired.
		2	In progress	In progress
Albite	Plagioclase Feldspar	1	(1) > 100 grams acquired (G&G collection, B0469) (2) Polished mount to be prepared	In progress
		2	In progress	In progress
Oligoclase	Plagioclase Feldspar	3	> 100 grams acquired (G&G collection, 008)	In progress
Andesine	Plagioclase Feldspar	1	(1) > 65 grams acquired (G&G collection, B0513) (2) Preliminary polished mount prepared	Preliminary homogeneity and quantitative chemical analysis acquired.
		2	In progress	In progress
Labradorite	Plagioclase Feldspar	1	(1) > 160 grams acquired (Naim, Labrador; RNG specimen) (2) Preliminary polished mount prepared	Preliminary homogeneity and quantitative chemical analysis acquired.
		2	In progress	In progress
Anorthite	Plagioclase Feldspar	1	Samples to be acquired	NA
		2	NA	NA

Table M3a.2. Status of tasks associated with mineralogical and chemical characterization of mineral components of aggregates (cont).

Mineral	Group	08 Qtr	(1) Acquisition Status (2) Microprobe Mount Status	Microprobe Analysis Status
Hornblende	Amphibole	1	(1) > 350 grams acquired (G&G collection, B0545) (2) Preliminary polished mount prepared	Preliminary homogeneity and quantitative chemical analysis acquired.
		2	In progress	In progress
Hornblende	Amphibole	1	(1) > 70 grams acquired (G&G collection, Room 008) (2) Polished mount to be prepared	In progress
		2	In progress	In progress
Augite	Pyroxene	1	(1) > 0 (?) grams acquired (G&G collection, B1007) (2) Preliminary polished mount prepared	Preliminary homogeneity and quantitative chemical analysis acquired.
		2	In progress	In progress
Augite	Pyroxene	1	(1) > 80 grams acquired (G&G collection, Room 008) (2) Polished mount to be prepared	In progress
		2	In progress	In progress
Forsteritic Olivine	Olivine	1	(1) > 280 grams acquired (San Carlos, AZ) (2) Polished mount to be prepared	In progress
		2	In progress	In progress

Table M3a.2. Status of tasks associated with mineralogical and chemical characterization of mineral components of aggregates (cont).

Mineral	Group	08 Qtr	(1) Acquisition Status (2) Microprobe Mount Status	Microprobe Analysis Status
Muscovite	Mica	1	(1) > 65 grams acquired (G&G collection, Room 008) (2) Polished mount to be prepared	Preliminary quantitative chemical analysis acquired.
		2	In progress	In progress
Biotite	Mica	1	(1) > 175 grams acquired (G&G collection, B0857) (2) Polished mount to be prepared	In progress
		2	In progress	In progress
Biotite	Mica	1	(1) > 150 grams acquired (G&G collection, Room 008) (2) Polished mount to be prepared	Preliminary quantitative chemical analysis acquired.
		2	In progress	In progress
Calcite	Carbonate	1	(1) > 100 grams acquired (Mexico; RNG specimen) (2) Polished mount to be prepared	In progress
		2	In progress	In progress
Dolomite	Carbonate	1	Samples to be acquired	NA
		2	NA	NA

Table M3a.2. Status of tasks associated with mineralogical and chemical characterization of mineral components of aggregates (cont).

Mineral	Group	08 Qtr	(1) Acquisition Status (2) Microprobe Mount Status	Microprobe Analysis Status
Hematite	Iron Oxide	1	Samples to be acquired	NA
		2	NA	NA
Magnetite	Iron Oxide	1	Samples to be acquired	NA
		2	NA	NA
Ilmenite	Iron Titanium Oxide	3	> 100 g sample (Ontario; RNG specimen)	NA
Goethite	Iron Oxyhydroxide	1	Samples to be acquired	NA
		2	NA	NA
Kaolinite (KGA-1B)	Clay Mineral	3	Samples acquired	NA
		2	Samples acquired	In progress
Kaolinite	Clay Mineral	3	Samples acquired	NA
		2	Samples acquired	In progress
Montmorillonite (SAz-2)	Clay Mineral	3	Samples acquired	NA
		2	Samples acquired	In progress
Chlorite	Clay Mineral	3	Samples acquired; ~25 g Calumet and New Melones (RNG)	NA
		2	Samples acquired	In progress

## Significant Results

### *Establishing a Surface Energy Predictive Model*

One of the first goals will be to establish a model for predicting aggregate bulk surface energies based on mineralogical composition. Improved prediction of aggregate bulk properties pertinent to moisture damage susceptibility can lead to better methods to measure material properties and moisture damage susceptibility of asphalt/aggregate mixes. Development of a simple visual field

test of aggregate surface energy properties will aid in on-site evaluation of aggregate moisture damage susceptibility.

We expect the bulk/total surface energy of an aggregate to be a function of the component surface energies of its mineralogical constituents as:

$$Se_{aggregate} = \sum (Se_{Mineral} \cdot SA) + \sigma$$

where  $Se$  is surface energy,  $SA$  is surface area, and  $\sigma$  is the error term. A visual inspection of rock mineralogy based on percent of constituents can accurately predict total surface energy of the sample.

Methods –A Universal Sorption Device can be used to measure pure phase mineral surface energies by calculating the amount of a reference gas (water, hexane, and methylpropyl ketone in this case) sorbed to the mineral surface at various pressures. The adsorption isotherm for each reference gas is used to calculate equilibrium spreading pressure for each of the vapors along with the specific surface area (SSA) using the BET Equation. The equilibrium spreading pressure of each vapor is then used to calculate the three surface energy components using GvOC Equations. These values will then be used to establish an additive model of total surface energy for previously characterized rock samples based on percent of each constituent at the surface. The validity of the model will be tested by using the same Universal Sorption Device technique on the aggregate samples. A statistical analysis will be performed on the observed measurements versus predicted values.

Experiments – Although rock mineralogy has the capacity to be very complex it is dominated by a relatively small group of minerals of predictable variability in North America. The mineralogy of common aggregates used in hot asphalt mixes across America is outlined in the aggregate analysis data from the Strategic Highway Research Program’s (SHRP) materials reference library. Pure phase minerals are being collected by Dr. Ray Guillemette based on the findings of the SHRP. These minerals are the dominant constituents in all major aggregates of the study. The chosen minerals are listed in table 1.

The surface energies of these pure phase minerals will be calculated using a Universal Sorption Device using three reference gases to determine spreading pressures. Each mineral will be crushed and passed through a number 10 sieve. Minerals will be washed with distilled water and heated for 24 hours at 80°Celsius in a Fisher Isotemp® Oven. Each reference gas will be used on a separate sample of each pure phase mineral. After the test is run each sample will be washed with distilled water and reheated at 80°C for future analysis.

After each of the pure phase mineral surface energies have been quantified the SHRP aggregate samples themselves will be crushed and analyzed in the Universal Sorption Device to statistically determine the linear additive model’s validity.

Data- The data gained from this experiment will be in  $erg / (cm)^2$  for each pure phase mineral and SHRP aggregate. In order to calculate mineral surface energy the isotherm for each

reference gas must be calculated. To obtain a full isotherm, the aggregate is exposed to ten equal increments of partial probe vapor pressure from vacuum to saturated vapor pressure. At each stage the adsorped mass is recorded after it reaches equilibrium. The adsorped mass of each stage is then used to plot the isotherm. The measured isotherm for hexane is then used to calculate the specific surface area (SSA) using the Branauer, Emmett, and Teller BET equation:

$$A = \left( \frac{N_m N_0}{M} \right) \alpha$$

where  $N_0$ =Avogadro's number;  $M$ =molecular weight of the probe vapor;  $\alpha$  = projected area of a single molecule; and  $N_m$ =monolayer capacity of the aggregate surface. The specific surface area and each adsorption isotherm are then used to calculate three surface energy components using the GvOC equation:

$$W = 2\sqrt{\gamma_s^{\text{LW}}\gamma_s^{\text{AB}}} + 2\sqrt{\gamma_s^{\text{+}}\gamma_s^{\text{-}}} + 2\sqrt{\gamma_s^{\text{-}}\gamma_s^{\text{+}}}$$

where  $\gamma^{\text{Total}}$  = total surface energy of the material;  $\gamma^{\text{LW}}$  = Lifhsitz–van der Waals or dispersive component;  $\gamma^{\text{AB}}$  = acid-base component;  $\gamma^{\text{+}}$  = Lewis acid component, and  $\gamma^{\text{-}}$  = Lewis base component.

### Current Results

In order to use the Universal Sorption Device as an appropriate measuring device for surface energy the reproducibility must first be known. In order to test the repoducability one of the SHRP aggregates was chosen at random and the surface energy was measured on the sorbtion device. The aggregate was RD-7, a shaly limestone composed primarily of calcite. Hexane and methylpropyl ketone were run in triplicate and water vapor was tested four times. The results indicated that there was a good deal of internal consistency between the test runs, and the overall surface energy calculation was within a 95 percent confidence interval to previous study of the aggregate over two years ago. In total 8 minerals are currently at various stages of testing. All minerals will be tested in triplicate for each vapor. The results to date are included in the following chart.

Mineral Surface Energy					
Mineral	SSA	Energy Components (ergs/cm <sup>2</sup> )			
		LW	Acid	Base	Total
RD-7	0.23	48.97	0.52	467.57	80.27
Quartz	0.08	32.73	0.05	142.01	37.91
Microcline	0.07	52.62	0.41	206.43	71.02
Calcite	0.09	41.68	0.11	152.76	49.86
Biotite	0.05	56.88	0.01	691.77	62.08
Labradorite	0.08	35.17	1.38	997.22	109.45
Andesine	0.07	50.39	1.08	11261.19	270.64
Albite	0.05	53.42	0.19	435.99	71.68
Siderite	NA	NA	NA	NA	NA



## Significant Problems, Issues and Potential Impact on Progress

No significant problems at this time.

## Work Planned Next Quarter

Work planned in the next quarter includes continued analysis of the aggregates and minerals, with specific reference to surface energies.

## **CATEGORY M4: MODELING**

### **Work Element M4a: Micromechanics Model (TAMU)**

#### Work Done This Quarter

The TAMU researchers continued to work this quarter on the development of a micromechanical model that couples the presence of moisture and mechanical loading. This work complements the work that is being conducted by the University of Nebraska on modeling of fracture in asphalt mixtures using cohesive zone elements under dry conditions (See Work Element F3b).

In the coupled moisture-mechanical model, the adverse effects of moisture on the viscoelastic properties of the bulk (i.e. mastic) and on the quality and strength of the aggregate-mastic interface are reflected in the mechanical response of the system. This modeling approach has been implemented using a sequentially coupled moisture-mechanical scheme in Abaqus<sup>®</sup>. This methodology consists of two main stages. During the first stage, moisture diffusion profiles under the absence of load are generated within the system. During the second stage, mechanical load is applied and the moisture profiles generated during the first simulation are used as prescribed conditions of the simulation. During this stage, the mechanical properties of the materials change through time as a function of the diffused moisture content. The current model is composed of five main elements: (1) microstructure geometry of asphalt mixtures; (2) mass transport processes; (3) viscoelastic properties of the bulk; (4) fracture mechanics principles; and (5) thermodynamics principles.

Figure M4a.1 presents the state of the two idealized microstructures that were subjected to moisture diffusion for thirty days under two diffusion coefficients ( $D_1 > D_2$ ) before applying a mechanical pressure at the top surface of the model. The only difference between these two specimens is the diffusivity of the mastic (it is assumed that both mastics have the same mechanical properties); therefore, the differences in the mechanical performance is exclusively due to the coupling between the amount of moisture diffused into the system and the mechanical properties of the materials. More details about the micromechanical model are available in Appendix A of this report.

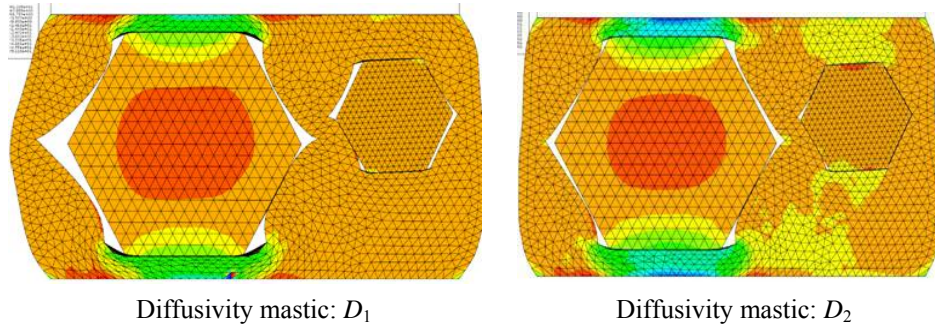


Figure M4a.1. Final state of the specimens conditioned for 30 days after mechanical test ( $D_1 > D_2$ )

### Significant Results

We have developed an approach for modeling coupled moisture-mechanical damage. The model accounts for the influence of moisture on the bond energy and bulk viscoelastic properties.

### Significant Problems, Issues and Potential Impact on Progress

The current challenges are (1) to incorporate more realistic microstructure, material properties and loading conditions in the micromechanical model, and (2) to develop a framework for accounting for the influence of material thermodynamic properties on moisture transport and moisture induced damage.

### Work Planned Next Quarter

A comprehensive sensitivity analysis will be conducted in order to identify the relative importance of the geometrical, physical and mechanical parameters in the development of failure. In addition, thermodynamic principles describing the saturation process occurring at the interface will be incorporated into the model.

### **Work Element M4b: Analytical Fatigue Model for Mixture Design**

### **Work Element M4c: Unified Continuum Model**

#### Work Done This Quarter

We have worked during this quarter on two aspects of the unified continuum model. The first aspect focused on developing the method for determining the elastoviscoplastic model parameters using experimental measurements. The data are from comprehensive experimental measurements that were conducted at the University of Nottingham. Dr. Gordon Airey and Dr. Andy Collop have provided us with access to their research team and research database. Dr. Eyad Masad spent a few days at the University of Nottingham this summer to discuss the experimental measurements. Once the model's parameters are determined, the model will be

used to predict performance of asphalt mixtures under different boundary conditions of wheel tracking experiments.

The Nottingham database is for two asphalt mixtures types: a 10 mm Dense Bitumen Macadam (DBM) and 30/10 Hot Rolled Asphalt (HRA). The DBM is a continuously graded mixture and the HRA is a gap graded mixtures. Granite aggregate and a 70/100 penetration grade asphalt binder are used in these mixtures. The binder contents were 5.5% and 8.0% for DBM and HRA mixtures, respectively. The specimen dimensions were 100 mm in diameter and 100mm in height. The database includes uniaxial and triaxial tests with compression and tension loading conditions. These tests performed at different temperatures and stress levels.

The tests in the Nottingham database include a uniaxial constant strain rate test, a constant stress creep test, a single creep recovery test, and a repeated creep recovery test. The uniaxial constant strain rate and constant stress creep tests were conducted using several constant strain rates and stress levels at different temperatures. The single creep recovery tests were conducted over a range of temperatures and stress levels. This test involved applying a constant load and then removing the load until the rate of recovered deformation was approximately zero. In the repeated creep recovery test, several combinations of loading and unloading times were conducted under different stress levels. This test included applying a constant stress and then removing the stress for several continuous loading-unloading cycles until failure occurred.

The triaxial tests were conducted under creep loading with several combinations of axial stress and confinement stress. This Nottingham database also includes wheel tracking data: small scale wheel tracking, large scale wheel tracking and full scale wheel tracking tests. The tested slab dimensions were 305 mm long, 281 mm wide and 100 mm deep. The contact length is 230 mm with a speed of 0.552 km/h. The range of applied loading was 540~1000 kPa at different temperatures.

The second aspect of this work element focused on developing the framework for coupling mechanical damage with moisture damage in the TAMU elastoviscoplastic model. The proposed mechanical damage can distinguish between crack nucleation and growth, and it is pressure sensitive, with damage induced more rapidly for tensile stresses than equal compressive stresses, which agrees well with the experimental results on asphaltic materials.

The degrading effect of moisture manifests in two physical phenomena: (1) adhesive moisture damage, which is the degradation of the bond strength between the aggregates and the asphalt mastic due to the existence and diffusion of moisture through the thin films surrounding the aggregate particles and along the aggregate-mastic interfaces; (2) cohesive moisture damage, which is the degradation of the cohesive strength of the asphalt mastic itself. In this study and for the first time, both of these phenomena are modeled independently, which allows one to introduce fundamental mechanical properties (e.g. bond strength and cohesive strength) and model the transition between adhesion and cohesion damage. The details of modeling moisture damage and coupling between mechanical and moisture damage mechanisms are documented in Appendix B.

### Significant Results

No significant results in this quarter.

### Significant Problems, Issues and Potential Impact on Progress

No significant problems.

### Work Planned Next Quarter

We will conduct extensive sensitivity analysis of the elastoviscoplastic model with damage under various loading and boundary conditions. We will also test the ability of the model to describe experimental measurements of asphalt mixtures with coupled mechanical and moisture damage.

## **CATEGORY M5: MOISTURE DAMAGE PREDICTION SYSTEM**

This area is planned to start later in the project.


Moisture Damage Year 2		Year 2 (4/08-3/09)												
		4	5	6	7	8	9	10	11	12	1	2	3	
<b>Adhesion</b>														
<b>M1a Affinity of Asphalt to Aggregate - Mechanical Tests</b>														
M1a-1	Select Materials						DP							
M1a-2	Conduct modified DSR tests					P					P		DP	
M1a-3	Evaluate the moisture damage of asphalt mixtures												DP	
M1a-4	Correlate moisture damage between DSR and mix tests													
M1a-5	Propose a Novel Testing Protocol													
<b>M1b Work of Adhesion</b>														
M1b-1	Adhesion using Micro calorimeter and SFE													
M1b-2	Evaluating adhesion at nano scale using AFM													
M1b-3	Mechanisms of water-organic molecule competition												JP,D	
<b>M1c Quantifying Moisture Damage Using DMA</b>														
<b>Cohesion</b>														
<b>M2a Work of Cohesion Based on Surface Energy</b>														
M2a-1	Methods to determine SFE of saturated binders													
M2a-2	Evaluating cohesion at nano scale using AFM													
<b>M2b Impact of Moisture Diffusion in Asphalt</b>														
M2b-1	Diffusion of moisture through asphalt/mastic films												JP,D	
M2b-2	Kinetics of debonding at binder-agreagte interface												JP,D	
<b>M2c Thin Film Rheology and Cohesion</b>														
M2c-1	Evaluate load and deflection measurements using the modified PATTI test		DP		JP						D		F	
M2c-2	Evaluate effectiveness of the modified PATTI test for Detecting Modification										D	DP	F	
M2c-3	Conduct Testing													
M2c-4	Analysis & Interpretation												P	
M2c-5	Standard Testing Procedure and Recommendation for Specifications													
<b>Aggregate Surface</b>														
<b>M3a Impact of Surface Structure of Aggregate</b>														
M3a-1	Aggregate surface characterization													
<b>Models</b>														
<b>M4a Development of Model</b>														
M4a-1	Micromechanics model development											JP		
M4a-2	Analytical fatigue model for use during mixture design													
M4a-3	Unified continuum model													

**LEGEND**

**Deliverable codes**

- D: Draft Report
- F: Final Report
- M&A: Model and algorithm
- SW: Software
- JP: Journal paper
- P: Presentation
- DP: Decision Point

[x]

-  Work planned
-  Work completed
-  Parallel topic

**Deliverable Description**


- Report delivered to FHWA for 3 week review period.
- Final report delivered in compliance with FHWA publication standards
- Mathematical model and sample code
- Executable software, code and user manual
- Paper submitted to conference or journal
- Presentation for symposium, conference or other
- Time to make a decision on two parallel paths as to which is most promising to follow through
- Indicates completion of deliverable x

Moisture Damage Year 2 - 5		Year 2 (4/08-3/09)				Year 3 (4/09-3/10)				Year 4 (04/10-03/11)				Year 5 (04/11-03/12)					
		Q1	Q2	Q3	Q4	Q1	Q2	Q3	Q4	Q1	Q2	Q3	Q4	Q1	Q2	Q3	Q4		
<b>Adhesion</b>																			
<b>M1a</b>	<b>Affinity of Asphalt to Aggregate - Mechanical Tests</b>																		
M1a-1	Select Materials		DP																
M1a-2	Conduct modified DSR tests		P		P														
M1a-3	Evaluate the moisture damage of asphalt mixtures				DP		P			P									
M1a-4	Correlate moisture damage between DSR and mix tests						P			P									
M1a-5	Propose a Novel Testing Protocol					P			P							JP, F			
<b>M1b</b>	<b>Work of Adhesion</b>																		
M1b-1	Adhesion using Micro calorimeter and SFE							JP					JP,F						
M1b-2	Evaluating adhesion at nano scale using AFM								JP						JP				
M1b-3	Mechanisms of water-organic molecule competition				JP,D	F						JP	D	F			JP, F		
<b>M1c</b>	<b>Quantifying Moisture Damage Using DMA</b>																		
													JP	D	F				
<b>Cohesion</b>																			
<b>M2a</b>	<b>Work of Cohesion Based on Surface Energy</b>																		
M2a-1	Methods to determine SFE of saturated binders															JP			
M2a-2	Evaluating cohesion at nano scale using AFM								JP						JP		JP, F		
<b>M2b</b>	<b>Impact of Moisture Diffusion in Asphalt</b>																		
M2b-1	Diffusion of moisture through asphalt/mastic films				JP,D	F						JP	D	F					
M2b-2	Kinetics of debonding at binder-agreagte interface				JP,D	F													
<b>M2c</b>	<b>Thin Film Rheology and Cohesion</b>																		
M2c-1	Evaluate load and deflection measurements using the modified PATTI test		DP	JP	D	F													
M2c-2	Evaluate effectiveness of the modified PATTI test for Detecting Modification				D	DP,F													
M2c-3	Conduct Testing							JP											
M2c-4	Analysis & Interpretation					P						D, JP		F					
M2c-5	Standard Testing Procedure and Recommendation for Specifications												D	P,F					
<b>Aggregate Surface</b>																			
<b>M3a</b>	<b>Impact of Surface Structure of Aggregate</b>																		
M3a-1	Aggregate surface characterization																		
<b>Models</b>																			
<b>M4a</b>	<b>Development of Model</b>																		
M4a-1	Micromechanics model development				JP				JP						M&A	D	DP	F, SW	
M4a-2	Analytical fatigue model for use during mixture design																	M&A,D	F
M4a-3	Unified continuum model								JP						M&A	D	DP	F, SW	

**LEGEND**

**Deliverable codes**

- D: Draft Report
- F: Final Report
- M&A: Model and algorithm
- SW: Software
- JP: Journal paper
- P: Presentation
- DP: Decision Point
- [x]

-  Work planned
-  Work completed
-  Parallel topic

**Deliverable Description**

- Report delivered to FHWA for 3 week review period.
- Final report delivered in compliance with FHWA publication standards
- Mathematical model and sample code
- Executable software, code and user manual
- Paper submitted to conference or journal
- Presentation for symposium, conference or other
- Time to make a decision on two parallel paths as to which is most promising to follow through
- Indicates completion of deliverable x

## APPENDIX A: DEVELOPMENT OF A COUPLED MICROMECHANICAL MOISTURE DAMAGE MODEL

Micromechanical modeling of moisture damage in asphalt mixtures is an efficient tool to understand the role and interaction of the different damage mechanisms occurring within the system through time. At the same time, these models can provide valuable information to guide the development of moisture damage models at the continuum level.

The main component of the micromechanical model currently under development at TAMU is the coupling between the presence of moisture and the mechanical performance of the mixture. In other words, the adverse effects of moisture on the viscoelastic properties of the bulk (i.e. mastic) and on the quality and strength of the aggregate-mastic interface are reflected in the mechanical response of the system. This modeling approach has been implemented using a sequentially coupled moisture-mechanical scheme in Abaqus<sup>®</sup>. This methodology consists of two main stages. During the first stage moisture diffusion profiles under the absence of load are generated within the system. During the second stage mechanical load is applied and the moisture profiles generated during the first simulation are used as prescribed conditions of the simulation. During this stage, the mechanical properties of the materials change through time as a function of the diffused moisture content. The current model is composed by five main elements: 1) microstructure geometry of asphalt mixtures; 2) mass transport processes; 3) viscoelastic properties of the bulk; 4) fracture mechanics principles; and 5) thermodynamics principles. Table 1 summarizes the current implementation of each one of these elements into the model.

Table 1. Components of the micromechanical model and their implementation.

Component of the model	Implementation
Microstructure geometry	Simplified geometries have been currently analyzed. However, the microstructure of the mixtures is well characterized (i.e. by means of X-Ray CT) and more realistic geometry will be incorporated in the near future.
Mass transport processes	The model is focused on one particular mode of moisture transport: moisture diffusion.
Viscoelastic properties of the bulk	The bulk (i.e., the mastic) is modeled as linear viscoelastic. The linear viscoelastic properties are function of the moisture content of the material.
Fracture mechanics principles	The interfaces of aggregate-mastic systems are modeled as cohesive zones ( <i>adhesive zones</i> ). The properties of the adhesive zones (i.e., response before damage, interface strength and critical energy released rate) are function of the amount of moisture at the interface. Crack initiation, propagation and arrest at the interface due to the combined action of moisture and mechanical load are a natural result of this numerical approach.
Thermodynamics principles	Thermodynamics principles have not been yet implemented. The rate of moisture saturation at the interface, which is function of the existing thermodynamic potential promoting debonding, will be included during the mass transport stage of the simulation.

## Example of the application of the modeling methodology

### • Geometry and material properties

In order to evaluate the capabilities of the model to couple the effects of moisture in the mechanical response of the materials, a simplified 2-dimensional model was developed. Figure 1 presents the geometry of the model and Table 2 contains the moisture diffusion coefficients and the mechanical properties of the materials.

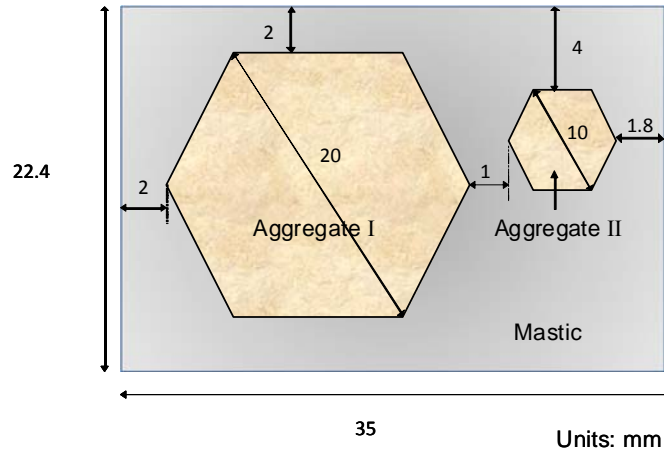


Figure 1. Geometry of the model.

Table 2. Components of the micromechanical model and their implementation.

	Aggregate	Mastic	Interface
Moisture diffusion coefficients (mm <sup>2</sup> /sec)	$2.44 \cdot 10^{-4}$	$D_1 = 2.78 \cdot 10^{-5}$ $D_2 = 5.56 \cdot 10^{-6}$	$1.00 \cdot 10^0$
Mechanical properties	$E = 5 \cdot 10^4$ MPa $\nu = 0.35$	Prony series for shear relaxation modulus [ $G(t)$ ], Kim et al. (2005)	$E_{\text{normal}} = E_{\text{shear}} = 150$ MPa  Failure criteria ( $n$ =normal, $s$ =shear): $\left( \frac{\epsilon_n}{\epsilon_{\text{max}}^n} \right)^2 + \left( \frac{\epsilon_s}{\epsilon_{\text{max}}^s} \right)^2 = 1$ Maximum displacement at failure: $\epsilon_{\text{max}}^s = \epsilon_{\text{max}}^n = 0.05$ mm.  Critical Energy Released rate, $G_C$ (mixed mode): $G_{Ic} = G_{IIc} = 0.297$ N/mm
Moisture dependency of mechanical properties	No moisture dependency	$G(t)$ decreases linearly from its original value in dry condition to 85% of the original value in saturated conditions.	Normal and shear moduli ( $E_{\text{normal}}$ , $E_{\text{shear}}$ ) decrease linearly from 150 MPa in dry condition to 0 MPa in saturated condition.



- **Simulation principle**

The simulation aims to represent an experimental program in which six identical specimens (Figure 1) are tested after being subjected to a moisture conditioning process. Three of the specimens contain mastic with moisture diffusivity  $D_1$ , while the other three contain mastic with moisture diffusivity  $D_2$  (Table 2). All specimens are placed inside an environmental chamber at constant relative humidity and temperature conditions. Moisture is allowed to diffuse into the specimens through the top and lateral sides. After 10 days, one specimen of each type is removed from the environmental chamber and tested. After 20 days, another specimen of each type is removed and tested. Finally, the remaining specimens are removed and tested after 30 days. The mechanical test is the same in all cases: pressure is applied to the top of the specimens during 40 seconds at a rate of 7.5MPa/sec. Figure 2 summarizes the simulation principle.

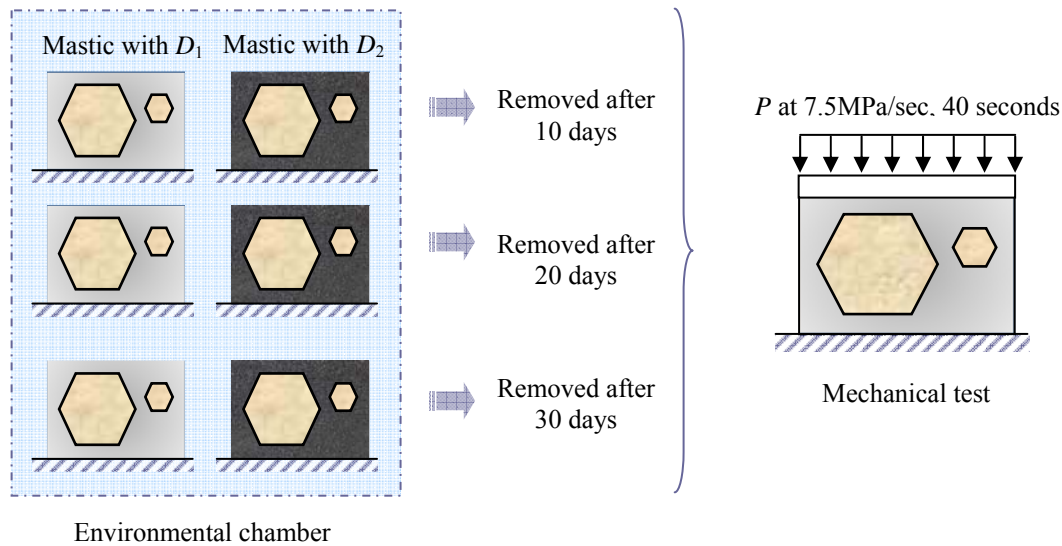


Figure 2. Simulation procedure.

- **Results**

Figure 3 presents the moisture profiles of the six specimens just before being subjected to the mechanical test. It can be observed that the specimen conditioned for 30 days containing mastic with diffusivity  $D_1$  presents larger values of moisture content, and is expected to perform poorly during the mechanical test.

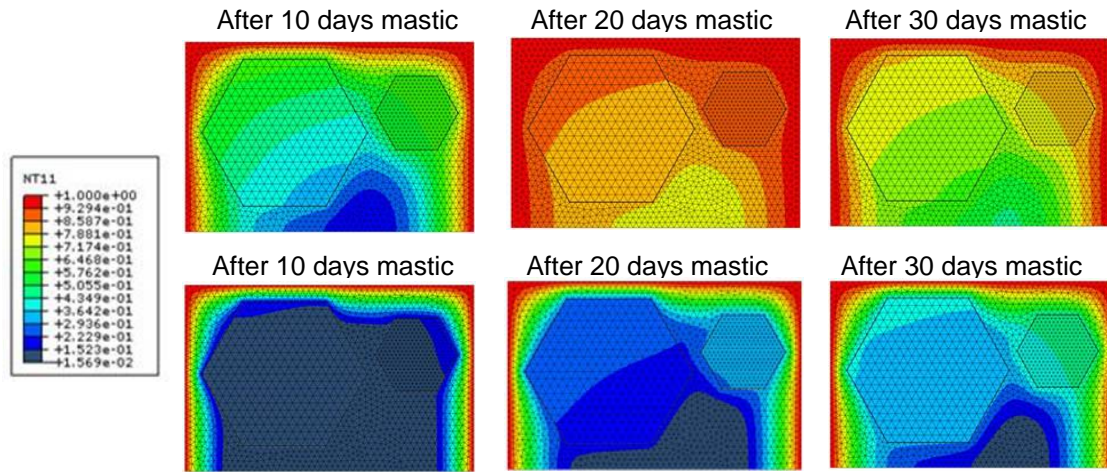


Figure 3. Moisture concentration profiles (concentration normalized with respect to saturation).

Figure 4 presents the state of the two specimens that were placed on the environmental chamber for 30 days after the application of the mechanical load. The only difference between these two specimens is the diffusivity of the mastic (it is assumed that both mastics have the same mechanical properties); therefore, the differences in the mechanical performance is exclusively due to the coupling between the amount of moisture diffused into the system and the mechanical properties of the materials.

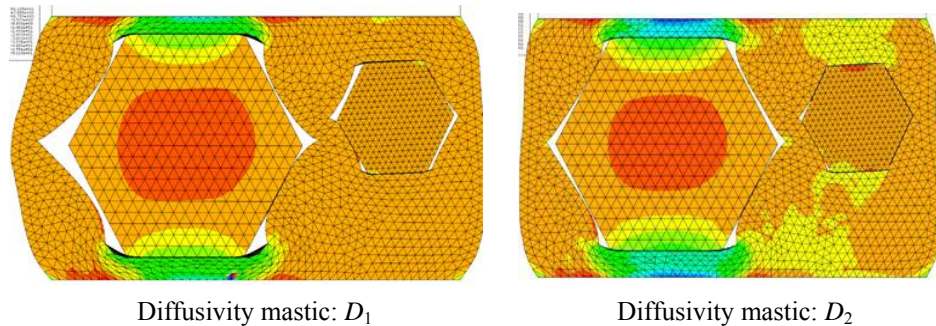


Figure 4. Final state of the specimens conditioned for 30 days after mechanical test ( $D_1 > D_2$ ).

The analysis of the performance of the system during the mechanical testing showed that cracks always initiated at the bottom-left side of the interface between the mastic and aggregate I. Figure 5 presents the relationship between crack length and time (i.e., crack propagation) for the six specimens. This figure demonstrates that: 1) cracking initiates first in the specimens with smaller diffusivity (specimens with mastic  $D_2$ ; Table 2), and 2) crack initiation is faster in the specimens subjected to longer periods of moisture conditioning.

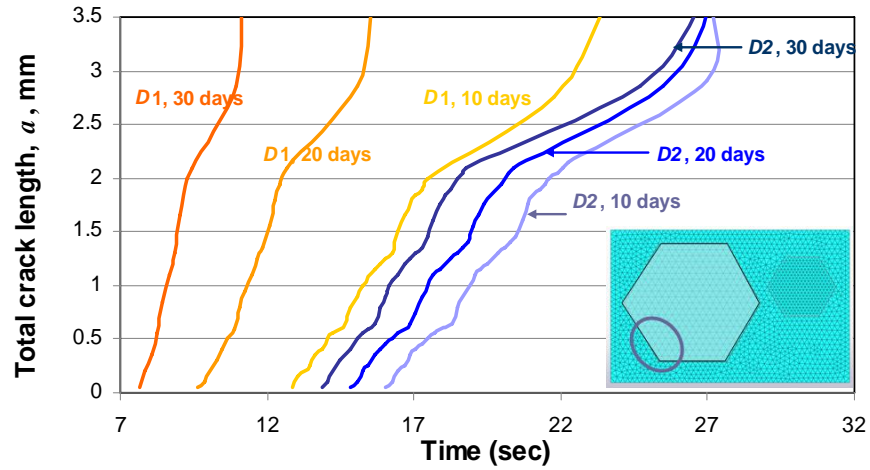


Figure 5. Crack length vs. time at the bottom-left zone of the mastic-aggregate I interface.

Finally, Figure 6 presents the viscoelastic response of the mastic for a point located close to the mastic-aggregate interface. Based on these results, it can be observed that the model is able to capture the effects of the moisture and adhesive failure on the viscoelastic response of the mastic.

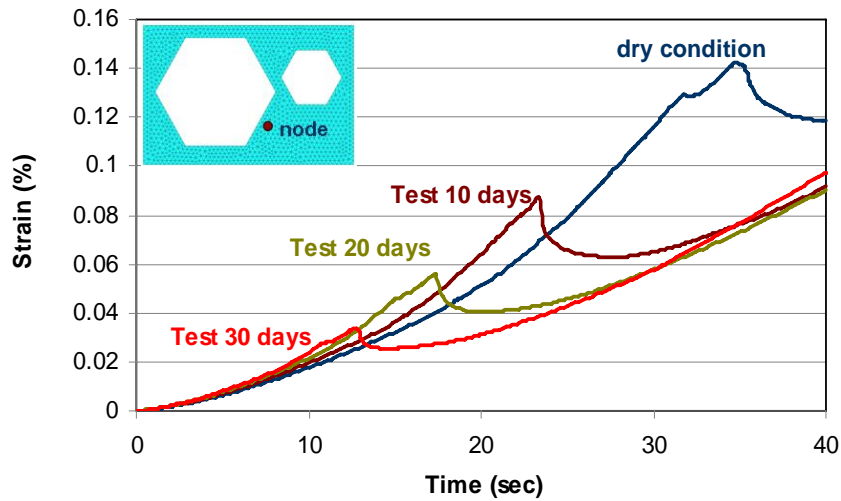


Figure 6. Viscoelastic response of the mastic.

## **APPENDIX B: A COUPLED MECHANICAL-MOISTURE-INDUCED DAMAGE MODEL FOR ASPHALTIC MIXES**

### **Summary**

Roadways are designed to last until rehabilitation or replacement, and it is their degraded performance that dictates the design of pavements. It is, therefore, essential to be able to predict the degradation (i.e. reduction in the mechanical and physical properties) of an asphalt concrete through the development of a robust computational model that can effectively simulate the performance of an asphalt pavement under different mechanical (e.g. traffic) and environmental (e.g. moisture) loading conditions.

There are two major contributors to damage evolution in asphalt pavements: mechanical and moisture. As trucks (and to a lesser extent, other vehicles) drive across a roadway, the repeated mechanical loading they impose damages the asphalt concrete. Moreover, as moisture is present in the form of water or relative humidity, it penetrates the asphalt microstructure and weakens the microstructure of asphalt concrete [see Caro et al. (2008a, 2008b) for more a comprehensive review of moisture damage]. Moisture-induced damage has for a long time been recognized by highway agencies and pavement industry as a serious contributor to premature degradation of asphalt pavements, which leads, in total, to an annual extra vehicle operating cost estimated at more than \$54 billion worldwide. Each of the mechanical- and moisture-induced damages seriously degrades the performance of the pavement and should be predicted in order to guide the design of better and more sustainable roadways. Both types of damages, moisture-induced damage and mechanical-induced damage, are coupled such that moisture damage strongly affects the mechanical damage.

In the last few decades, significant progress has been made in the development of test methods and standards to identify and remediate asphalt mixtures that are prone to mechanical and moisture damage. However, most of these aimed at trial-and-error comparative measures of moisture damage via visual observations from field data or comparative laboratory tests, which led to very slow advancements in mitigating or alleviating the susceptibility of asphalt pavements to a coupled mechanical and moisture damage. Moreover, these methods do not give any fundamental insight into the causes and evolution of the damage in time within the asphalt mix, nor can they directly be used for mix improvements. Therefore, the main objective of this study is to develop simple but effective and robust computational models that can be used by pavement engineers to predict the onset and evolution of damage in asphaltic mixes, to assess the remaining life of roadways, and to guide the design of better asphaltic mixes.

In the following, a brief description of the formulated and implemented computational damage model is described. Two models are developed: (1) mechanical-induced damage model which can be used to predict the nucleation and growth of cracks due to traffic loadings, and (2) moisture-induced damage model that can be used to predict the degradation in stiffness and strength of pavements due to presence of moisture and can distinguish between moisture-induced damage due to either adhesive-damage at the aggregate-mastic interface and cohesive-damage within the mastic itself.

## Mechanical-Induced Damage Model

The proposed mechanical damage is based on the framework of continuum damage mechanics (CDM). CDM is a framework for modeling the nucleation, growth, and propagation of numerous micro-cracks and their evolution into macro-cracks that ultimately leads to failure (see e.g. Voyiadjis and Kattan 1999; Abu Al-Rub and Voyiadjis 2003). CDM can be effectively used in predicting the onset (site and time or where and when) of damage nucleation (cracking potential) and its evolution (crack propagation). The proposed mechanical damage can distinguish between crack nucleation and growth due to compressive and extension imposed stresses and deformations. This can be achieved by adapting the following stress-based expression for the damage driving force,  $Y^m$  :

$$Y^m = \text{Maximum}\left(\tau - \alpha I_1, Y_o^m\right) \text{ with } \tau = \frac{\sqrt{J_2}}{2} \left(1 + \frac{1}{d} + \left(1 - \frac{1}{d}\right) \frac{J_3}{J_2^{3/2}}\right) \quad (1)$$

where  $Y_o^m$  is the threshold value of the mechanical damage force, which is a material property.  $I_1$  is the first stress invariant,  $J_2$  and  $J_3$  are the second and third deviatoric stress invariants,  $d$  is a parameter that distinguishes between the different strength in extension and compression ( $d \approx 0.7$ ), and  $\alpha$  is a pressure sensitivity parameter that is related to the asphalt angle of friction. Note that the superscript  $m$  indicates mechanical. The crack-density due to mechanical loading,  $\phi^m$ , can be calculated by using the following exponential law:

$$\phi^m = 1 - \exp\left[k^m \left(1 - \frac{Y^m}{Y_o^m}\right)\right] \geq 0 \quad (2)$$

where  $k^m$  is a material constant which controls the rate of damage growth. The mechanical damage variable  $\phi^m$  has a range of  $0 \leq \phi^m \leq 1$  with  $\phi^m = 1$  indicates complete failure.

It is noteworthy that the proposed mechanical-induced damage law is driven by the state of stress and is pressure sensitive, with damage induced more rapidly for tensile stresses than equal compressive stresses, which agrees well with the experimental results on asphaltic materials. Extensions in a compressive state of stress also induce damage more rapidly than further compressions.

## Moisture-Induced Damage Model

The degrading effect of moisture manifests in two physical phenomena: (1) adhesive moisture damage,  $\phi_a^M$ , which is the degradation of the bond strength between the aggregates and the asphalt mastic due to the existence and diffusion of moisture through the thin films surrounding the aggregate particles and along the aggregate-mastic interfaces; (2) cohesive moisture damage,  $\phi_c^M$ , which is the degradation of the cohesive strength of the asphalt mastic itself. Both (1) and

(2) may ultimately lead to erosion of the mastic film due to jetting water flow imposed by passing traffic (Kringos, 2007). In this study and for the first time, both of these phenomena are modeled independently, which allows one to introduce fundamental mechanical properties (e.g. bond strength and cohesive strength) and model the transition between adhesion and cohesion damage.

The decay in the aggregate-mastic bond strength and mastic cohesive strength due to the presence of moisture content,  $\theta$ , can be computed using the following evolution law:

$$X_i^M(t) = X_{i,0}^M + \int_0^t \dot{X}_i^M(\theta(\xi)) d\xi \quad (3)$$

where  $X_i^M(t)$  is the average bond strength of the aggregate-mastic adhesive strengths for  $i = a$  (i.e. adhesive) and the average mastic cohesive strength for  $i = c$  (i.e. cohesive) at time  $t$ ,  $X_{i,0}^M$  is the initial adhesive or cohesive strengths ( $i = a, c$ ), and  $\dot{X}_i^M(\theta(\xi))$  is the rate of decay of the average adhesive or cohesive strengths for a moisture content  $\theta$  at time  $\xi$ , where time  $t = 0$  is some time before moisture diffusion. The moisture content  $\theta$  can be computed effectively in many finite element codes (e.g. Abaqus) using standard fluid-diffusion constitutive equations. However, the asphalt mix diffusion coefficient needs to be identified in order to accurately estimate the level of moisture content.

For simplicity, the rate of decay in the adhesive/cohesive strength can be assumed to have the following linear evolution equation:

$$\dot{X}_i^M(\theta) = -k_i^M \theta(t) \quad \text{for } i = a, c \quad (4)$$

where  $k_i^M$  ( $i = a, c$ ) are material properties that can be identified through measuring the surface energy at the aggregate-binder interface and the surface energy of the binder. Also,  $k_i^M$  can be a function of the binder film thickness, aggregate size, aggregate physical and physio-chemical properties, and binder physio-chemical properties. Furthermore, one can define nonlinear evolution laws for  $\dot{X}_i^M$  other than the assumed simple form in Eq. (4).

It is noteworthy that the above evolution law provides an effective and robust approach for modeling adhesive/cohesive moisture damage, wherein the current moisture content drives the change in the bond/cohesive strength, but a decreased moisture level does not correspond to an anticipated restoration of strength (i.e. no healing). Though asphalt concretes exhibit healing, this would not be properly expressed by ignoring the moisture loading history. A dry asphalt concrete specimen that has never been exposed to moisture would be expected to have different behavior than a dry asphalt concrete specimen that has spent extended time in high moisture conditions.

Now, one can define two moisture-induced damage variables that are associated with degradation in the adhesive strength of the aggregate-mastic interface,  $\phi_a^M$ , and degradation in the cohesive strength of the mastic,  $\phi_c^M$ , that are defined through the following equations:

$$\phi_i^M = 1 - \frac{X_i^M}{X_{i,0}^M} \quad \text{for } i = a, c \quad (5)$$

### Coupling between Mechanical- and Moisture-Induced Damages

Moisture-induced damage is coupled with mechanical-induced damage in the proposed model to reflect reality. In particular, damage from exposure to moisture accelerates the damage due to mechanical loading, allowing mechanical damage to accumulate earlier and faster under the same loading conditions. This coupling can be enhanced by replacing the mechanical damage driving force  $Y^m$  in Eq. (1)<sub>1</sub> by the coupled mechanical-moisture-induced damage force,  $Y^{mM}$ , such that:

$$Y^{mM} = \frac{Y^m}{(1-\phi_a)(1-\phi_c)} \quad (6)$$

Furthermore, the total nominal stress  $\sigma$  in the damaged material can be related to the stress in the intact (undamaged) material  $\bar{\sigma}$  by the following relation:

$$\sigma = (1-\phi^{mM})^2 \bar{\sigma} \quad (7)$$

where the total coupled mechanical-moisture-induced damage variable  $\phi^{mM}$  can be defined as a coupled form of mechanical-induced damage,  $\phi^m$ , moisture-induced adhesive damage,  $\phi_a^M$ , and moisture-induced cohesive damage,  $\phi_c^M$ , such that:

$$\phi^{mM} = 1 - \sqrt{(1-\phi^m)^2 (1-\phi_a^M)^2 (1-\phi_c^M)^2} \quad (8)$$

Therefore, assuming the validation of the strain equivalence hypothesis (Lemaitre, 1992), which states that the strain in the damaged configuration is the same as the strain in the undamaged configuration, one can express the degraded (or damaged) stiffness of the asphalt mix as follows:

$$E^D = (1-\phi^{mM})^2 E \quad (9)$$

where  $E^D$  is the damaged stiffness and  $E$  is the initial stiffness.

In order to facilitate the use of the proposed model by pavement engineers, it has been implemented in the well-known finite element code Abaqus (2006) through the user material

subroutine UMAT. The model will be calibrated and validated against the large amount of experimental data obtained by researchers at Texas A&M University and by many others.

### **Advantages of the Proposed Model**

The proposed approach for modeling different types of damage closely reflects the degradation of asphalt concretes. The following characteristic of the proposed damage model are briefly summarized: (1) the damage driven by mechanical loading is pressure-sensitive such that tension induces more damage than compression and extension while under compression induces more damage than more compression (as shear stresses change). (2) The moisture-induced damage model distinguishes between the damage due to degradation in the adhesive strength between the aggregate and mastic and the degradation in the cohesive strength of the mastic. (3) The associated material parameters are related to fundamental asphaltic material properties (e.g. adhesive strength, cohesive strength, surface energy, etc) which allows one to optimize the design of pavements to mitigate mechanical and/or moisture induced failures or to predict the onset of pavement distress that guide the health monitoring of pavements. (4) Moisture damage accelerates mechanical damage as described by proper coupled laws. (5) Moisture damage itself accumulates during the presence of moisture, proportional to the concentration and duration of moisture and the damage remains when the moisture is removed.

The conducted study will lead to the development of a computational software that is simple and easy to use by pavement engineers to predict the time frame over which mechanical-moisture-induced damages may occur under different environmental and traffic loading conditions. This computational tool will give highway agencies and contractors the ability to easily perform “what-if” scenarios for asphaltic pavements, tweaking mix designs and compositions for maximum performance while producing quality asphalt mix in compliance with required specifications. Therefore, the proposed model, which is developed based on fundamental moisture-induced damage mechanisms, can be used for predicting moisture-induced damage as a durability indicator and to modify mix composition that increases durability and minimizes the risk of failure. Lowering the risk translates to lower cost to the highway agency and the public, reduce maintenance operations, and extending the pavement’s service life.

### **References**

Abaqus, 2006. Version 6.5, Habbitt, Karlsson and Sorensen, Inc: Providence, RI.

Abu Al-Rub, R. K., and G. Z. Voyiadjis, 2003, On the coupling of anisotropic damage and plasticity models for ductile materials. *Int. J. Solids Struct.*, 40: 2611-2643.

Caro, S., E. Masad, A. Bhasin, and D. N. Little, 2008a, Moisture susceptibility of asphalt mixtures, Part 1: mechanisms. *International Journal of Pavement Engineering*, 9: 81-98.

Caro, S., E. Masad, A. Bhasin, and D. N. Little, 2008b, Moisture susceptibility of asphalt mixtures, Part 2: characterization and modeling. *International Journal of Pavement Engineering*, 9: 99-114.



Kringos, N., 2007. *Modeling of Combined Physical-Mechanical Moisture Induced Damage in Asphaltic Mixes*. Ph.D. Dissertation, Delft University, The Netherlands.

Lemaitre, J., 1992, *A Short Course in Damage Mechanics*. Springer-Verlag, New York.

Voyiadjis, G.Z. and P. I. Kattan, 1999, *Advances in Damage Mechanics: Metals and Metals Matrix Composites*. Elsevier, Oxford.



## **PROGRAM AREA: FATIGUE**

### **CATEGORY F1: MATERIAL AND MIXTURE PROPERTIES**

#### **Work Element F1a: Cohesive and Adhesive Properties**

##### ***Subtask F1a-1: Critical Review of Measurement and Application of Cohesive and Adhesive Bond Strengths (TAMU)***

###### Work Done This Quarter

The work on improving the white paper relating the ideal work of fracture to the practical work of fracture was continued. This involved a continued review of the pertinent literature and a discussion of specific experts at Imperial College and the University of Nottingham. Two of the ARC graduate students (Ms. Silvia Caro and Mr. Jonathan Howson) spent one month at the University of Nottingham and Imperial College to collaborate on various aspects of this work element.

###### Significant Results

None.

###### Significant Problems, Issues and Potential Impact on Progress

None.

###### Work Planned Next Quarter

Improvements to this white paper will be made continually based on literature review. In addition, researchers are in the process of validating the findings from this paper based on testing of selected bituminous and aggregate materials and by accomplishing the various other subtasks in this work element.

##### ***Subtask F1a-2: Develop Experiment Design (TAMU)***

###### Work Done This Quarter

The experiment design was completed and reported in the last quarterly report.

###### Significant Results

None.

Significant Problems, Issues and Potential Impact on Progress

None.

Work Planned Next Quarter

At this time, researchers do not anticipate any changes to this experiment design. However, as the work progresses in this subtask and in the area of modeling, some refinement to the proposed experiment design may be required in the future.

***Subtask F1a-3: Thermodynamic Work of Cohesion and Adhesion (Year 1 start)***

Work Done This Quarter

The objective of this subtask is to provide the surface free energy of asphalt binders that will be used in other subtasks as a material property input or for the comparison with results from other test methods. Based on the requirements from other tasks, tests under this subtask will continue through the remainder of this project.

Significant Results

None.

Significant Problems, Issues and Potential Impact on Progress

None.

Work Planned Next Quarter

Based on the requirements from other tasks, tests under this subtask will continued through the remainder of this project.

***Subtask F1a-4: Mechanical Work of Adhesion and Cohesion***

Work Done This Quarter

The test protocols to evaluate the mechanical work of adhesion and cohesion were further developed during this quarter. Some of the problems that were encountered and overcome while developing the test protocol are discussed in the following sub section.

Significant Results

None.

## Significant Problems, Issues and Potential Impact on Progress

The initial tests on measuring the tensile strength of thin films in the transverse mode were conducted using a 5kN universal testing machine with conventional Linear Variable Deflection Transducers (LVDTs). However, these LVDTs were mounted to the loading frame. Consequently, the measured deformation was the sum of the deformation due to the loading frame and the deformation of the specimen. The deformation of thin films (about 100 microns) at the time of failure is of the order of just a few microns, which is significantly large compared to the deformation within the loading frame itself. Therefore, the deformation recorded using these LVDTs had a very large bias and resulted in unrealistic stress-strain relationships. To rectify this situation, researchers changed to the use of laser or optical LVDTs that used specimen end plates as a datum or reference point. However, due to the specimen end plate geometry, the laser LVDTs amplified even the slightest distortion in the specimen geometry resulting in unrealistic strain measurements. Finally, a high-resolution camera was successfully used to record and measure the strain in the thin film during loading and failure. The final test protocol is now close to be finalized. Examples of horizontal displacement and shear strain fields in an asphalt binder are shown in figure F1a.1.

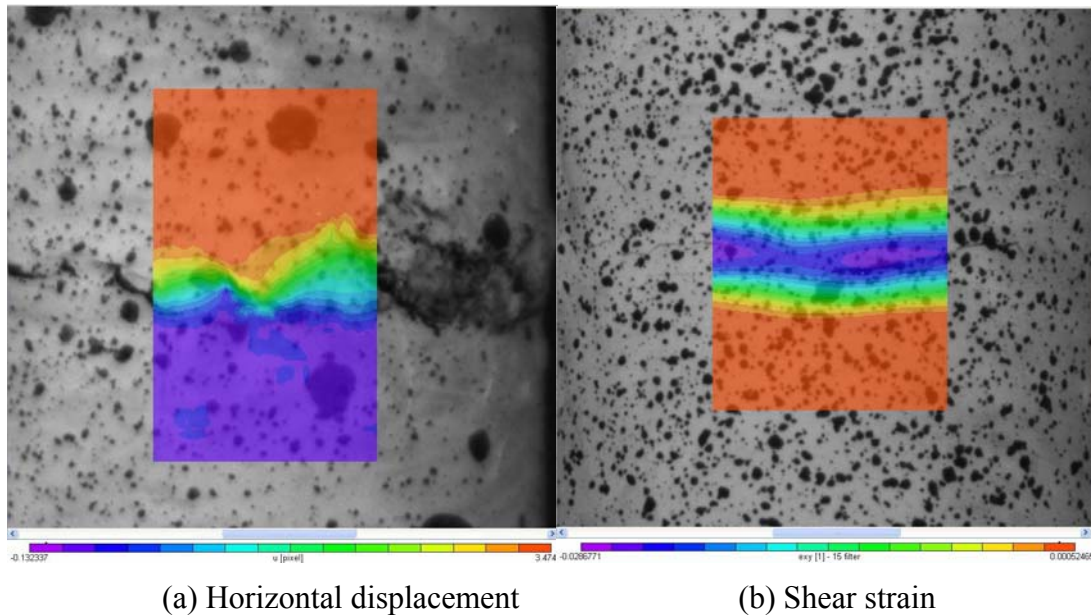


Figure F1a.1. Examples of (a) horizontal displacement and (b) shear strain in an asphalt binder specimen in the pull-off test.

## Work Planned Next Quarter

Researchers will begin executing the tests as per the experiment design developed in Subtask F1a-4 and reported in the previous quarterly report.

### ***Subtask F1a-5: Evaluate Acid-Base Scale for Surface Energy Calculations***

#### Work Done This Quarter

No activity was planned for this quarter.

#### Significant Results

None.

#### Significant Problems, Issues and Potential Impact on Progress

None.

#### Work Planned Next Quarter

Work on this subtask is planned in year 4 of this project.

### **Work Element F1b: Viscoelastic Properties (Year 1 start)**

#### ***Subtask F1b-1: Separation of Nonlinear Viscoelastic Deformation from Fracture Energy under Cyclic Loading (TAMU)***

#### Work Done This Quarter

The main objective of this task was to develop an approach to determine three main aspects of material response during cyclic loading:

- i) identify the limiting stress or strain amplitude that results in a nonlinear viscoelastic response without causing damage,
- ii) model and monitor the change in the nonlinear viscoelastic parameters with increasing number of load cycles, and
- iii) model and monitor the change in the nonlinear viscoelastic parameters within each cycle.

Researchers have made significant progress in achieving the first two steps. A test protocol was developed to evaluate the fatigue cracking characteristics of sand-asphalt mixtures or Fine Aggregate Matrix (FAM) using the Dynamic Mechanical Analyzer (DMA). Data from DMA testing were analyzed to quantify the amount of fatigue damage using the dissipated energy approach (crack growth index) and the non-linear viscoelastic modeling approach. Results from both approaches were consistent.

#### Significant Results

Preliminary results from the test and data analysis protocols that were developed support the following conclusion. When FAM specimens are tested within a certain range of stress

amplitude or strain amplitude, the results from the controlled stress mode of loading are equivalent to the results from the controlled strain mode of loading. The following criterion should be satisfied in order for the controlled-stress and controlled strain results to rank mixtures in the same order:

$$(0.75 \times stress)_{stress\ con} \leq \left( \frac{stress\ @\ N_f + stress\ @\ N=1}{2} \right)_{strain\ con} \leq (1.25 \times stress)_{stress\ con}$$

An example of the comparison of controlled strain to controlled stress results is shown in figure F1b.1. The details of the findings from this study will be documented in the forthcoming detailed technical report and journal paper.

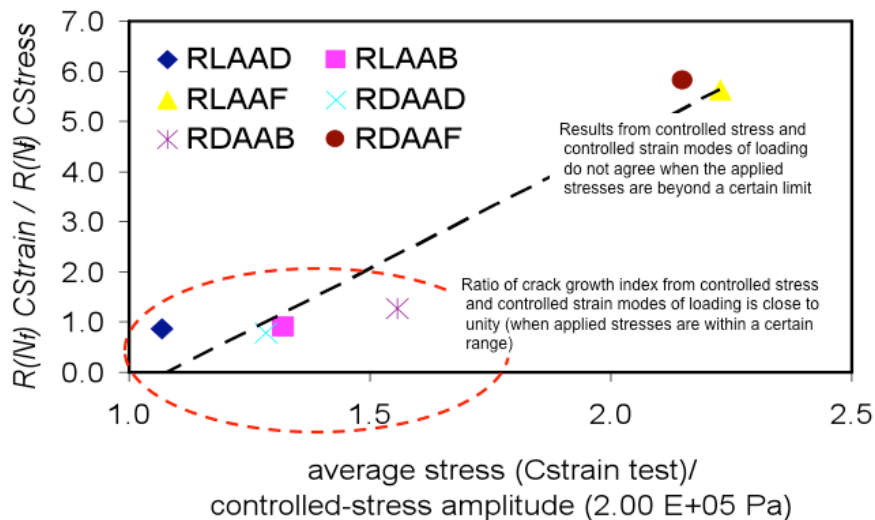


Figure F1b.1. Illustration of the uniformity of results from controlled stress and controlled strain modes of loading within a certain stress range.

### Significant Problems, Issues and Potential Impact on Progress

None.

### Work Planned Next Quarter

The draft technical report is under review (final edit) and will be produced as a deliverable to FHWA during the next quarter (reporting period). An appendix to this report will be a protocol for DMA testing and full data analysis using the crack growth index (CGI) approach. This protocol has been prepared in AASHTO Standard format. The DMA testing procedure and associated analysis were presented by the ARC members to the mixture expert task group that was held in Reno, Nevada on September 2008. The presentation is provided in Appendix C.

The researchers will begin work on the last component of this work element, i.e., developing a model to represent the differences in phase angle during each load cycle and validating it. In the next quarter, researchers will provide a detailed experiment design that will be used to accomplish this objective.

***Subtask F1b-2: Separation of Nonlinear Viscoelastic Deformation from Fracture Energy under Repeated and Monotonic Loading***

Work Done This Quarter

The analysis method presented in Subtask F1b-1 is being extended to the analysis of asphalt mixtures subjected to relaxation tests followed by repeated loads.

Significant Results

None.

Significant Problems, Issues and Potential Impact on Progress

None.

Work Planned Next Quarter

The results of this work are being prepared in the form of a research report, similar to the DMA report, to be delivered to FHWA. A journal technical paper will be prepared.

**Work Element F1c: Aging**

***Subtask F1c-1: Critical Review of Binder Oxidative Aging and Its Impact on Mixtures (TAMU)***

Work Done This Quarter

*Review of Kinetics of Binder Oxidation*

A study of binder oxidation at elevated constant air pressure and of binder oxidation in solution at different asphalt concentrations suggests that three generic processes are involved in binder oxidation (Herrington 1998). Two processes (sulfoxide and “slow” carbonyl formation) are first order reactions with respect to sulfide and asphalt concentration in solution. The third process (“fast” carbonyl formation) may not be first order but does give rise to an exponential decrease in the rate of product formation.

In Herrington’s work, two binders (of seven neat binders studied) were aged at 300 psi constant air pressure (equivalent to 4 atm oxygen pressure) and at three elevated temperatures 60, 70,



80°C. Viscosities were measured in glass capillary viscometers at 60°C. The log viscosity increase with aging time fits the following equation:

$$P = P_{f\infty} \cdot (1 - e^{-k_f \cdot t}) + k_s \cdot t$$

Where P is log viscosity as a function of oxidation time,  $P_{f\infty}$  is the final log viscosity value due to first order “fast” reaction,  $k_f$  and  $k_s$  are reaction constants. A set of these three parameters was obtained from non-linear regression, for each test temperature. Note this equation for asphalt oxidation is essentially the same as the one for tar oil oxidation proposed by Dickinson and Nicholas (1949) except that it is in terms of log viscosity instead of oxygen uptake.

The change of peak areas of sulfoxide and carbonyl group also were measured. While sulfoxide formation obeys first order kinetics, carbonyl formation consists of a fast-rate increase and a constant-rate increase, as presented in the literature review in the last quarterly report. To understand carbonyl formation more completely, the researchers studied binder oxidation in solutions (with an inert solvent) of different asphalt concentrations. It was found that the “slow” (constant-rate) reaction is first order with respect to asphalt concentration, while data for “fast” reaction shows great variation, and thus does not lead to a clear conclusion.

Nonetheless, due to the abundance of asphalt binder in mixtures and because of the observed behavior of viscosity change, it is more likely that the constant-rate reaction is a pseudo-zero order, while the fast-rate reaction is first order.

### Significant Results

Literature reports provide important insight into binder oxidation kinetics during both the fast-rate and constant-rate period binder kinetics and in both neat films and pavements. More data are needed, to understand specific binder kinetics and to provide a better understanding of hardening in pavements and as a function of climate and mixture parameters.

### Significant Problems, Issues and Potential Impact on Progress

There are no problems or issues.

### Work Planned Next Quarter

Review previous work. This is an on-going effort. A white paper of pavement temperature modeling is being prepared.

### Cited References

Herrington, P. R., 1998, Oxidation of Bitumen in the Presence of a Constant Concentration of Oxygen. *Petroleum Science and Technology*, 16 (9&10): 1061-1084.

Dickinson E. J., and J. H. Nicholas, 1949, The Reaction of Oxygen with Tar Oils, Road Research Technical Paper, No. 16.

***Subtask F1c-2: Develop Experimental Design (TAMU)***

Work Done This Quarter

In this quarter, work on the experimental design for both a pilot experiment and an expanded experiment focused on mixture testing and analysis described further in Work Element F2c. These experiments are aimed at achieving the following three objectives associated with this Work Element F1c:

- (1) Determine fundamental mixture parameters that control the decline of mixture fatigue resistance with aging (Subtask F1c-4 including polymer modified asphalt materials in Subtask F1c-5)
- (2) Develop enhanced mixture testing protocol (Work Element F2c)
- (3) Validate transport model of binder oxidation (Subtask F1c-3 including polymer modified asphalt materials in Subtask F1c-5)

For both the pilot experiment and the expanded experiment, the following elements are included:

- Materials
- Specimens (lab-mixed, lab –computed (LMLC), Field Cores)
- Aging Protocol
- Laboratory Testing Protocols and Measured Properties
- Analysis Methods

Changes to both experiments since the last quarterly report include the following:

- The LMLC specimens (6 inch in diameter and more than 7 inch in height) are fabricated using the Superpave Gyratory Compactor (SGC) and then cored and cut to 4 inch in diameter by 4 inch in height. The specimens are now cut from both top and bottom to facilitate a more uniform AV distribution and thus more uniform failure in the middle of the specimen height.
- A newly developed viscoelastic characterization (VEC) test replaces the resilient modulus test. This VEC test is now conducted at 10, 20, and 30°C in tension only to allow for determination of Poisson’s ratio, complex modulus, phase angle, and master curves as a function of frequency for each of these parameters.
- The revised repeated-load direct tensile (RDT) test at 20°C includes multiple 1000 cycle loading periods after different rest or healing periods of 1000, 500, 250, 120, 60, 30, 15, 8, and 4 seconds.

Also in this quarter, a draft report was prepared for FHWA that details the five elements listed above for both the pilot and expanded experiments. This report is now being formatted for submittal to FHWA.

### Significant Results

The pilot experiment design was completed, and specimen fabrication (Subtask F1c-4) continued. All component binder and aggregate materials are being stored in the TTI McNew Laboratory. Approximately 50% of the 96 LMLC specimens are now fabricated, and all of the aged specimens are now in the 60°C environmental room.

### Significant Problems, Issues and Potential Impact on Progress

Input from the entire ARC team with approval from FHWA is needed for verification testing and for selecting asphalt binder materials and field validation sections. The component materials are needed to fabricate LMLC specimens that will be aged in the 60°C environmental room for up to a year prior to material characterization and evaluation of mixture fatigue resistance. Cores from field validation sections must be collected on multiple dates to assess the effect of aging on mixture fatigue resistance.

### Work Planned Next Quarter

With input from the entire ARC team and approval from FHWA core asphalt binder materials and the field validation sections will be selected and the expanded experimental design will be finalized. In the next quarter, the draft report on the experimental design for this Work Element F1c will be submitted to FHWA. This report, currently being formatted for FHWA, includes details on the pilot experiment and enhanced CMSE\* testing and analysis protocols and as much detail as possible on the expanded experiment.

### ***Subtask F1c-3: Develop a Transport Model of Binder Oxidation in Pavements (TAMU)***

#### Work Done This Quarter

The asphalt binder oxidation model can be used to predict asphalt binder properties in the pavement over a defined period of time. However, computationally, it previously was implemented only for a constant pavement temperature condition, which was inadequate for using as a tool to understand asphalt binder oxidation in pavements under actual weather conditions.

In order to calculate asphalt binder properties under actual pavement temperatures, the pavement temperature prediction model developed over previous reporting periods and which showed significant improvements over several models reported in the literature, has been computationally coupled with the asphalt binder oxidation model. As a result, the aged properties of an asphalt binder can be calculated over time using pavement conditions – actual air void distributions in pavements and actual pavement temperature profiles. In addition, the simulation of oxidation effects on pavements in various climatic regions can be achieved because

the temperature prediction model is capable of calculating pavement temperature in numerous areas due to availability of weather data input. Pavement oxidation simulations of various climatic locations will be studied in detail during the next quarter.

#### Significant Results

Significant progress in modeling binder oxidation in pavements has been made. This progress includes work on both temperature modeling and oxygen transport modeling. This modeling effort provides the basis for planning both laboratory and field experiments.

#### Significant Problems, Issues and Potential Impact on Progress

The principal issue with the transport model that remains is the question of how accurately the cylindrical continuum transport model is able to represent actual pavement oxidation. If the model captures the essential elements, then it will be able to provide very valuable insight for pavement performance prediction.

The modeling work within this subtask and the significant results outlined in the previous section are excellent candidates for presentation at the next Models and Fundamental Properties Expert Task Group meeting.

#### Work Planned Next Quarter

The results obtained on pavement oxidation with temperature profile predicted from the model will be compared to actual pavement oxidation data acquired from the field. Several important model parameters, such as diffusivity and asphalt binder film thickness, will be estimated to improve the accuracy of the pavement oxidation model.

Pavement oxidation simulations of several climate regions throughout the country will be conducted to investigate the effect of asphalt binder oxidation under those specified weather conditions.

#### ***Subtask F1c-4: The Effects of Binder Aging on Mixture Viscoelastic, Fracture, and Permanent Deformation Properties (TAMU)***

#### Work Done This Quarter

During this quarter, specimen fabrication for the pilot experiment (Subtask F1c-2) continued. Approximately 50% of the 96 LMLC specimens are now fabricated, and all of the aged specimens are now in the 60°C environmental room.

#### Significant Results

None to report at this time.

### Significant Problems, Issues and Potential Impact on Progress

Due to problems with the MTS equipment used for direct tension testing discovered in the last quarter and corresponding data measurement equipment upgrades, data acquired using “dummy” specimens were carefully checked prior to continuation of the development of the enhanced CMSE\* mixture testing protocol (Work Element F2c).

In addition, TTI Administration approved the request submitted by ARC researchers to: (1) upgrade the existing TTI MTS system and (2) purchase a second MTS system for mixture testing. These purchase requests are now in the appropriate office at Texas A&M University.

### Work Planned Next Quarter

Next quarter, specimen fabrication for the pilot experiment (Subtask F1c-2) will be completed. With input from the entire ARC team and approval from FHWA with respect to the core asphalt binder materials and the field validation sections, material procurement and specimen fabrication will commence for the expanded experiment.

Mixture testing utilizing the enhanced CMSE\* testing protocol (Work Element F2c) will also commence for the pilot experiment specimens. At the end of the protocol measurements of extracted binder properties will also commence. Specifically, air void (AV) characterization (total and water accessible) through determination of specific gravities and X-ray CT and image analysis will commence.

### ***Subtask F1c-5: Polymer Modified Asphalt Materials (TAMU)***

#### Work Done This Quarter

No activity this quarter.

#### Significant Results

No activity.

#### Significant Problems, Issues and Potential Impact on Progress

No activity.

#### Work Planned Next Quarter

No work planned.

## **Work Element F1d: Healing**

### ***Subtask F1d-1: Critically Review Previous Work on Healing under FHWA Contracts DTFH61-C-92-00170 and DTFH61-C-99-00022 (TAMU)***

#### Work Done This Quarter

The literature review was continued in this quarter.

#### Significant Results

None.

#### Significant Problems, Issues and Potential Impact on Progress

None.

#### Work Planned Next Quarter

This is an ongoing subtask that will be continued through this project.

### ***Subtask F1d-2: Select Materials with Targeted Properties (TAMU)***

#### Work Done This Quarter

In the previous quarter the relationship between molecular morphology and surface free energy and molecular morphology and self-diffusivity of molecules were evaluated. In the case of the latter molecular morphology was quantified as the methylene to methyl hydrocarbon ratio (MMHC). Molecular modeling techniques were used to establish these relationships. Both, surface free energy and self-diffusivity are related to the self-healing properties of asphalt binder. Researchers are documenting these findings in the form of both a journal and conference paper. The abstract of the conference paper was accepted for presentation at an international pavement conference in Italy on 2009. The journal paper is under progress and will be submitted to ASCE journal of materials in the next few weeks. A second journal paper was submitted to the Transportation Research Board and is under review for publication in the TRB Journal.

Molecular modeling techniques are useful in validating hypotheses of material behavior and in conducting virtual parametric analyses of the effects of molecular variables on material behavior. However, these hypotheses must be eventually put into practice to measure material properties and select materials with a variety of different healing characteristics. To this end, researchers have documented the intrinsic healing properties of six different asphalt binders using the DSR (see subtask F1d-4). The next step is to determine the molecular morphological characteristics such as MMHC ratio for these binders using an FTIR.

### Significant Results

Although this work is still in progress, we feel it is significant that our hypotheses, derived from the literature and our own experimental work, are being validated by this molecular modeling. The modeling is also providing extremely valuable insight into our work.

### Significant Problems, Issues and Potential Impact on Progress

None.

### Work Planned Next Quarter

In the next quarter we will complete and submit the journal paper that compares the morphological properties of bitumen molecules to its self-diffusivity using molecular modeling techniques. We will also determine the morphological properties such as MMHC ratio for the six asphalt binders using the FTIR and compare these properties to the long term intrinsic healing characteristics of the asphalt binders measured using the DSR.

### ***Subtask F1d-3: Develop Experiment Design (TAMU)***

#### Work Done This Quarter

No activity this quarter.

#### Significant Results

None.

#### Significant Problems, Issues and Potential Impact on Progress

None.

#### Work Planned Next Quarter

A detailed experiment design to validate the healing model and properties will be developed based on the significant progress we have made in subtasks F1d-2 and F1d-4. The information from these subtasks is necessary in order to develop an efficient experimental design. We anticipate that the experiment design will be developed in the last quarter of this project year or early in the next project year (late spring).

***Subtask F1d-4&5: Investigate Test Methods to Determine Material Properties Relevant to Asphalt Binder Healing (TAMU)***

Work Done This Quarter

One of the material properties related to the self-healing in asphalt binders is the self-diffusivity of bitumen molecules. Molecular modeling work from subtask F1d-2 demonstrates that MMHC ratio can be related to the self-diffusivity and consequently to the long term healing rate of asphalt binders. Researchers have completed some preliminary work to determine the MMHC ratio for the selected asphalt binders.

Significant Results

None.

Significant Problems, Issues and Potential Impact on Progress

None.

Work Planned Next Quarter

Complete measuring the MMC ratio for the same set of five asphalt binders that were used with the DSR to determine the intrinsic healing function. Complete molecular modeling of self-diffusivity as it relates to MMHC and compare with the empirical results from Subtasks F1d-2 and F1d-3.

***Subtask F1d-5: Testing of Materials for model validation\* (TAMU)***

Work Accomplished This Quarter

No activity planned.

Significant Results

None.

Significant Problems, Issues and Potential Impact on Progress

None.

Work Planned Next Quarter

Work in this subtask is planned after completion of Subtask F1d-3.

\*Note: Title of the subtask was changed to clarify that the testing in this subtask is not to obtain material properties but to validate the model. The former is accomplished in subtask F1d.4.



### ***Subtask F1d-6: Evaluate Relationship Between Healing and Endurance Limit of Asphalt Binders (UWM)***

#### Work Done This Quarter

Work is currently being done to evaluate a new proposed test procedure based on both Texas A&M University's (TAMU's) incremental damage amplitude threshold (see ARC Q3 2007 report) and University of Illinois at Urbana–Champaign's "plateau value" concept (Carpenter and Shen 2006) using haversine load pulses spaced at varying intervals. The concept is as follows:

- First, identify the threshold stress amplitude where consecutive load cycles at constant stress lead to an increasing strain response. This concept is consistent with what TAMU has been exploring on fine aggregate matrix (FAM) specimens. For binder specimens, a stress sweep is being conducted as a series of time sweep steps. Each step consists of 20 cycles at 1 Hz with one data point collected every 2 cycles. The stress amplitude is held constant within each step and then increased after each additional step. The strain response is measured for each step; constant strain readings within each step indicate that there is no incremental damage occurring between load cycles of constant amplitude, but an increasing strain response at constant stress amplitude indicates the opposite effect. The stress amplitude at which this occurs is the incremental damage threshold stress value, which will be used in an upcoming test to evaluate healing.
- Second, apply a series of 1 Hz cycles at the incremental damage threshold stress amplitude at varying intervals. This largely follows the concept introduced by Carpenter and Shen (2006). To begin, apply a single load cycle at 1 Hz using a stress amplitude already known to cause damage to a binder specimen and measure the strain response (or  $|G^*|$ ). Let the material rest for a given amount of time (5 minutes, for example), and then apply another load cycle. The next rest period should be shorter (4 minutes in the continued example). This continues as the subsequent rest periods get progressively shorter until the material is unable to recover the damage from the previous load cycle. This will give an idea of the relation between healing rate versus a constant amount of damage. This loading scheme can be thought to mimic traffic loading, and the strain at which incremental damage occurs can be thought of as the critical strain in the pavement and used for pavement design.

This concept is illustrated in figure F1d-6.1.

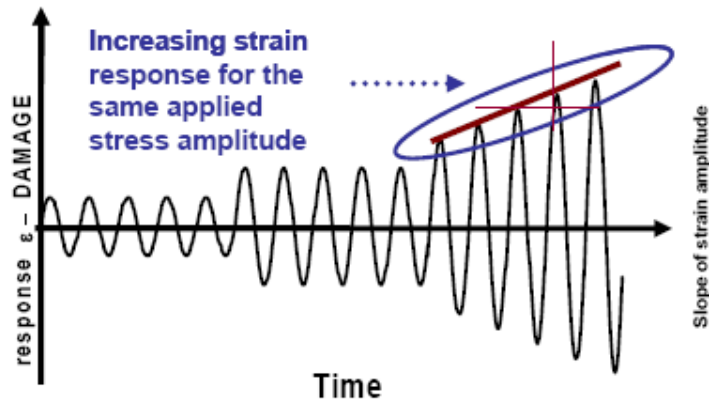


Figure F1d-6.1. Graph. TAMU concept for incremental damage threshold.

### Significant Results

A preliminary set of data was generated using one base binder (a PG 64-22) and two polymer modifiers – linear styrene-butadiene-styrene (LSBS) and ethylene terpolymer. The stress sweep was first performed in order to determine the incremental damage threshold stress amplitude, as described above and illustrated in figure F1d-6.2. For preliminary analysis purposes, the stress amplitude that yielded greater than a 20% reduction in  $|G^*|$  after 20 cycles was deemed the incremental damage threshold value.

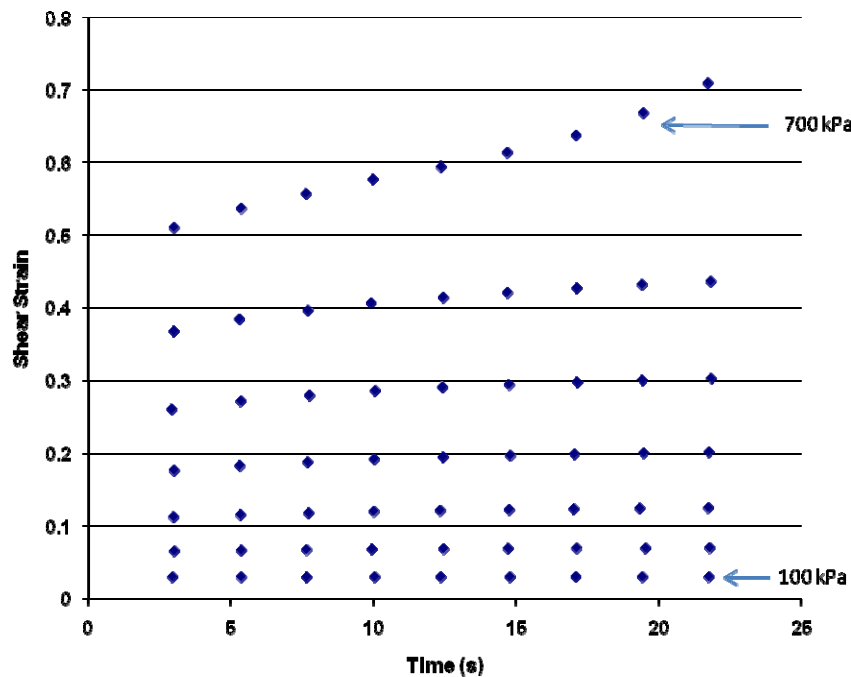


Figure F1d-6.2. Graph. Typical results from stress sweep testing at 25 °C, 1 Hz.

After determining the appropriate stress amplitude, a series of 1 Hz load cycles was applied at systematically decreasing interval lengths, as illustrated in figure F1d-6.3. The first load cycle was applied, and then the specimen was allowed to rest for 300 seconds. Another load cycle was then applied, and the specimen was allowed to rest for 240 seconds. This cycle was then repeated for rest intervals of 180, 120, 60, 45, 30, 15, 10 and 5 seconds. For this data set, specimens failed after the 30-second rest period and subsequent load application.

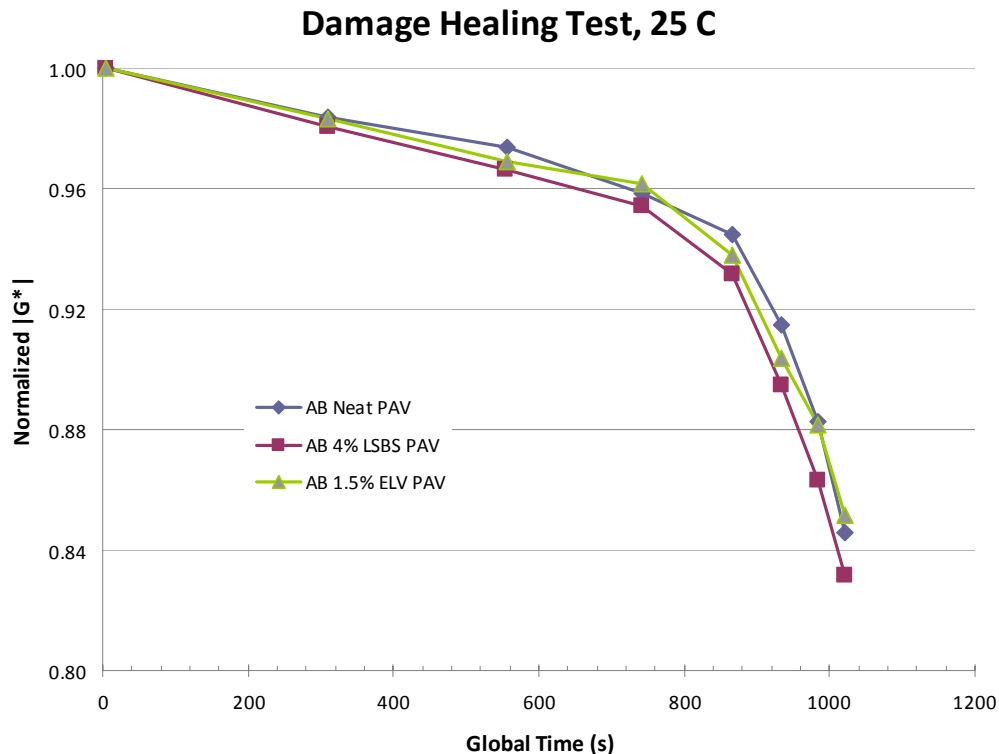


Figure F1d-6.3. Graph. Results from the proposed damage-healing test.

The proposed analysis method is as follows:

- From the stress sweep test, calculate the rate of damage per cycle. This can be done by noting the decrease in  $|G^*|$  per cycle or by the increase in dissipated energy ( $W_i$ ) per cycle.
- From the results of the damage-healing test, either  $|G^*|$  or  $W_i$  can be measured for each load application. From one load application to the next, there should be a predicted amount of damage induced in the specimen, as calculated from the stress sweep test. However, the intervals in between load applications allow for healing to take place. By comparing the measured  $|G^*|$  or  $W_i$  at a given cycle to what is predicted from the rate of damage per cycle, the healing rate per rest interval can be calculated.

### Significant Problems, Issues and Potential Impact on Progress

None.

### Work Planned Next Quarter

Refinement of the testing and analysis methods will continue. Work will also be done to verify whether results of this test procedure can fit within the framework proposed by TAMU (Bhasin et al. 2008).

### Cited References

Bhasin, A., D. N. Little, R. Bommavaram, and K. L. Vasconcelos, 2008, A framework to quantify the effect of healing in bituminous materials using material properties. *Road Materials and Pavement Design*, 219-242.

Carpenter, S. H., and S. Shen, 2006, Dissipated energy approach to study hot-mix asphalt healing in fatigue. *Transportation Research Record*, no. 1970, 178-185.

### ***Subtask F1d-7: Coordinate with Atomic Force Microscopic (AFM) Analysis (WRI)***

#### Work Done This Quarter

The detailed work plan, submitted as part of the Year 2 Work Plan, was approved during the past quarter.

#### Significant Results

None.

### Significant Problems, Issues and Potential Impact on Progress

None.

### Work Planned Next Quarter

No work in this subtask will be conducted in the next quarter.

### ***Subtask F1d-8: Coordinate Form of Healing Parameter with Micromechanics and Continuum Damage Models (TAMU)***

#### Work Done This Quarter

Work has been accomplished with respect to the nature of healing as reported under work elements F1d and F2c. The results of these mixture healing responses will be used as an

empirical basis for further development of the healing model (or parameter to be used in a micromechanical and/or continuum damage model.

#### Significant Results

None.

#### Significant Problems, Issues and Potential Impact on Progress

None.

#### Work Planned Next Quarter

Work on this subtask is scheduled for the later years of this research.

#### ***Subtask F1d-9: Design Experiment on Selected Binders with Synchrotron (TAMU)***

#### Work Done This Quarter

No activity this quarter.

#### Significant Results

None.

#### Significant Problems, Issues and Potential Impact on Progress

None.

#### Work Planned Next Quarter

No work planned.

### **CATEGORY F2: TEST METHOD DEVELOPMENT**

#### **Work Element F2a: Binder Tests and Effect of Composition (UWM)**

#### Work Done This Quarter

During this quarter, the binders selected for this study were tested before and after modification with two polymers. The chosen base binders were:

- FH, a PG 64-22 neat binder with a high content of asphaltenes (16.25% as determined per ASTM D4124-01).

- CRM, a PG 58-28 neat binder with a low content of asphaltenes (9.06% as determined per ASTM D4124-01).

The binders were tested according to the Multiple Stress Creep and Recovery (MSCR) procedure in their un-aged condition and in the rolling thin film oven (RTFO)-aged condition. Aging of the binders was completed, and fatigue test data were collected and analyzed, following the proposed work plan approved for Year 2. The fatigue testing included the stress sweep protocol and the monotonic Binder Yield Energy Test (BYET).

A presentation on the effects of polyphosphoric acid (PPA) on the rheology of base binders after various storage temperatures was submitted and accepted for the Petersen Asphalt Research Conference in Laramie, Wyoming, July 16, 2008. The study also covered the effects of surface area-to-volume ratio.

### Significant Results

Table F2a.1 presents the results obtained during stress sweep testing of the CRM and FH base binders. Stress at failure is defined as the stress value at 50% reduction in initial G\*. All testing was done at the intermediate temperature of the grade of the base asphalt.

Table F2a.1. Stress sweep testing results.

<b>Stress at failure, kPa</b>					
	Run 1	Run 2	Average	Standard deviation	Coefficient of variation
CRM	645	652	648.5	4.9	0.76
CRM+0.7 ELV	636	645	640.5	6.4	0.99
CRM+2LSBS	676	682	679	4.2	0.62
FH	942	946	944	2.8	0.30
FH+0.7 ELV	1060	N/A	1060	N/A	N/A
FH+2LSBS	1140	1090	1115	35.4	3.17

For the CRM base binder, the value for stress at failure was not affected significantly by the type of polymer modification. A similar trend was also observed for the FH binder. It is noted that for the FH material, the value of the stress at failure is much higher than for the CRM material. This trend is also evident in the graphs shown in figures F2a.1 and F2a.2.

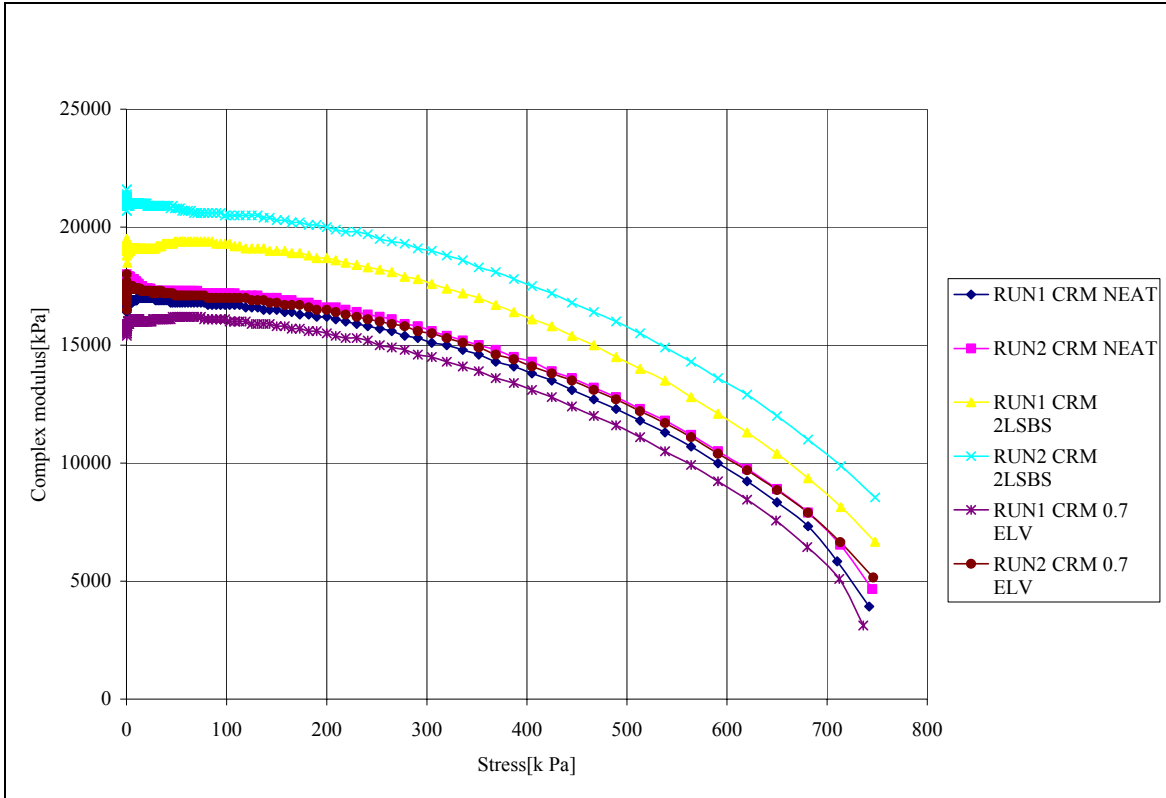


Figure F2a.1. Graph. Complex modulus versus stress for CRM base binder.

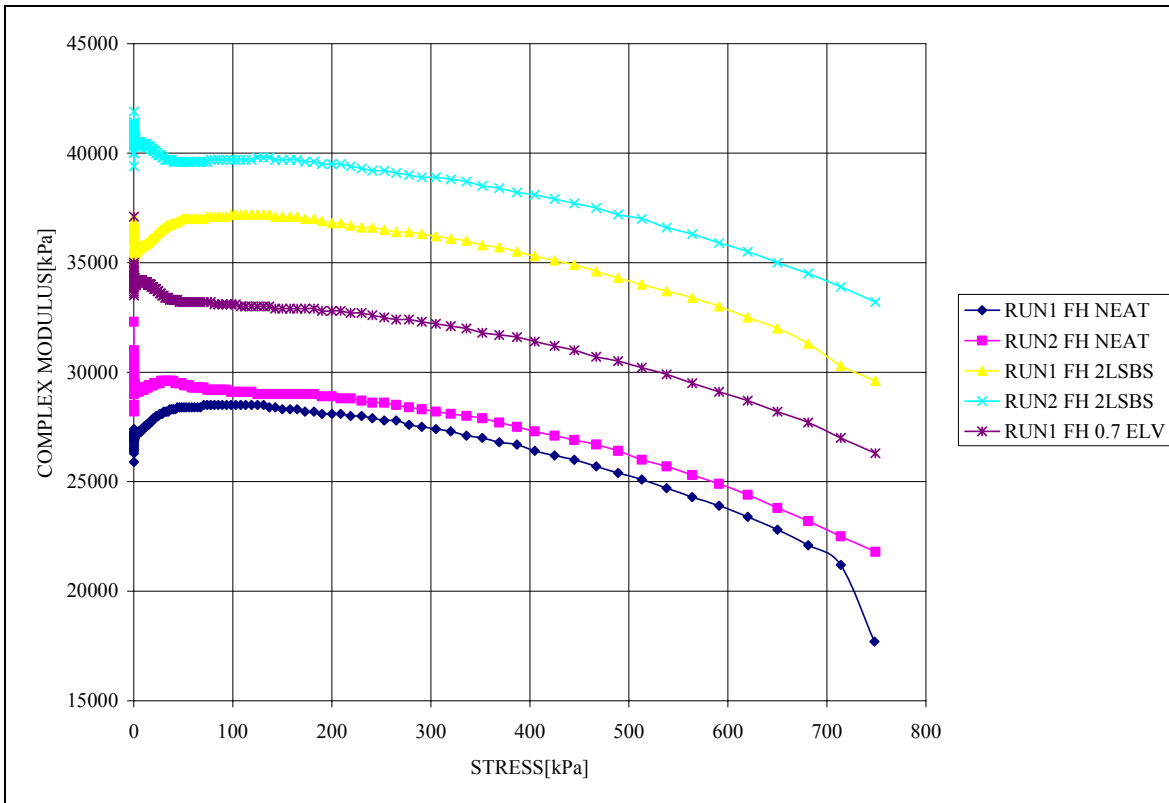


Figure F2a.2. Graph. Complex modulus versus stress for FH base binder.

Tests were also performed for CRM modified with 4% wt linear styrene-butadiene-styrene (LSBS) copolymer (CRM+2LSBS), CRM modified with 1.5% wt Elvaloy terpolymer (CRM+1.5ELV), FH modified with 4% wt LSBS copolymer (FH+4LSBS) and FH modified with 1.5% wt Elvaloy terpolymer (FH+1.5ELV). Data analysis was not completed at the time this report was submitted.

Figures F2a.3 through F2a.6 show the results obtained during MSCR tests. The parameter Jnr represents nonrecoverable compliance.



Figure F2a.3. Graph. MSCR results for FH un-aged base binder.

Figure F2a.3 shows that at 100 Pa, the Elvaloy-modified FH binder recovers more than the LSBS-modified binder. The opposite is true at 3200 Pa.

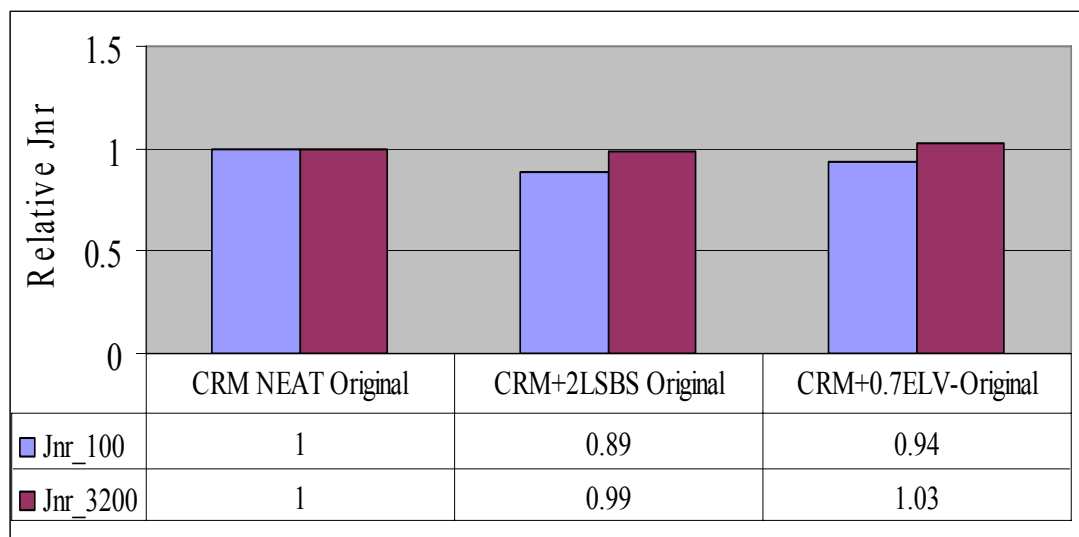


Figure F2a.4. Graph. MSCR results for CRM un-aged base binder.



Figure F2a.4 shows that for the CRM binder at 100 Pa, the Elvaloy-modified material recovers more than the LSBS-modified material. At 3200 Pa, the recovery of the polymer-modified materials is similar to that of the unmodified material.

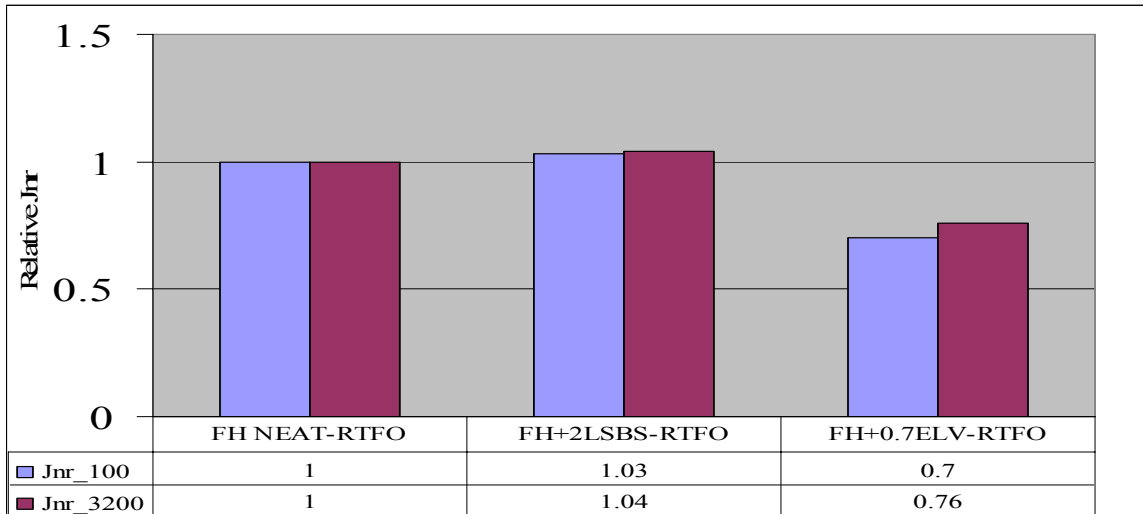


Figure F2a.5. Graph. MSCR results for the RTFO-aged FH base binder.

Figure F2a.5 shows the results for the RTFO-aged FH binder. For the LSBS-modified material at 100 Pa and 3200 Pa, a significant change in recovery was not observed. The Elvaloy-modified binder recovered more at 100 Pa than at 3200 Pa.

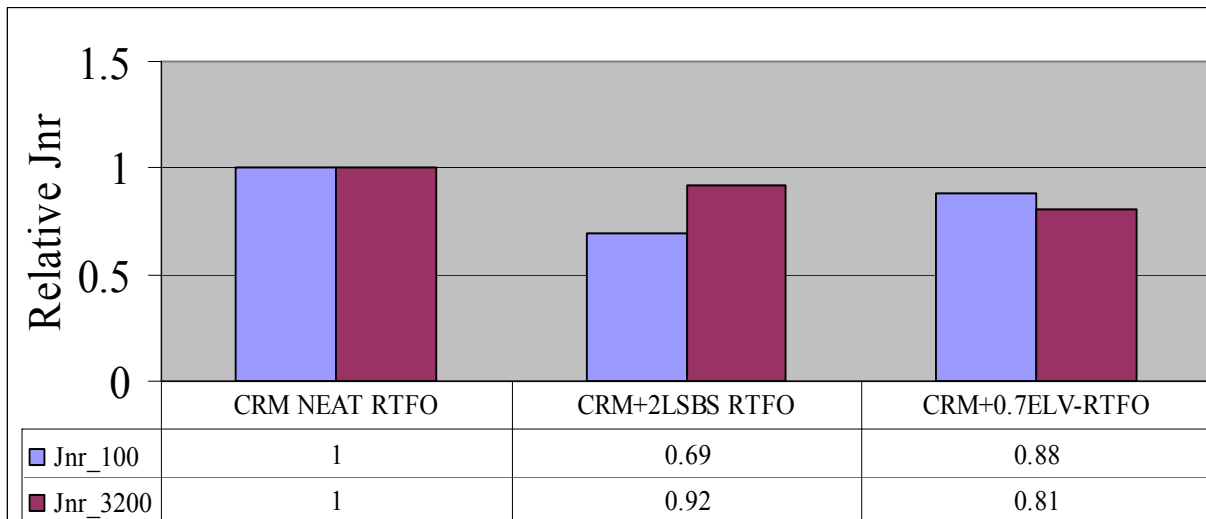


Figure F2a.6. Graph. MSCR results for RTFO-aged CRM base binder.

As shown in figure F2a.6, the RFTO-aged LSBS-modified binder recovered more than the Elvaloy-modified binder at 100 Pa. At 3200 Pa, the opposite was true.

Tests were also performed on CRM binder modified with 4% wt LSBS, CRM binder modified with 1.5% wt Elvaloy, FH binder modified with 4% wt LSBS and FH binder modified with 4% wt Elvaloy, but the data were not yet analyzed at the time this report was submitted.

As part of the fatigue testing program, the selected materials were subjected to monotonic stress testing: the Binder Yield Energy Test (BYET). Results of testing on the pressure aging vessel (PAV)-aged binders are shown in figures F2a.7 and F2a.8.

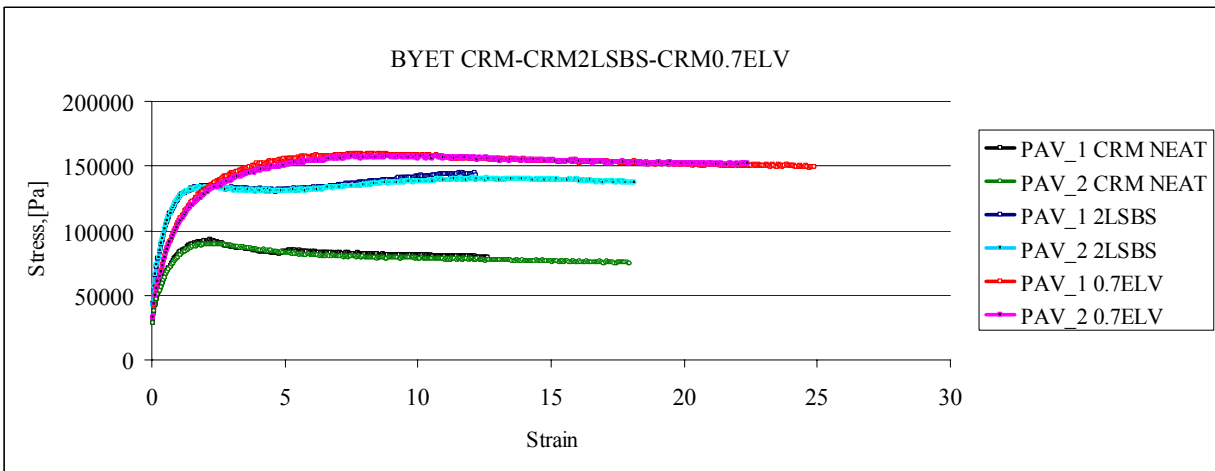


Figure F2a.7. Graph. BYET results for the CRM base binder.

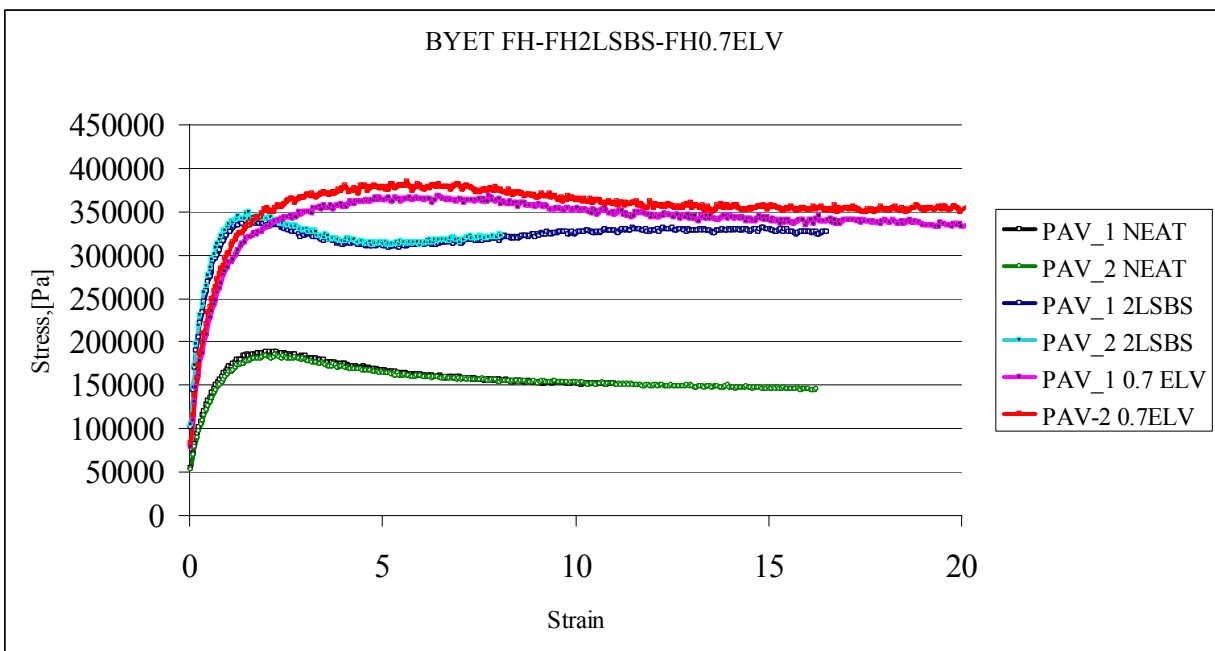


Figure F2a.8. Graph. BYET results for the FH base binder.

The above graphs show the same trend for the BYET energy for both base binders. It is clear that the presence of polymer modifiers stiffens the binders and increases the yield energy very significantly. The graphs also show that the Elvaloy-modified binders have a higher strain tolerance than the LSBS-modified ones. This is indicated by the peak stress occurring at a higher strain value for the Elvaloy-modified materials than for the LSBS-modified materials.

Yield energy to peak stress and strain at maximum stress for both base binders are shown in tables F2a.2 and F2a.3. It was generally observed that strains at maximum stress are higher for CRM base binders than FH base binders.

Table F2a.2. Yield energy and strain at maximum stress for CRM base binder.

Yield Energy (kPa)					
	Run 1	Run 2	Average	Standard deviation	Coefficient of variation (%)
CRM NEAT	166.9	186.5	176.5	13.6	7.72
CRM 2LSBS	1523.3	1577.9	1550.6	38.6	2.49
CRM 0.7ELV	1492.2	1082.7	1287.4	289.5	22.49
Strain at Max Stress					
	Run 1	Run 2	Average	Standard deviation	Coefficient of variation (%)
CRM NEAT	2.19	2.44	2.31	0.18	7.64
CRM 2LSBS	11.53	12.04	11.78	0.36	3.06
CRM 0.7ELV	10.59	7.83	9.21	1.95	21.19

Table F2a.3. Yield energy and strain at maximum stress for the FH base binder.

Yield Energy (kPa)					
	Run 1	Run 2	Average	Standard deviation	Coefficient of variation (%)
FH NEAT	305.15	339.19	322.17	24.06	7.47
FH 2LSBS	439.60	391.14	415.38	34.27	8.25
FH 0.7ELV	1896.19	2116.14	2006.17	155.53	7.75
Strain at Max Stress					
	Run 1	Run 2	Average	Standard deviation	Coefficient of variation (%)
FH NEAT	1.90	2.20	2.05	0.21	10.35
FH 2LSBS	1.50	1.40	1.45	0.07	4.88
FH 0.7ELV	5.60	6.40	6.00	0.57	9.43

Frequency sweep tests were also performed for all binders in preparation for the viscoelastic continuum damage (VECD) analysis. Data analysis and modeling were not performed.

## Significant Problems, Issues and Potential Impact on Progress

None.

## Work Planned Next Quarter

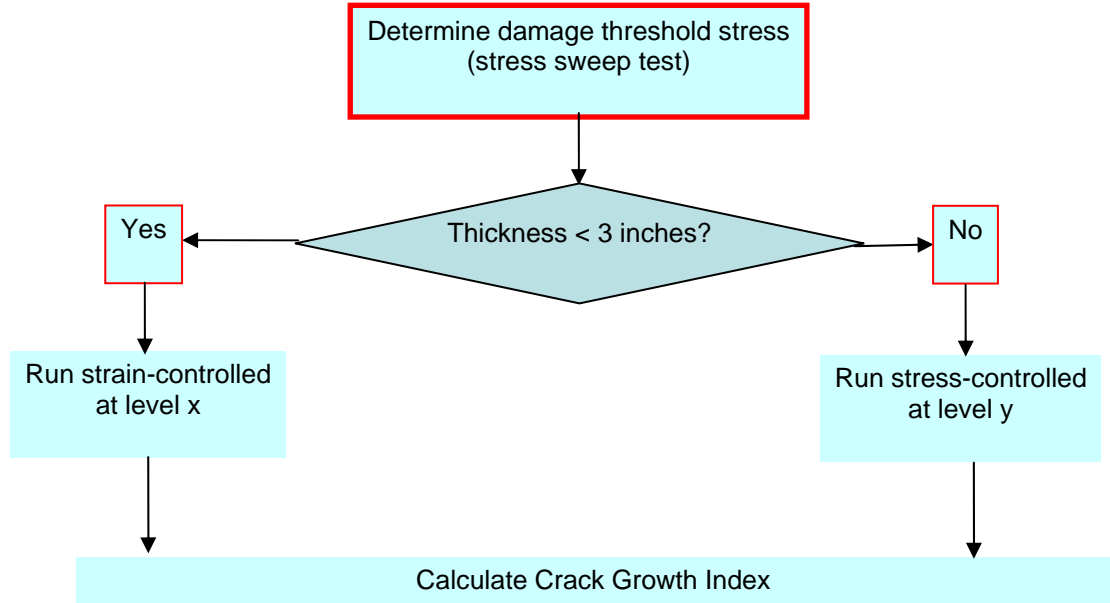
During the next quarter, the research team will continue conducting laboratory aging on the selected materials and will run more fatigue tests. At the same time, data analysis of the test results will be performed.

## **Work Element F2b: Mastic Testing Protocol (TAMU)**

### Work Done This Quarter

Improvements to the test protocol to determine fatigue-cracking resistance of FAM specimens using the DMA were made in Subtask F1b-1. Further work on this subtask will be carried out in coordination with the technology development area. The tentative protocol was presented to the mixture ETG at the semi-annual meeting in Reno, NV. A summary of the DMA test method is presented herein (see figure F2b.1):

- 1) Conduct a stress sweep test to determine the nonlinear viscoelastic properties and stress value at which damage is initiated (damage threshold stress).
- 2) Conduct a time sweep test (fatigue test) using the damage threshold stress or associated damage threshold strain depending on pavement thickness.
- 3) Record the material properties (dynamic modulus and phase angle) during fatigue loading.
- 4) Use the damage growth index and modified Schapery's theory to characterize the resistance of fine aggregate mixture to fatigue damage.
- 5) In comparing different FAMs, use the highest damage threshold stress or highest damage threshold strain.



x : highest damage threshold strain for all systems  
 y : highest damage threshold stress for all systems

Figure F2b.1. An outline of the procedure for conducting the DMA test.

Significant Results

None.

Significant Problems, Issues and Potential Impact on Progress

None.

Work Planned Next Quarter

Researchers will coordinate with the technology development work area to further develop the test protocols as stated under subtask F2c.

**Work Element F2c: Mixture Testing Protocol (TAMU)**

Work Done This Quarter

During this quarter, a new viscoelastic characterization (VEC) test protocol was developed that is easier and faster and can be accomplished with the currently available equipment. This test protocol provides sufficient information to determine the relaxation modulus as a function a

time, complex modulus as a function of frequency, phase angle as a function of frequency, and Poisson's ratio as a function of frequency. The lab-mixed-lab-compacted (LMLC) specimens used in this test protocol were 4 inches in diameter and 4 inches in height. Taller specimens (6 inches in height) were not used because the air void contents near the end of the samples (within 1 inch of each end) were significantly higher than those in the middle third of the sample. The percent air voids was approximately uniform after cutting 1 inch from the top and the bottom of the 6-inch high LMLC specimens.

In the newly developed VEC test protocol, a uniaxial increasing tensile stress that is a function of time was applied. The loading time was carefully controlled to assure no damage was introduced to the specimen. The axial and radial deformations of the specimen were recorded by three vertical linear variable differential transformers (LVDTs) and three radial LVDTs. Figure F2c.1 shows the configuration of the specimen mounted with LVDTs in the environmental chamber of the Material Test System (MTS).



Figure F2c.1. Configuration of test protocol for viscoelastic characterization of asphalt mixture.

The axial strain and radial strain are calculated using raw deformation data. Both axial strain and radial strain were functions of time. The stress data and strain data were presented as functions of time. By applying the Laplace transform to the stress function and axial strain function, the relaxation modulus was calculated according to linear viscoelasticity theory. The complex modulus and phase angle as a function of frequency were then determined using the relationship between the relaxation modulus and complex modulus (Findley 1989). The viscoelastic Poisson's ratio was determined using Dr. Zachary Grasley's method (Grasley 2007).

The VEC test was conducted on every specimen at three temperatures (10°C, 20°C, and 30°C). Using the time-temperature superposition principle, master curves were constructed for the magnitude of complex modulus and phase angle. The magnitude of the complex modulus was fit into a newly developed model that includes six fitting parameters and provides an S-shape curve to express this complex modulus. The master curve for the phase angle was found to be of a shape similar to that of a probability density function. A model was developed to fit the phase angle data. All the findings from the VEC test protocol agree with viscoelasticity theory.

The repeated direction tension (RDT) test protocol was improved to characterize the fatigue response of asphalt mixtures. A haversine tensile load was applied to the specimen at a frequency of 10 Hz. After the first 1,000 continuous loading cycles, the specimen was allowed to rest for 1,000 seconds. Then a second 1,000 loading cycles was applied, and the specimen was allowed to rest for 500 seconds. After the third segment of 1,000 loading, the specimen was allowed to rest for 250 seconds, followed by a subsequent 1,000-cycle loading period followed by only a 4-second rest period. The entire test thus includes nine 1000-cycle loading periods and nine rest periods. This modified RDT test protocol is able to not only determine the crack growth index and the rate of fracture damage accumulation (determined in the previous CMSE approach) but also to calculate the rate of plastic deformation accumulation, Paris' law coefficients, and average crack radius. In addition, this protocol provides sufficient information to characterize the short-term and long-term healing properties of the mixture since the test protocol includes rest (healing) periods that vary in length. Another improvement to the modified protocol is that it does not include the 0.9 second rest period between two adjacent load pulses that was used in the original protocol. As a result, the modified protocol better captures true material properties.

### Significant Results

A new viscoelastic characterization (VEC) test protocol was developed. Compared to other available test protocols, the new protocol is easier and faster. The LMLC specimens were not damaged in the test because the loading time and level were carefully controlled to assure that the material deformed within a linear range. After the new VEC test protocol, the same specimen was tested again using the modified RDT test protocol that provided the complete mixture fatigue and healing properties. The two test protocols are able to characterize viscoelastic, fracture, and healing properties of asphalt mixtures in a feasible and efficient way.

### Significant Problems, Issues and Potential Impact on Progress

Problems with the MTS equipment were identified. It was found that the MTS equipment was not able to control the specimen displacement at a constant level. Therefore, the original relaxation modulus test protocol could not accurately determine the relaxation modulus.

The data acquisition system of the MTS was not stable or reliable. The "controlled" LVDT could not be well controlled by the data acquisition system, and reliable data using LVDT-controlled protocols could not be obtained.

The new VEC test protocol does not require the MTS to hold the specimen at a constant strain level, so more reliable data were obtained from the MTS. In addition, the LVDT-controlled protocol was not used. Instead, the machine displacement controlled protocol was utilized to assure reliable data.

#### Work Planned Next Quarter

In the next quarter, work will commence toward development of a test protocol to determine the viscoelastic anisotropic properties of the mixture under compressive stress using the Universal Testing Machine (UTM) and the Rapid Triaxial Testing (RaTT) Cell. The RaTT Cell will be mounted inside the UTM and used to apply triaxial compressive stress to the LMLC specimen. From this test protocol, viscoelastic properties (modulus, phase angle, Poisson's ratio, etc.) in the direction of mixture compaction and perpendicular to the direction of compaction will be obtained.

#### Cited References

Findley, W. N., J. S. Lai, and K. Onaran, 1989, *Creep and Relaxation of Nonlinear Viscoelastic Materials with an Introduction to Linear Viscoelasticity*. Dover Publication, Inc., Mineola, New York.

Grasley, Z. C., 2007, "Analysis of the Viscoelastic Poisson's Ratio as Applied to Portland Cement Paste." Unpublished work.

### **Work Element F2d: Tomography and Microstructural Characterization (TAMU)**

#### Work Done This Quarter

While no work was accomplished this quarter toward accomplishing specific work element deliverables, work with the AFM was accomplished. The AFM was used to evaluate various microstructural properties of a variety of asphalts as well as to evaluate trial viscoelastic responses.

#### Significant Results

None.

#### Significant Problems, Issues and Potential Impact on Progress

None.

#### Work Planned Next Quarter

Work on this task will begin next quarter. In the initial phase researchers will try to determine simple viscoelastic properties (creep and relaxation) for the different phases in an asphalt binder



using an Atomic Force Microscope (AFM). This will be the first step towards determining the mechanical properties and contribution of individual phases in bitumen to fatigue cracking and self-healing.

### Work Element F2e: Verification of the Relationship between DSR Binder Fatigue Tests and Mixture Fatigue Performance (UWM)

#### Work Done This Quarter

Work continued on applying nonlinear viscoelastic behavior characteristics to the constitutive modeling of asphalt binders tested under monotonic constant shear through the Binder Yield Energy Test (BYET). As shown in the previous quarterly technical progress report, a frequency sweep consisting of increasing applied strain amplitudes can show differences in linear and nonlinear viscoelastic behavior without damage. These differences in response are shown in figure F2e.1. By using the  $G^*(\omega)$  master curves generated at nonlinear strain levels, a nonlinear relaxation modulus can be calculated and used for constitutive modeling.

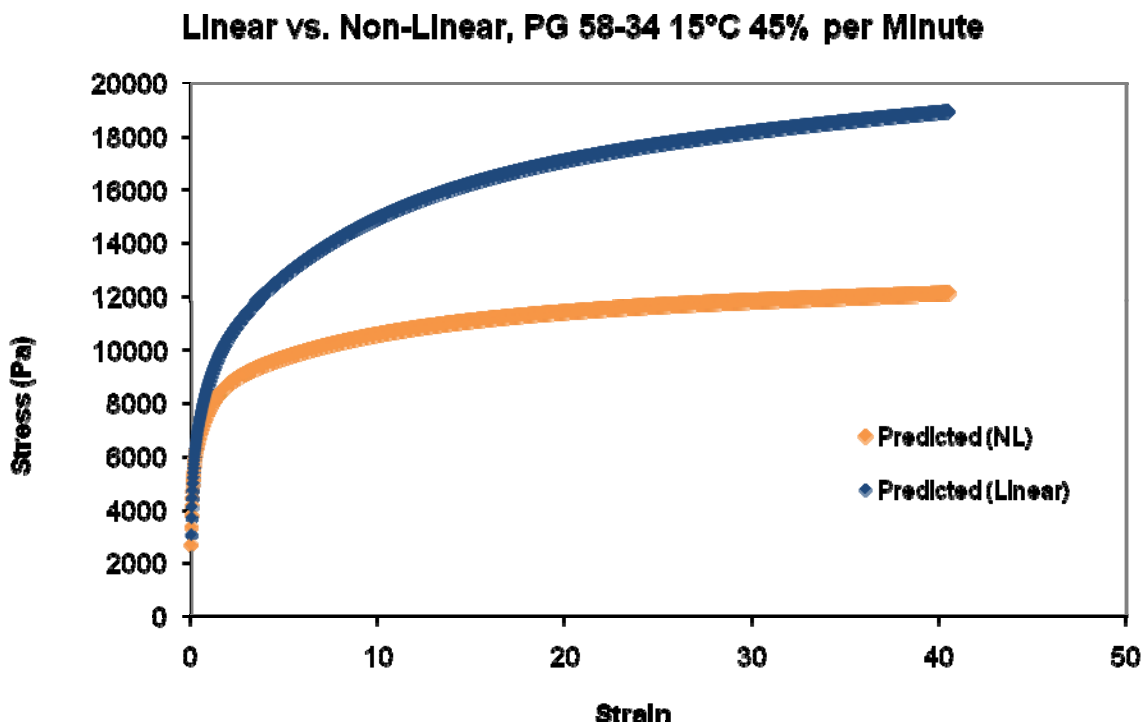


Figure F2e.1. Graph. Monotonic shear undamaged response: linear versus nonlinear (NL).

By accounting for the nonlinearity of asphalt binder when modeling the monotonic shear response, it can effectively be kept separate from the calculation of damage. This same approach will also be used to explore whether effects of visco-plasticity are present during monotonic shear. This concept is depicted in figure F2e.2.

### Predicted vs. Measured, PG70-22, 19°C, 0.005/s

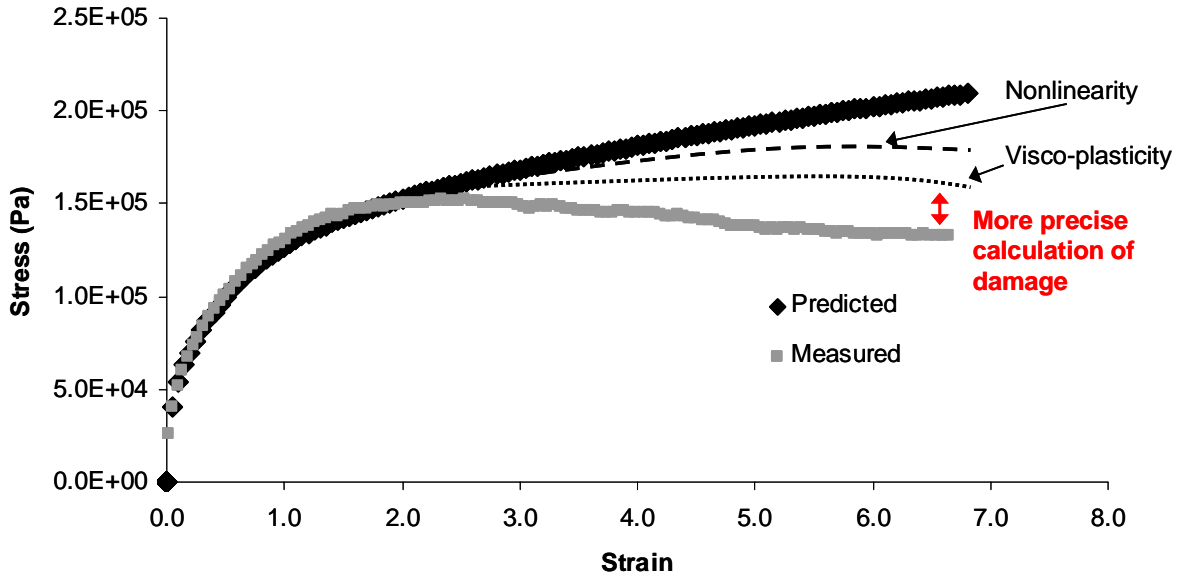


Figure F2e.2. Graph. Conceptual figure showing the proposed separation of nonlinearity and visco-plasticity from damage calculation.

Also, the application of viscoelastic continuum damage (VECD) concepts to both stress and strain sweep test results began in order to explore whether the testing mode had an effect on damage characteristics of asphalt binder. As evident in figure F2e.3, preliminary results show that the strain-controlled test gave a more gradual accumulation of damage compared to the stress-controlled test. This is consistent with concepts behind stress-controlled or strain fatigue testing: Strain-controlled cyclic tests require an increase in number of cycles to failure when compared to stress-controlled cyclic tests.

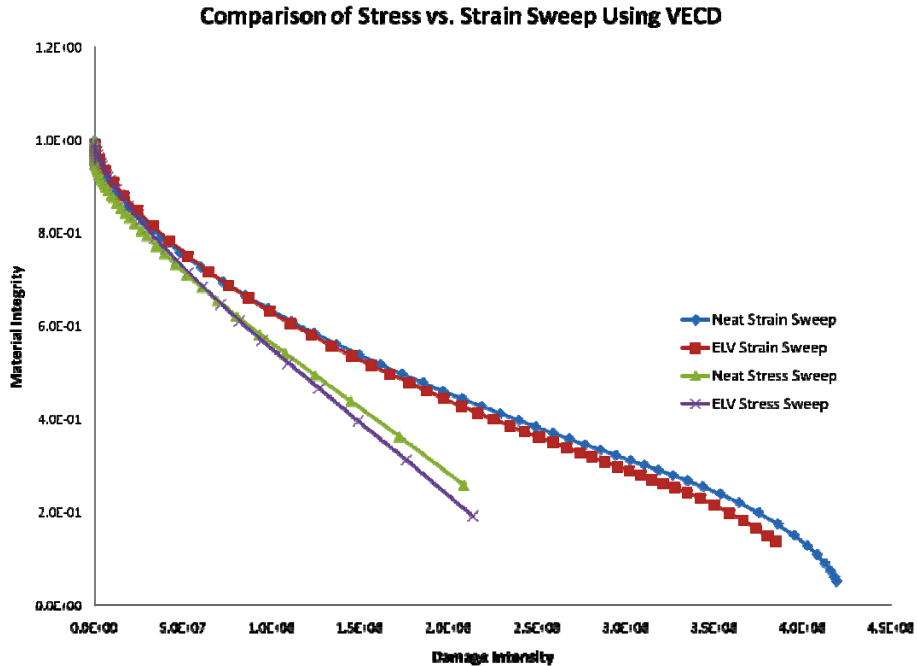


Figure F2e.3. Graph. VECD  $M(D)$  plots for stress and strain sweep results.

Progress from this work element was presented at the Petersen Asphalt Research Conference held July 14-16, 2008, and at the FHWA Binder ETG meeting September 16, 2008. Also, two papers focusing on this work element were submitted for consideration to TRB and AAPT.

### Significant Results

Monotonic shear response was modeled using nonlinear viscoelastic properties without damage, which is promising for inclusion in VECD models. Accounting for nonlinearity, as similarly described in work element F1b-1, can give a more accurate depiction of damage accumulation.

It was also shown that amplitude sweep results can be analyzed within the VECD framework. Differences exist in the preliminary data between stress- and strain-controlled test procedures, which could possibly help discriminate between the two and identify which is the more promising accelerated fatigue procedure.

### Significant Problems, Issues and Potential Impact on Progress

None.

### Work Planned Next Quarter

Work will continue on determining the extent of visco-plastic behavior present in the intermediate temperature binder response. Comparison between monotonic, stress sweep and strain sweep response will be investigated. Also, work will begin on preliminary mixture fatigue evaluation for comparison to relevant binder fatigue data.

## **CATEGORY F3: MODELING**

### **Work Element F3a: Asphalt Microstructural Model (WRI)**

#### Work Done This Quarter

The detailed work plan, submitted as part of the Year 2 Work Plan, was approved during the past quarter.

#### Significant Results

None.

#### Significant Problems, Issues and Potential Impact on Progress

None.

#### Work Planned Next Quarter

A kick off meeting of the members of the asphalt microstructure modeling team will take place in January 2009 sometime during the TRB Meeting in Washington D.C. Prior to this, the subcontract approval process by the FHWA Contracting Office will be initiated. Hopefully, the approval process with the Contracting Office will proceed quickly and subcontracts will be established between WRI and the members of the asphalt microstructure modeling (AMM) team. Specific year-by-year work plans with a detailed first-year and first quarter of the first year plans will constitute the negotiation of a subcontract between WRI and an AMM team member.

### **Work Element F3b: Micromechanics Model (TAMU)**

#### ***Subtask F3b-1: Model Development***

#### ***Subtask F3b-2: Account for Material Microstructure and Fundamental Material Properties***

Note: These two subtasks work together until such time as the development progresses. Subtask F3b-2 will begin in the latter part of the Year 2 Work Plan.

#### Work Done This Quarter

Work during this quarter focused on the development of laboratory tests to obtain key model input parameters such as the linear viscoelastic (LVE) properties and the cohesive zone (CZ) fracture properties of asphalt matrix phase (referred to as the fine aggregate matrix (FAM) in other tasks related: M1c, F1b, F2b) and to determine the proper dimension of the representative volume elements (RVEs) of asphalt concrete mixtures where damage events are involved.

As illustrated in figure F3b.1, the microstructure of a general asphalt concrete mixture exhibits two distinct phases: a portion of relatively coarse aggregate particles (in white) and an asphalt

matrix phase (in black) comprised of asphalt cement, fine aggregates, and entrained air voids. At approximately room temperature the coarse aggregate particles typically demonstrate linear elastic behavior, while the asphalt matrix phase is viscoelastic and is subjected to damage such as cracking that subsequently results in failure of the overall asphalt concrete mixture. The computational micromechanics modeling approach led by the University of Nebraska uses material properties of each individual phase (i.e., aggregate and asphalt matrix) and fracture properties of asphalt matrix phase for model inputs, therefore the measurement of the LVE properties and the CZ fracture properties of the asphalt matrix phase is one of key tasks of this work.

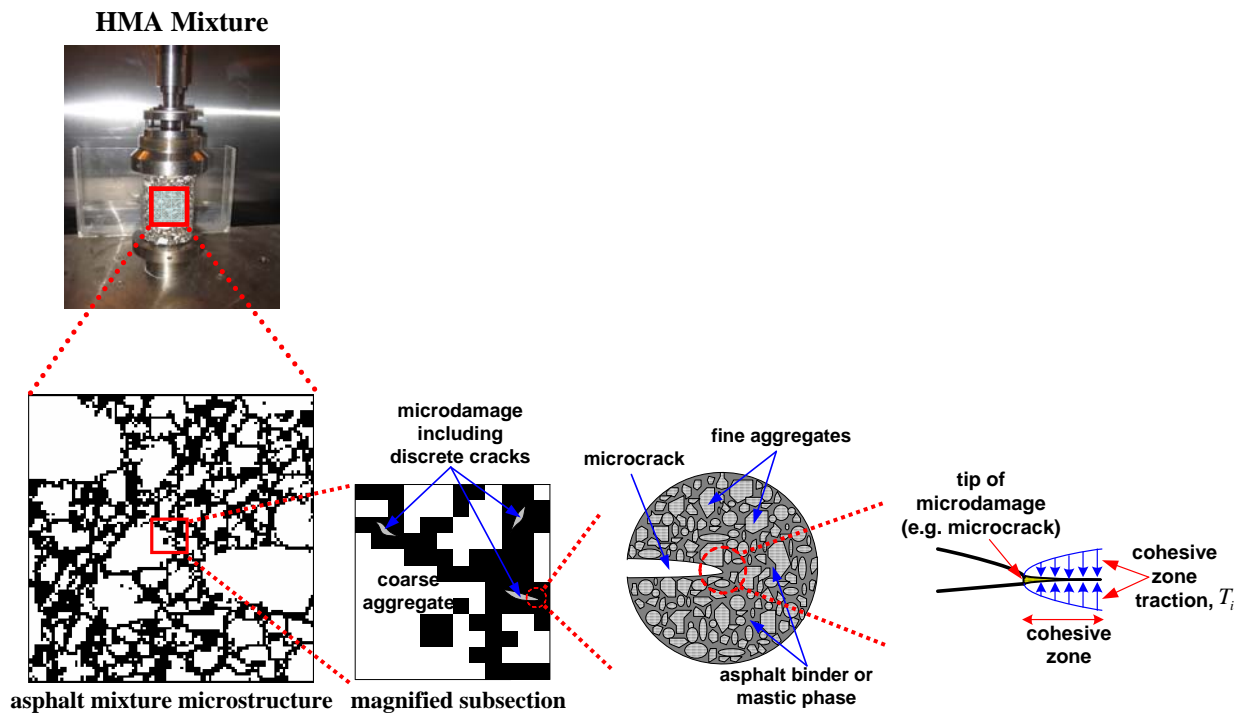


Figure F3b.1. Asphalt concrete microstructure with two distinct phases (aggregates and matrix).

Figure F3b.2 presents a complete set of test results (dynamic modulus master curves at a reference temperature of 23°C) obtained during this quarter by performing the DMA tests (dynamic strain sweep tests followed by dynamic frequency sweep tests) (Kim et al. 2002, 2003, 2006). A total of five asphalt matrix mixtures with different hydrated lime addition rates (0.5% to 3.0%) were tested, as shown in the figure F3b.2.

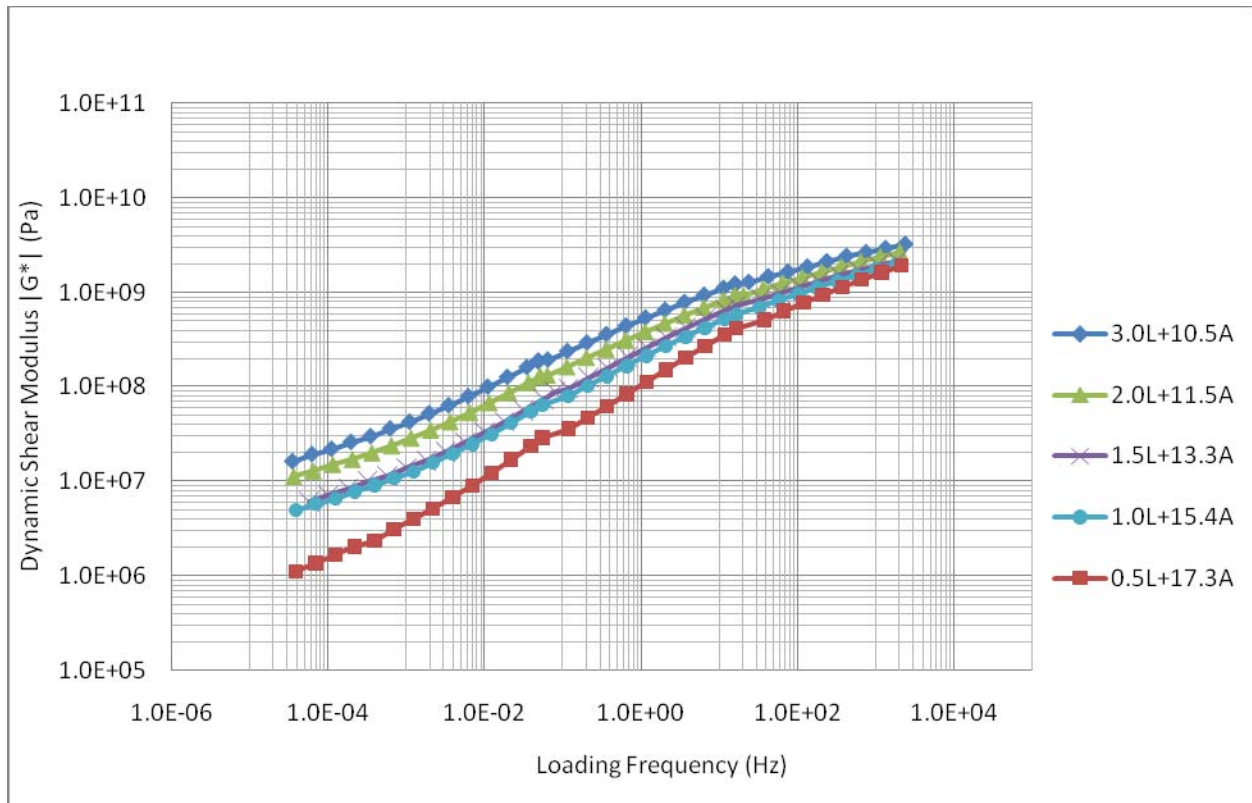


Figure F3b.2. Test results (dynamic modulus master curves at a reference temperature of 23°C) obtained during this quarter by performing the DMA tests.

For the CZ fracture properties of asphalt matrix phase, we have revised the fracture testing system that has been originally used for characterizing fracture properties of asphalt binder samples. A transition from the testing of asphalt binder to asphalt matrix has been pursued as illustrated in figure F3b.3 during this quarter because of technical limitations in simulating realistic asphalt film thickness for the fracture test. For an accurate characterization of the fracture behavior, the testing needs to be performed with an extremely thin asphalt film (approximately 10 $\mu\text{m}$ ) which is typically the known film thickness of an asphalt concrete mixture however, this accurate simulation of real asphalt film thickness was not trivial. Alternatively, test results at several different film thicknesses were used to approximately determine the fracture parameters at a film thickness of 10 $\mu\text{m}$  by relating film thickness to fracture behavior obtained from those several film thicknesses tested (Kim et al. 2008). This limitation can be overcome through the transition from the use of asphalt binder sample to asphalt matrix sample. However, based on preliminary results, it was found that the initial displacements recorded during the test included erroneous data due to the insufficient power of a driving motor. Currently, researchers are working on the system revision to further improve the precision and accuracy of fracture characteristics in the asphalt matrix phase.

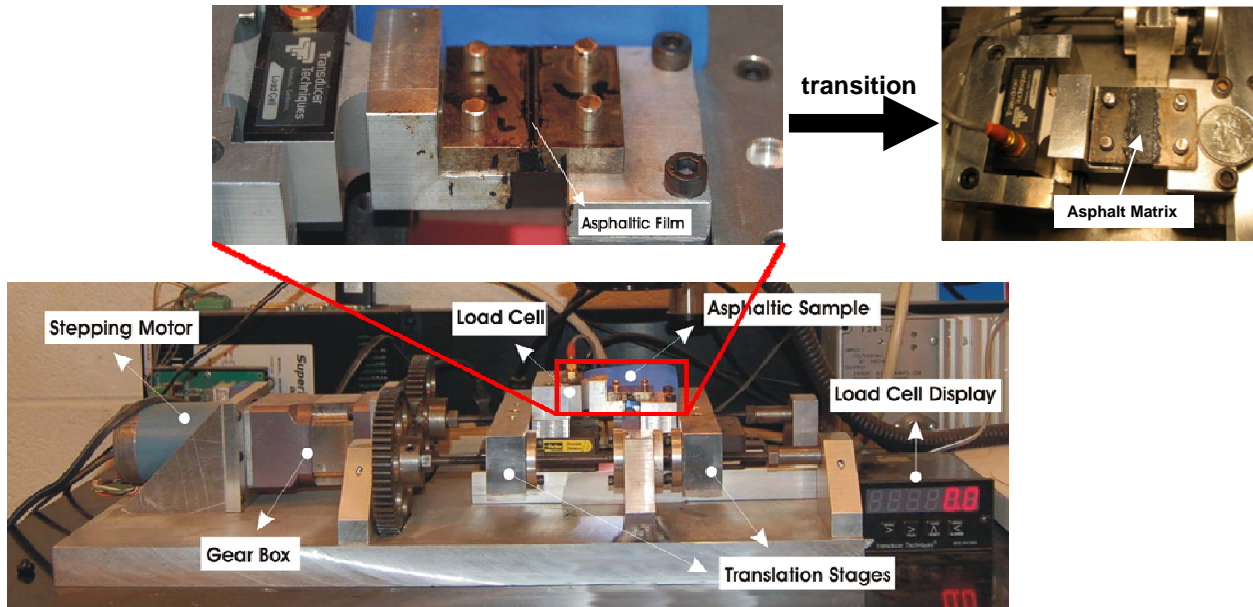


Figure F3b.3. Fracture testing system for the CZ model parameters.

As briefly summarized in the last quarterly report, the RVEs of asphalt concrete mixtures without damage were studied through a simple method based on geometric analyses of asphalt mixture heterogeneity. Analysis results and related research concepts were presented in a journal article submitted to the TRB 2009 annual meeting. During this quarter, as a follow-up study, we initiated a testing set-up that will possibly identify asphalt concrete RVEs when damage events are included. For this task, we have initiated a digital image correlation (DIC) testing system as shown in figure F3b.4 and could obtain preliminary test results. DIC can be used to capture real-time and continuous variations in three-dimensional deformation and strain of mixture components with high-resolution video cameras. Changes in the spatial homogeneity of a mixture can be easily monitored as damage progresses, and the RVEs of asphalt concrete mixtures into which damages have been incorporated can be appropriately defined. We will continue the testing and data analyses.

In addition to the experimental progress, we have also accomplished several computational modeling activities including the implementation of the Xu and Needleman's CZ model (1993, 1994) presented in figure F3b.5(a) and the bilinear CZ model (Geubelle and Baylor 1998; Espinosa and Zavattieri 2003) shown in figure F3b.5(b) into the finite element (FE) framework, CZ model validations with analytical solutions as presented in figure F3b.6, and numerical convergence studies of the bilinear model to the size of time increment and the cohesive zone element in a double cantilever beam (DCB) specimen. Simulation results are demonstrated in figure F3b.7.

### Significant Results

Significant findings from the experimental and modeling activities described above will be reported for the next quarter and in the technical reports with details.



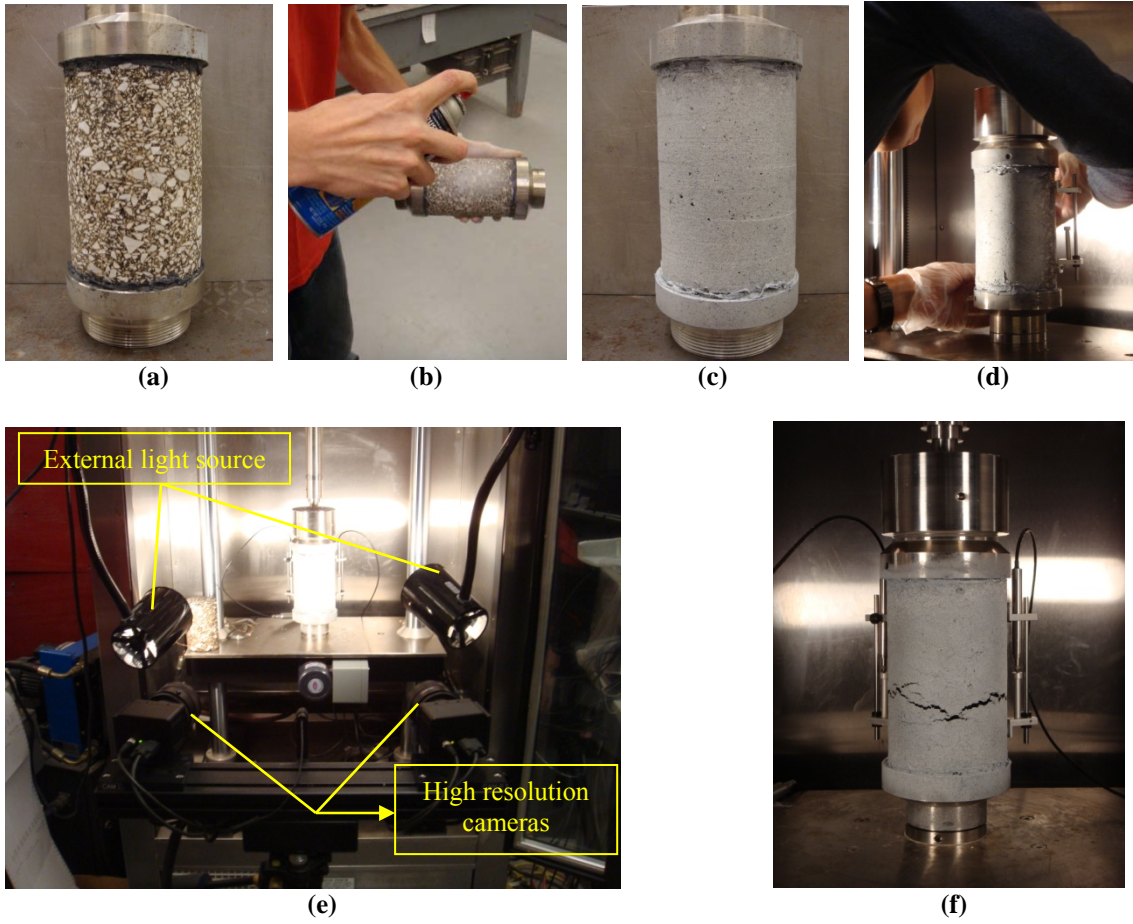


Figure F3b.4. Digital image correlation (DIC) testing system and sample preparation steps.



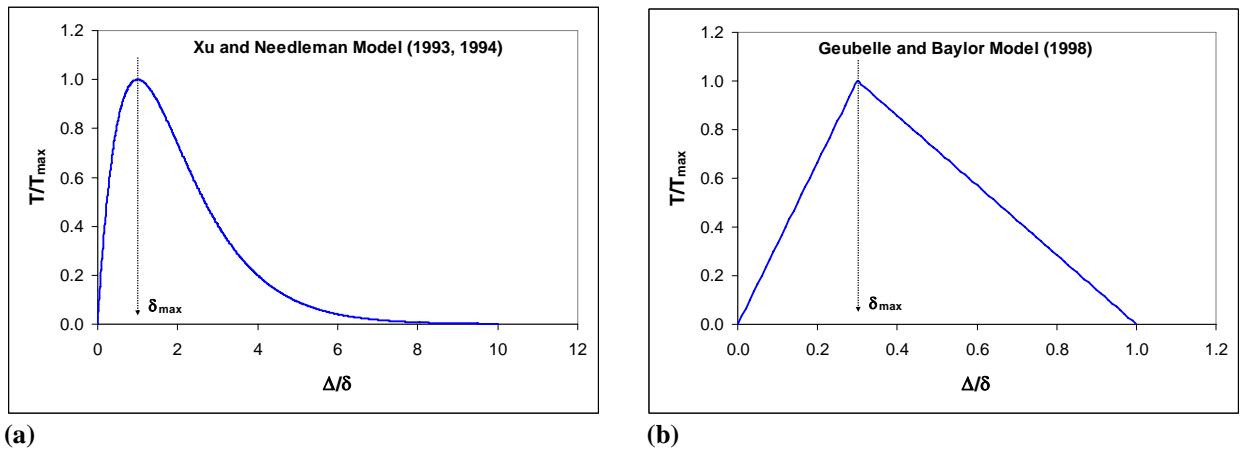


Figure F3b. 5. CZ models implemented during this quarter: (a) Xu and Needleman CZ Model; (b) Bilinear CZ Model.

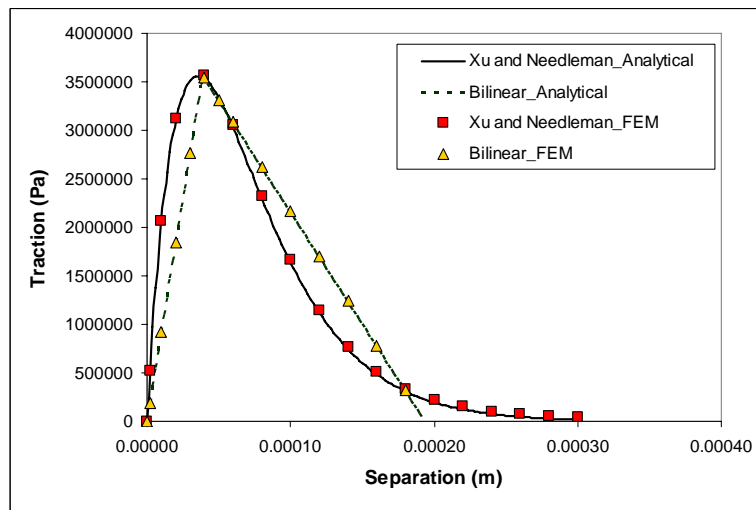
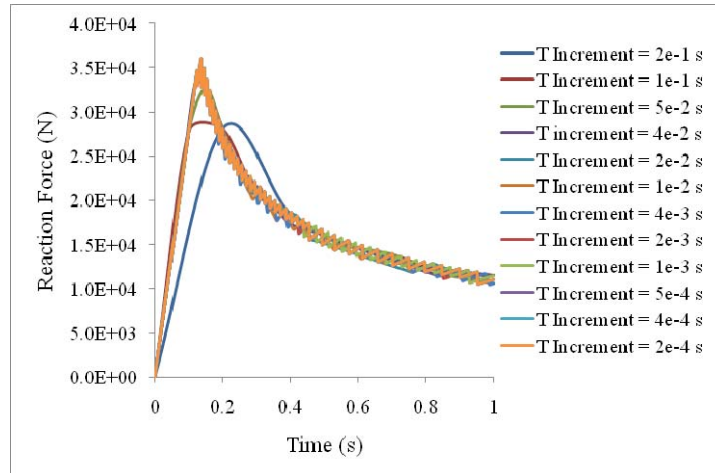
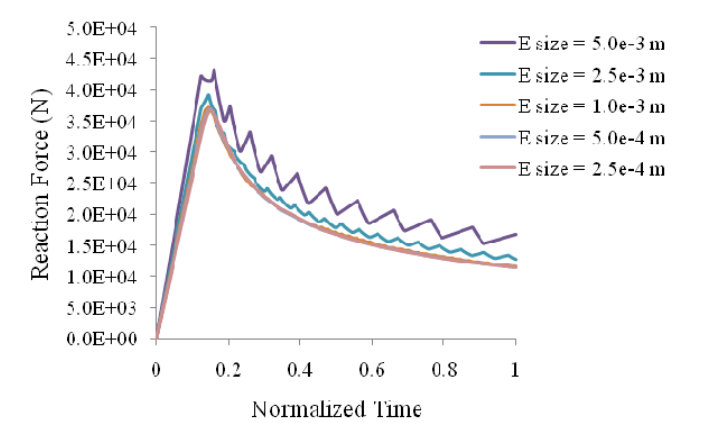


Figure F3b.6. CZ model validations with analytical solutions.



(a)



(b)

Figure F3b.7. Numerical convergence studies: (a) size of time increment; (b) size of cohesive zone element.

Significant Problems, Issues and Potential Impact on Progress

None.

Work Planned Next Quarter

Laboratory testing systems will be set and used to obtain CZ model parameters. Analysis of DIC test data will also be conducted to determine the influence of damage on the size of the asphalt concrete RVEs. In addition, CZ models implemented in the finite element framework will be further investigated for a better understanding of their features, characteristics, benefits, and limitations to the modeling of asphalt concrete fracture. All modeling activities planned will be closely collaborated with researchers at the Texas A&M University (Drs. Little and Masad) and the University of Texas-Austin (Dr. Bhasin) where various laboratory activities to identify fundamental material properties are in progress.

## References Cited

Espinosa, H. D., and P. D. Zavattieri, 2003, A Grain Level Model for the Study of Failure Initiation and Evolution in Polycrystalline Brittle Materials. Part I: Theory and Numerical Implementation. *Mechanics of Materials*, 35: 333-364.

Geubelle, P. H., and J. Baylor, 1998, The Impact-Induced Delamination of Laminated Composites: A 2D Simulation. *Composites, Part B*, 29B: 589-602.

Kim, Y., D. H. Allen, and D. N. Little, "Damage Modeling of Asphalt Concrete Mixtures through Computational Micromechanics and Cohesive Zone Fracture." In review, submitted in 2008, *Journal of the Association of Asphalt Paving Technologists*, AAPT.

Kim, Y., D. N. Little, and R. L. Lytton, 2002, Use of Dynamic Mechanical Analysis (DMA) to Evaluate the Fatigue and Healing Potential of Asphalt Binders in Sand Asphalt Mixtures. *Journal of Association of Asphalt Paving Technologists*, AAPT, 71, 176-206.

Kim, Y., D. N. Little, and R. L. Lytton, 2003, Fatigue and Healing Characterization of Asphalt Mixtures. *Journal of Materials in Civil Engineering*, ASCE, 15(1), 75-83.

Kim, Y., H. J. Lee, D. N. Little, and Y. R. Kim, 2006, A Simple Testing Method to Evaluate Fatigue Fracture and Damage Performance of Asphalt Mixtures. *Journal of the Association of Asphalt Paving Technologists*, AAPT, 75, 755-787.

Xu, X. P. and A. Needleman, 1993, Void Nucleation by Inclusion Debonding in a Crystal Matrix. *Modelling and Simulation in Materials Science and Engineering*, 1: 111-132.

Xu, X. P. and A. Needleman, 1994, A Numerical Simulations of Fast Crack Growth in Brittle Solids. *Journal of the Mechanics and Physics of Solids*, 42(9): 1397-1434.

## **Work Element F3c: Development of Unified Continuum Model (TAMU)**

### Work Done This Quarter

The progress in this task is reported under work element M4c and in appendices B and C.

### Significant Results

No significant results.

### Significant Problems, Issues and Potential Impact on Progress

No significant problems.

### Work Planned Next Quarter

We will conduct extensive sensitivity analysis of the elastoviscoplastic model with damage under various loading and boundary conditions. We will also test the ability of the model to describe experimental measurements of asphalt mixtures with couples mechanical and moisture damage.

### **Work Element F3d: Calibration and Validation**




This work element is planned to start later in the project.

Fatigue Year 2		Year 2 (4/08-3/09)											
		4	5	6	7	8	9	10	11	12	1	2	3
<b>Material Properties</b>													
<b>F1a</b>	<b>Cohesive and Adhesive Properties</b>												
F1a-1	Critical review of literature						JP(1)						
F1a-2	Develop experiment design												
F1a-3	Thermodynamic work of adhesion and cohesion												
F1a-4	Mechanical work of adhesion and cohesion												
F1a-5	Evaluate acid-base scale for surface energy calculations												
<b>F1b</b>	<b>Viscoelastic Properties</b>												
F1b-1	Separation of nonlinear viscoelastic deformation from fracture energy under cyclic loading								JP		D		F
F1b-2	Separation of nonlinear viscoelastic deformation from fracture energy under monotonic loading								JP		D		F
<b>F1c</b>	<b>Aging</b>												
F1c-1	Critical review of binder oxidative aging and its impact on mixtures												
F1c-2	Develop experiment design						D(3)	F(3)					
F1c-3	Develop transport model for binder oxidation in pavements					P(4)						P	JP
F1c-4	Effect of binder aging on properties and performance							JP(2)					P
F1c-5	Polymer modified asphalt materials												
<b>F1d</b>	<b>Healing</b>												
F1d-1	Critical review of literature												
F1d-2	Select materials with targeted properties												
F1d-3	Develop experiment design												
F1d-4	Test methods to determine properties relevant to healing								JP				
F1d-5	Testing of materials												
F1d-6	Evaluate relationship between healing and endurance limit of asphalt binders										DP	P	
F1d-7	Coordinate with AFM analysis												
F1d-8	Coordinate form of healing parameter with micromechanics and continuum damage models												
<b>Test Methods</b>													
<b>F2a</b>	<b>Binder tests and effect of composition</b>												
F2a-1	Analyze Existing Fatigue Data on PMA								DP				
F2a-2	Select Virgin Binders and Modifiers and Prepare Modified Binder								DP				
F2a-3	Laboratory Aging Procedures												
F2a-4	Collect Fatigue Test Data					P						JP	
F2a-5	Analyze data and propose mechanisms												P
<b>F2b</b>	<b>Mastic testing protocol</b>												
F2b-1	Develop specimen preparation procedures								D(5)				
F2b-2	Document test and analysis procedures in AASHTO format								D(5)				
<b>F2c</b>	<b>Mixture testing protocol</b>												
<b>F2d</b>	<b>Tomography and microstructural characterization</b>												
F2d-1	Micro scale physicochemical and morphological changes in asphalt binders												
<b>F2e</b>	<b>Verify relationship between DSR binder fatigue tests and mixture fatigue performance</b>												
F2e-1	Evaluate Binder Fatigue Correlation to Mixture Fatigue Data												
F2e-2	Selection of Testing Protocols						D, JP				DP, F		
F2e-3	Binder and Mixture Fatigue Testing												
F2e-4	Verification of Surrogate Fatigue Test											P	
F2e-5	Interpretation and Modeling of Data						JP					P	
F2e-6	Recommendations for Use in Unified Fatigue Damage Model												
<b>Models</b>													
<b>F3a</b>	<b>Asphalt microstructural model</b>												
<b>F3b</b>	<b>Micromechanics model</b>												
F3b-1	Model development										JP		
F3b-2	Account for material microstructure and fundamental material properties												
<b>F3c</b>	<b>Develop unified continuum model</b>												
F3c-1	Analytical fatigue model for mixture design												
F3c-2	Unified continuum model								JP				
F3c-3	Multi-scale modeling												

**LEGEND**

**Deliverable codes**

- D: Draft Report
- F: Final Report
- M&A: Model and algorithm
- SW: Software
- JP: Journal paper
- P: Presentation
- DP: Decision Point
- [x]

-  Work planned
-  Work completed
-  Parallel topic

**Deliverable Description**

- Report delivered to FHWA for 3 week review period.
- Final report delivered in compliance with FHWA publication standards
- Mathematical model and sample code
- Executable software, code and user manual
- Paper submitted to conference or journal
- Presentation for symposium, conference or other
- Time to make a decision on two parallel paths as to which is most promising to follow through
- Indicates completion of deliverable x

JP (1) A draft paper on the comparison of surface energy to total energy of fracture was prepared and reviewed jointly by ARC researchers and ETG members from TU-Delft  
 JP (2) 1 submitted for presentation only (accepted) 1 not accepted  
 D(3)/F(3) draft report is being finalized and formatted for final submission on October 31, 2008  
 P(4) presentations made at 45th Petersen Asphalt Research Conference in July 2008 entitled "Forward and Inverse Self-Consistent Micromechanics Model of an Asphalt Concrete Mixture" and "Modeling Pavement Temperature History for Pavement Perf  
 D(5) Researchers are preparing a single consolidated report for F2b-1 and F2b-2. The draft report is complete and is being reviewed internally. The draft will be submitted to FHWA for review by mid November

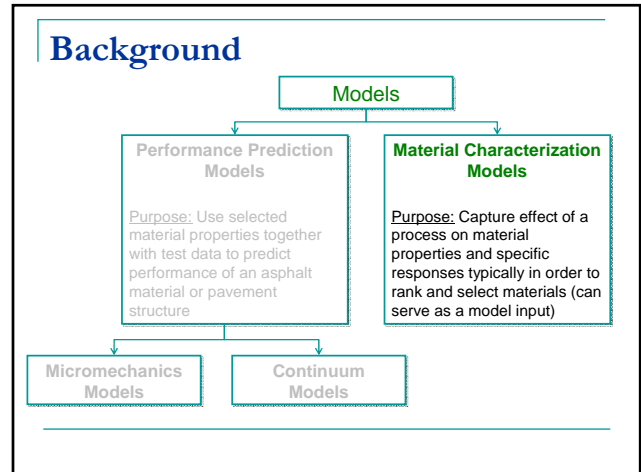
Fatigue Year 2 - 5		Year 2 (4/08-3/09)				Year 3 (4/09-3/10)				Year 4 (04/10-03/11)				Year 5 (04/11-03/12)				
		Q1	Q2	Q3	Q4	Q1	Q2	Q3	Q4	Q1	Q2	Q3	Q4	Q1	Q2	Q3	Q4	
<b>Material Properties</b>																		
<b>F1a</b>	<b>Cohesive and Adhesive Properties</b>																	
F1a-1	Critical review of literature			JP														
F1a-2	Develop experiment design																	
F1a-3	Thermodynamic work of adhesion and cohesion																	
F1a-4	Mechanical work of adhesion and cohesion					JP	D	F										
F1a-5	Evaluate acid-base scale for surface energy calculations														JP			
<b>F1b</b>	<b>Viscoelastic Properties</b>																	
F1b-1	Separation of nonlinear viscoelastic deformation from fracture energy under cyclic loading			D,JP	M&A, F			JP		JP		P		JP,M&A,D		F		
F1b-2	Separation of nonlinear viscoelastic deformation from fracture energy under monotonic loading			D,JP	M&A, F			JP		JP		P		JP,M&A,D		F		
<b>F1c</b>	<b>Aging</b>																	
F1c-1	Critical review of binder oxidative aging and its impact on mixtures																	
F1c-2	Develop experiment design			D, F														
F1c-3	Develop transport model for binder oxidation in pavements			P		P, JP		P		P, JP		P		P, JP		D, M&A	F	
F1c-4	Effect of binder aging on properties and performance			JP	P			JP	D	F					JP	D	F	
F1c-5	Polymer modified asphalt materials							P				P				D	F	
<b>F1d</b>	<b>Healing</b>																	
F1d-1	Critical review of literature																	
F1d-2	Select materials with targeted properties																	
F1d-3	Develop experiment design																	
F1d-4	Test methods to determine properties relevant to healing					JP				JP	D	F						
F1d-5	Testing of materials							JP							M&A,D	JP, F		
F1d-6	Evaluate relationship between healing and endurance limit of asphalt binders			DP				P	D,JP,F	P		D,F	P		DP,JP	P	D	F
F1d-7	Coordinate with AFM analysis																	
F1d-8	Coordinate form of healing parameter with micromechanics and continuum damage models													JP			JP,D	F
<b>Test Methods</b>																		
<b>F2a</b>	<b>Binder tests and effect of composition</b>																	
F2a-1	Analyze Existing Fatigue Data on PMA			DP														
F2a-2	Select Virgin Binders and Modifiers and Prepare Modified Binder			DP														
F2a-3	Laboratory Aging Procedures																	
F2a-4	Collect Fatigue Test Data			P		JP		P		P				JP, D,F				
F2a-5	Analyze data and propose mechanisms					P			P				P			P	D	F
<b>F2b</b>	<b>Mastic testing protocol</b>																	
F2b-1	Develop specimen preparation procedures			D														
F2b-2	Document test and analysis procedures in AASHTO format			D														
<b>F2c</b>	<b>Mixture testing protocol</b>																	
F2c-1	Evaluate Binder Fatigue Correlation to Mixture Fatigue Data			D, JP	F													
<b>F2d</b>	<b>Tomography and microstructural characterization</b>																	
F2d-1	Micro scale physicochemical and morphological changes in asphalt binders							JP				JP		M&A,D	F			
<b>F2e</b>	<b>Verify relationship between DSR binder fatigue tests and mixture fatigue performance</b>																	
F2e-1	Evaluate Binder Fatigue Correlation to Mixture Fatigue Data			D, JP	DP, F													
F2e-2	Selection of Testing Protocols																	
F2e-3	Binder and Mixture Fatigue Testing																	
F2e-4	Verification of Surrogate Fatigue Test					P	JP			P	JP	D	F, DP					
F2e-5	Interpretation and Modeling of Data			JP		P	JP			DP	P	JP		M&A				
F2e-6	Recommendations for Use in Unified Fatigue Damage Model																D	F
<b>Models</b>																		
<b>F3a</b>	<b>Asphalt microstructural model</b>							JP						JP			M&A	F
<b>F3b</b>	<b>Micromechanics model</b>																	
F3b-1	Model development					JP				JP				M&A	D	DP	F, SW	
F3b-2	Account for material microstructure and fundamental material properties											JP			D		F	
<b>F3c</b>	<b>Develop unified continuum model</b>																	
F3c-1	Analytical fatigue model for mixture design																M&A,D	F
F3c-2	Unified continuum model					JP				JP				M&A	D	DP	F, SW	
F3c-3	Multi-scale modeling												JP	M&A	D		F	

**LEGEND**  
**Deliverable codes**  
D: Draft Report  
F: Final Report  
M&A: Model and algorithm  
SW: Software  
JP: Journal paper  
P: Presentation  
DP: Decision Point  
[x]  
Work planned  
Work completed  
Parallel topic

**Deliverable Description**  
Report delivered to FHWA for 3 week review period.  
Final report delivered in compliance with FHWA publication standards  
Mathematical model and sample code  
Executable software, code and user manual  
Paper submitted to conference or journal  
Presentation for symposium, conference or other  
Time to make a decision on two parallel paths as to which is most promising to follow through  
Indicates completion of deliverable x

**APPENDIX C: SLIDES PRESENTED AT THE RENO ETG MEETING**

**Asphalt Research Consortium**  
**Material Characterization Models**  
 Mixture ETG – Reno, September, 2008



### Material Characterization Models

- **Purpose**


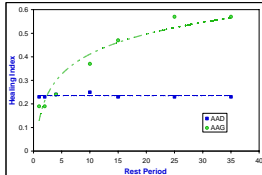
Capture the effect of a process or processes that alter the material properties and consequently the engineering response of the material or composite
- **Examples of Models**
  - rate of crack wetting and/or intrinsic healing of asphalt binders (*healing*)
  - fatigue characterization of FAM using DMA (*fatigue cracking*)
  - fatigue characterization of asphalt binders<sup>AB1</sup>

### Material Characterization Models

#### *Healing*

- **Healing model and its components**

$$R = \int_{t=-\infty}^{t-t} R_n(t-\tau) \frac{d\phi(\tau, X)}{d\tau} d\tau$$
  - Healing function that describes relationship between % strength recovered and duration of rest period
  - Typically obtained from mechanical fatigue tests with intermediate rest periods



## Material Characterization Models

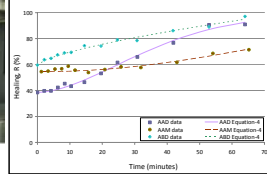
### Healing

- Healing model and its components

$$R = \int_{\tau=-\infty}^{\tau=t} R_h(t-\tau) \frac{d\phi(\tau, X)}{dt} d\tau$$

$$R_h(t) = R_0 + p(1 - e^{-at})$$

- Intrinsic healing function and is a material property input in the model



## Material Characterization Models

### Healing

- Healing model and its components

$$R = \int_{\tau=-\infty}^{\tau=t} R_h(t-\tau) \frac{d\phi(\tau, X)}{dt} d\tau$$

$$\frac{d\phi(t, X)}{dt} = \dot{a}_0 = \beta \left[ \frac{1}{D_0 k_m} \left\{ \frac{\pi W_c}{4(1-\nu^2)} \sigma_c^2 \beta - D_0 \right\} \right]^{1/n}$$

- Wetting function can be determined from material properties such as the viscoelastic properties of the material

## Material Characterization Models

### Healing

- Healing model – summary

$$R = \int_{\tau=-\infty}^{\tau=t} R_h(t-\tau) \frac{d\phi(\tau, X)}{dt} d\tau$$

A macroscopic healing parameter that can be used to rank healing characteristics of different materials using simple laboratory tests (binders, mastics, FAM, and mixtures)

A model that is based on the healing mechanism to relate fundamental material properties to macroscopic healing

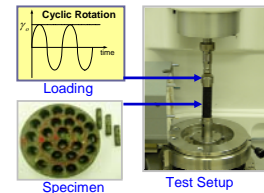
## Material Characterization Models

### Fatigue Cracking of FAM

- Fatigue cracking

$$\Delta R(N) = \left[ (2n+1)^{n+1} \left( \frac{G_R b}{4 \pi G_I \Delta G_I} \right)^n N \right]^{1/(2n+1)}$$

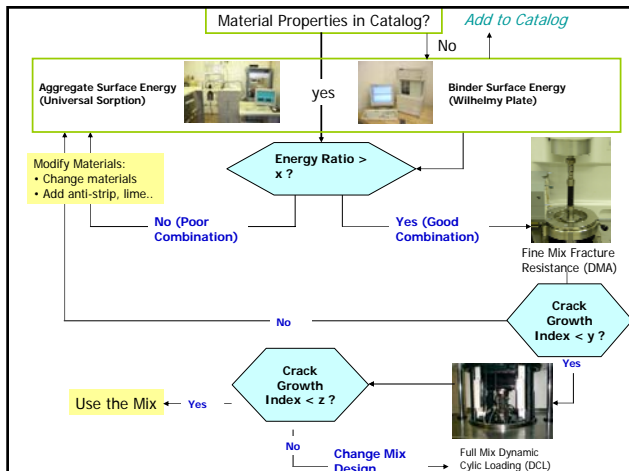
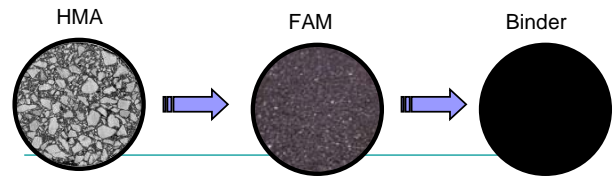
- Crack growth index as a relative measure of fatigue cracking
- This is a one dimensional analytical model based on fracture mechanics and can be extended to other modes of loading and/or materials (FAM or mixtures)



## Three-Step Approach for the Evaluation of Fatigue Cracking and Moisture Damage

### ■ Three-level system:

- Evaluate compatibility of asphalts and aggregates based on surface energy values
- Evaluate compatibility of asphalt-aggregate systems by DMA testing of FAM
- Evaluate of mixture design by testing of full HMA mixture



## Why three-level system?

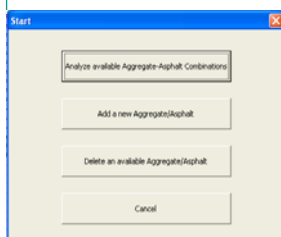
- Full HMA is a complex system and it is difficult to determine causes of failure (asphalt, aggregate or mixture design)
- Avoid using materials that have poor compatibility based on fundamental material properties
- Evaluate compatibility separately from the influence of air void distribution or full mixture design

## Step 1: Surface energy measurements of binders and aggregates

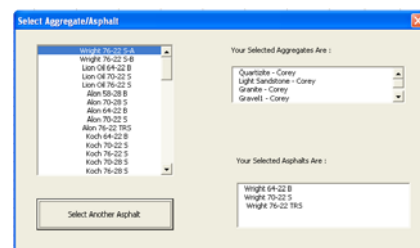
- Total number of binders tested to date with Wilhelmy plate: **96**  
(including modified, aged, and different batches)
- A wide variety of PG's as well as various modifications have been included in the testing spectrum
- Total number of aggregates tested to date with USD: **19**
- Detailed analysis of results and documentation in database is in progress

## Surface Energy Database

- A Visual Basic program in Excel has been created, which will calculate the **total bond energy**, both **dry** and in the **presence of water, for any combination of asphalt and aggregate** stored in the database
- Easy addition of asphalts and aggregates into database



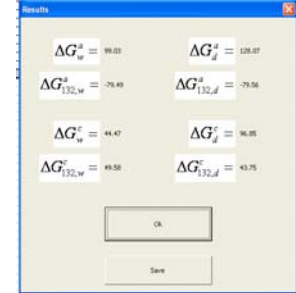
This screen greets you when you first start the program. You can either choose one of the option, or exit the program and browse the Excel file.



The program allows you to select as many or as few aggregates and asphalts to analyze as you want. However, it will not allow you select more then are in the database.

Start	Save Results To a File								Print Results
Combinations	$\Delta G_w^a$	$\Delta G_d^a$	$\Delta G_{132,w}^a$	$\Delta G_{132,d}^a$	$\Delta G_w^c$	$\Delta G_d^c$	$\Delta G_{132,w}^c$	$\Delta G_{132,d}^c$	
1 Quartzite - Corey--Weight 64-22 B	90.11	156.10	-166.36	-135.52	41.74	96.31	60.69	44.80	
2 Quartzite - Corey--Weight 76-22 S	91.04	141.50	-173.04	-150.86	40.33	94.52	49.08	37.49	
3 Quartzite - Corey--Weight 76-22 TRS	116.34	147.64	-145.06	-144.06	44.47	96.06	49.50	43.75	
4 Quartzite - Corey--Weight 76-22 S-A	94.72	157.19	-169.99	-130.91	45.54	96.40	59.25	36.11	
5 Quartzite - Corey--Weight 76-22 S-B	93.44	140.59	-173.00	-156.45	45.62	97.59	44.94	35.42	
6 Quartzite - Corey--Lion Of 64-22 B	92.29	171.07	-163.80	-132.18	59.59	99.36	79.16	24.76	
7 Light Sandstone - Corey--Weight 64-22 B	81.93	135.64	-74.69	-56.20	41.74	96.31	60.69	44.80	
8 Light Sandstone - Corey--Weight 76-22 S	83.36	126.18	-80.96	-66.41	40.33	94.52	49.08	37.49	
9 Light Sandstone - Corey--Weight 76-22 TRS	99.84	130.60	-64.66	-42.03	44.47	96.06	49.50	43.75	
10 Light Sandstone - Corey--Weight 76-22 S-A	86.97	135.66	-73.76	-60.67	45.54	96.40	59.25	36.11	
11 Light Sandstone - Corey--Weight 76-22 S-B	84.80	126.27	-81.79	-70.90	45.62	97.59	44.94	35.42	
12 Light Sandstone - Corey--Lion Of 64-22 B	89.68	143.29	-66.62	-60.09	59.59	99.36	79.16	24.76	

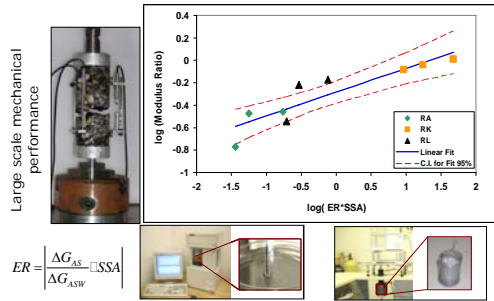
The results page displays all relevant information for every asphalt-aggregate combination you have selected to save. From here it is possible to save the results in a new Excel file, or print them.



The results for a particular combination of aggregate and asphalt are shown in a very easy to read format. These particular results can be saved here or the results from all combinations can be saved in the previous window.

## Recent Advances – Moisture Damage

Comparing Material Property to Mixture Performance - Lab



## Step 2: Dynamic Mechanical Analysis of DMA

Test protocols for the most recent procedure used to prepare, test and analyze performance using DMA have been prepared in AASHTO format.

Preparation and testing of fine graded asphalt mixes by means of the Dynamic Mechanical Analyzer (DMA)



Designation: ACME-Lab DMA PROCEDURE

### 1. SCOPE

This document presents the procedure for specimen preparation, mixture design, testing and data analysis of fine graded asphalt mixtures to be analyzed in the Dynamic Mechanical Analyzer. The document also explains how the results obtained by these procedures can be used in a more complete fracture mechanics model that characterizes viscoelastic materials.

### 2. REFERENCE DOCUMENTS

#### AASHTO Standards

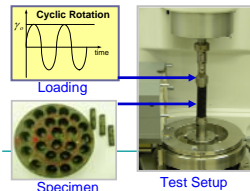
- T 11, Specific Gravity and Absorption of Coarse Aggregates
- T 112, C.A. Protocol and Determining the Density of the Hot-Mix Asphalt (DMA)
- Superpave 19, Control of Aggregate Gradation Compaction
- T 196, Bulk Specific Gravity of Compacted Hot-Mix Asphalt Using Suspended Surface (SUS)
- T 209, Standard Minimum Specific Gravity and Density of Bituminous Paving Mixtures
- T 11, Superpave Volumetric Design for Hot-Mix Asphalt (DMA)
- T 104, Dynamic Determination of Asphalt Stiffness Using Resonant Frequency

### 3. SIGNIFICANCE AND USE

This standard is used to characterize the rheological properties of fine graded asphalt mixtures. The standard refers mainly to two different test methods: Superpave using the DMA, and Superpave 19 using the DMA. Both methods are used to determine the dynamic modulus and phase angle of the asphalt mixtures, which is compared by the Superpave 19 test results.

The results from these procedures can be used to:

- Determine the fatigue life at different test conditions (i.e. temperature and frequency).
- Characterize the continuous damage of the sample in terms of the dissipated power as a function of the number of cycles.



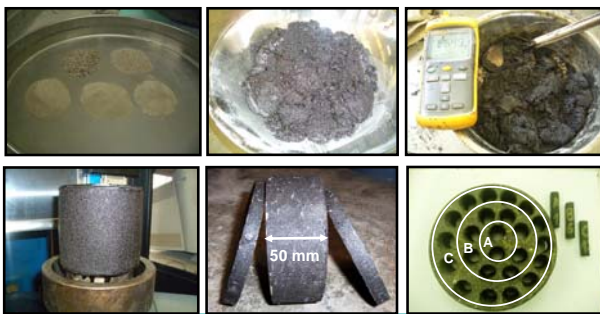
## Standard Contents

- Scope
- Reference documents
- Significance of use
- Summary of method
- Apparatus
- Hazards
- Mix design
- Mix preparation
- Test procedures
- Data analysis
- Key words

## Specimen Preparation

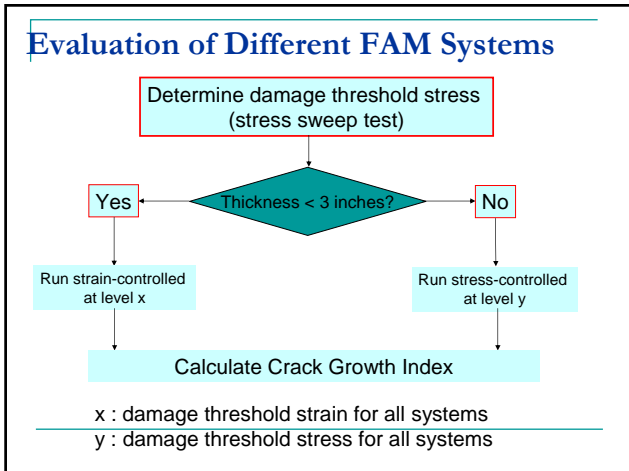
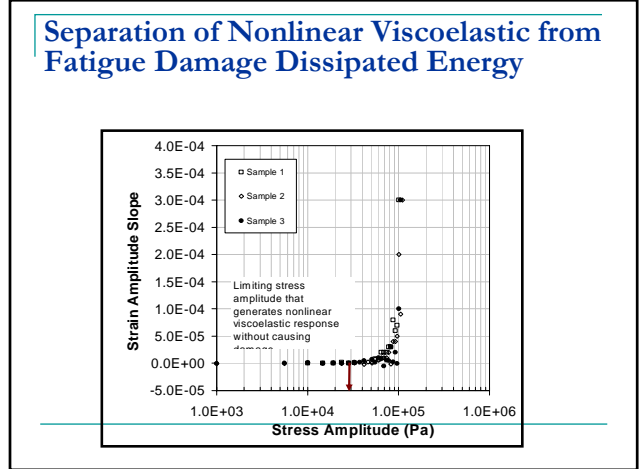
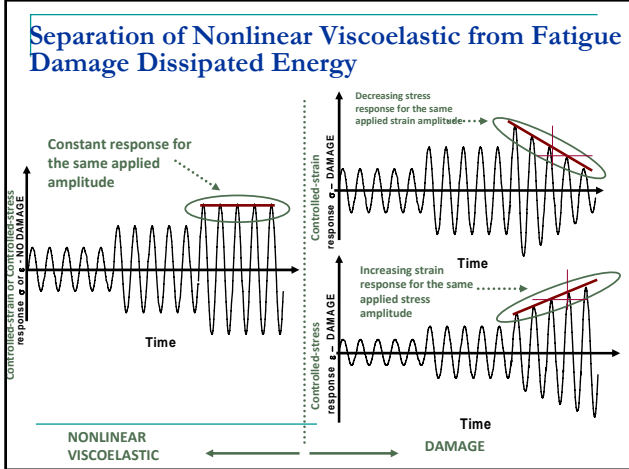
- Prepare gyratory specimens with fine aggregate portion of the mixture
- Use asphalt content similar to the mixture design
- Core 32 DMA specimens from one gyratory specimen

## Specimen Preparation



## DMA Test Method

- Run stress sweep test to determine the load level at which damage initiates
- Determine stress and strain levels at which damage initiates
- Run fatigue test (time sweep test) at stress or strain levels at which damage initiates
- Calculate the crack growth index



### Test Variability

Test	CGI/ R(N)		Fatigue Life		Cumulative DPSE (J/m <sup>2</sup> )	
	Ave.	CV(%)	Ave.	CV(%)	Ave.	CV(%)
CStrain-0.1%	89.38	10	7,200	63	1.3 × 10 <sup>6</sup>	58
CStress-initial	142.10	18	6,620	81	2.7 × 10 <sup>6</sup>	52
CStress-30%	126.26	28	18,000	54	6.1 × 10 <sup>6</sup>	70
CStress-50%	124.70	28	20,250	70	7.2 × 10 <sup>6</sup>	49
CStress-70%	125.41	42	76,750	83	3.3 × 10 <sup>7</sup>	50
CStrain-0.2%	112.25	13	6,325	56	3.5 × 10 <sup>6</sup>	35
CStress-initial*	215.42	6	8,100	84	5.8 × 10 <sup>6</sup>	64
CStress-30%	119.27	3	5,140	55	1.3 × 10 <sup>6</sup>	31
CStress-50%	117.58	17	22,000	75	7.4 × 10 <sup>6</sup>	63
CStress-70%	89.76	36	22,625	47	5.4 × 10 <sup>6</sup>	54
All tests	126.21	28	19,301	111	7.3 × 10 <sup>6</sup>	125
All tests, except*	116.30	15	-	-	-	-

↓ CV

## Test Variability

Parameter	Mixture ID	Controlled-Strain		Controlled-Stress	
		Ave.	CV (%)	Ave.	CV (%)
Fatigue Life	A	69,000	75	139,600	45
	B	6,325	53	22,000	70
	C	7,750	52	20,875	56
Cumulative DPSE (J/m <sup>3</sup> )*	A	7.60×10 <sup>7</sup>	79	3.74×10 <sup>7</sup>	42
	B	4.99×10 <sup>6</sup>	61	3.91×10 <sup>6</sup>	78
	C	6.03×10 <sup>6</sup>	54	6.56×10 <sup>6</sup>	67
CGI at N=50,000*	A	122.34	8	96.85	21
	B	179.03	13	174.44	28
	C	229.97	7	276.26	13

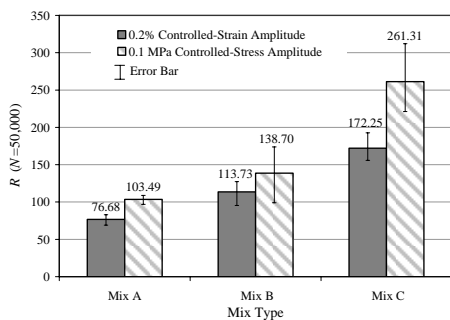
↓ CV

## DMA Results Example

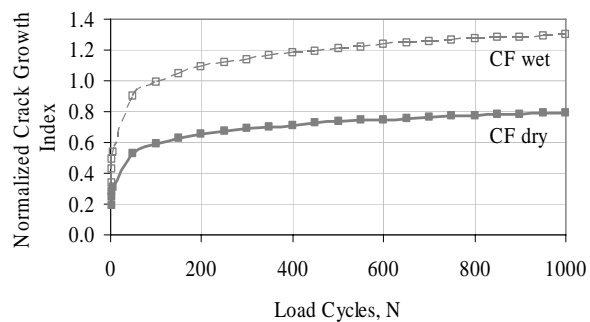
- Asphalt mixes with known field performance from Texas and Ohio

Mix label	Highway	Mix type	Location	Field moisture performance	Aggregate type	Binder grade
AF	Texas	Superpave	Atlanta, TX	Good	River Gravel	PG 76-22
	IH 20					
BF	Ohio	Type 1	Ashland County, OH	Fair to Poor	Gravel, Limestone, Reclaimed Asphalt Pavement (RAP)	PG 64-22
	SR 511					
CF	Ohio	Type 1 Intermediate	Wayne County, OH	Poor	Gravel, RAP	PG 64-28

## DMA Results Example



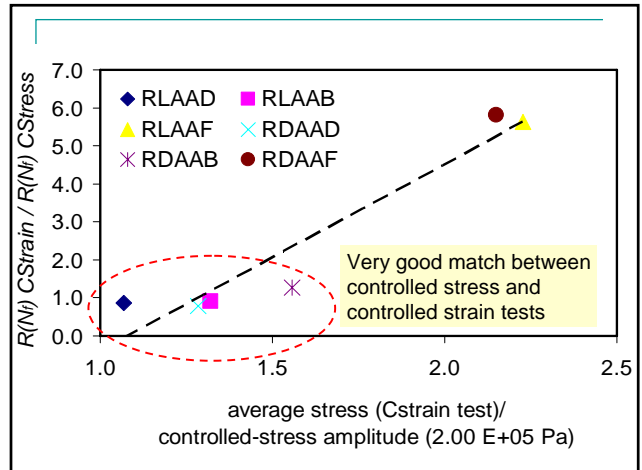
## DMA Results Example



## DMA - Summary

Where we are....

- Great effort to refine specimen fabrication and testing procedures (available in an AASHTO format)
- Use of CSI based on material properties substantially reduces variability in fatigue data
- Within a certain range of stress and strain amplitudes, the tests can be conducted in either controlled-stress or controlled-strain modes



## DMA - Summary

Examples of how we have used the DMA....

- Rank fatigue cracking of FAMs
- Evaluate the effect of fillers (hydrated lime)
- Evaluate the impact of aggregate properties on warm asphalt mixtures
- Impact of moisture conditioning on fatigue cracking life

## DMA - Summary

What we want to do now....?

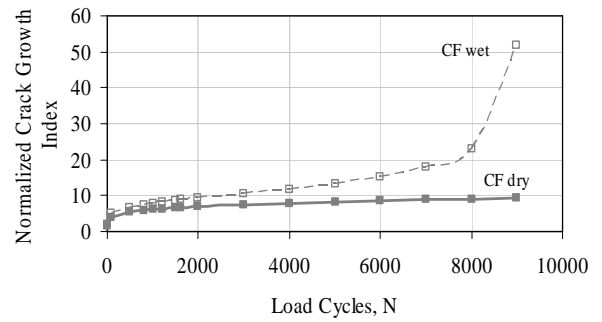
- **Ruggedness testing and standardization**
- Refine the analytical procedures to evaluate results from different modes of loading



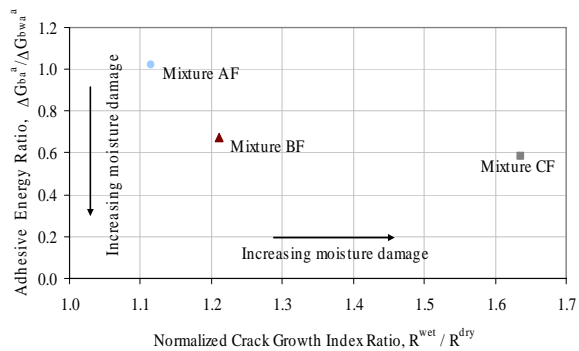
### Step 3: Repeated Direct Tension of Full Mixtures



### Mixture Results



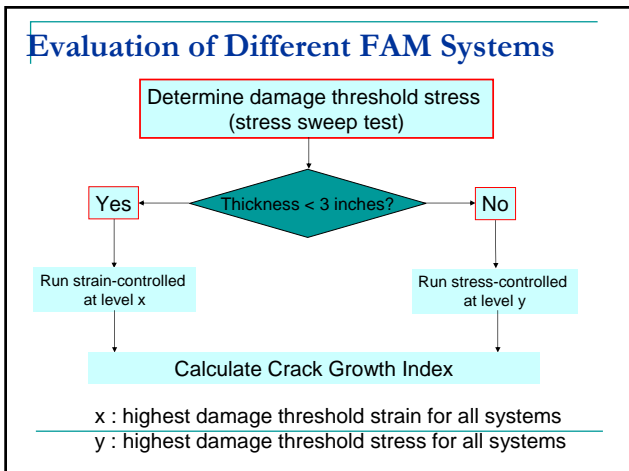
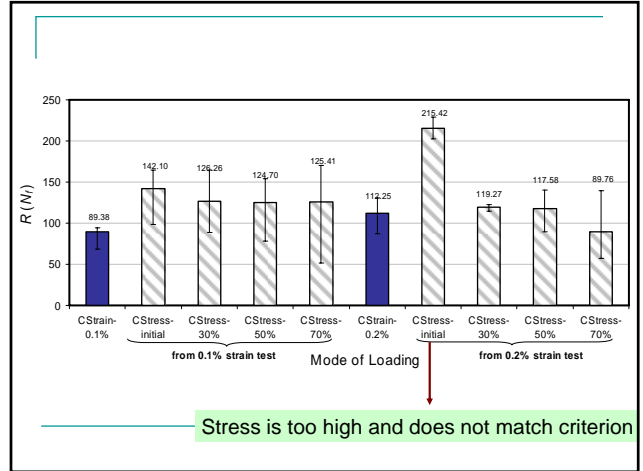
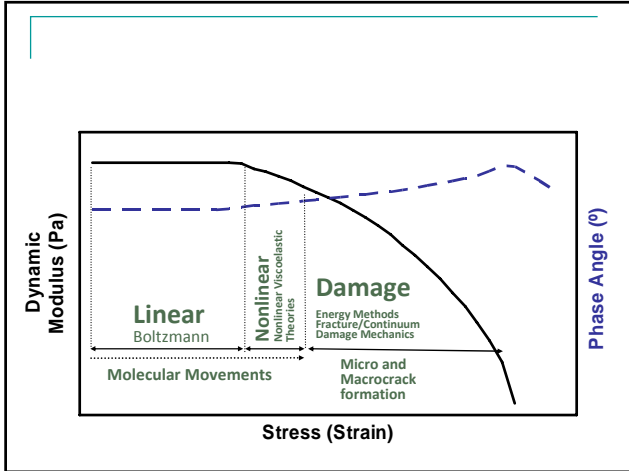
### Bond energy ratio versus normalized crack growth index ratio for the asphalt



### Stress vs. Strain Controlled

- A unified method for the analysis of controlled-stress and controlled-strain tests.
- Both modes of loading give similar ranking provided that:

$$(0.75 \times stress)_{stress\ con} \leq \left( \frac{stress\ @\ N_j + stress\ @\ N=1}{2} \right)_{strain\ con} \leq (1.25 \times stress)_{stress\ con}$$



## **PROGRAM AREA: ENGINEERED MATERIALS**

### **CATEGORY E1: MODELING**

#### **Work element E1a: Analytical and Micro-mechanics Models for Mechanical Behavior of Mixtures (TAMU)**

##### Work Done This Quarter

A technical paper was finished that summarized the theoretical derivation, computer programming and data analysis of the inverse and forward self-consistent micromechanics models. This paper was submitted to The 88<sup>th</sup> Annual Meeting of the Transportation Research Board and has been accepted for presentation.

Preliminary findings on the self-consistent micromechanics models of asphalt mixtures were reported at the 2008 Petersen Asphalt Conference in Laramie, Wyoming, on July 14, 2008. Positive comments were received on the developed models.

A new test protocol was developed to characterize an asphalt mixture's viscoelastic properties that will be taken as an input to the self-consistent micromechanics model that was developed and programmed in the previous quarters. In the newly developed test protocol, an increasing uniaxial tensile stress was applied to a lab-mixed-lab-compacted (LMLC) specimen while the axial and radial deformation of the specimen was recorded and used to calculate the axial and radial strain. The uniaxial tensile load was carefully controlled to assure no damage was introduced to the specimen. The time-dependent stress and axial strain were fit into functions of time. Applying the Laplace transform to the stress function and axial strain function, the relaxation modulus as a function of time was determined using the Boltzmann superposition principle and the convolution theorem. Then the relation between the relaxation modulus and the complex modulus (Findley 1989) was used to determine the complex modulus as a complex function of frequency and the phase angle as a function of frequency.

The test was conducted at three temperatures (10°C, 20°C and 30°C) in order to construct a master curve for the magnitude of the complex modulus and for the phase angle. Less loading time and loading level were applied to the specimen because the specimen was less stiff at a higher temperature and less loading time and level should be used to avoid damaging the specimen. Based on the calculated complex moduli at three temperatures, the time-temperature superposition principle was used to construct the master curves for the magnitude of the complex modulus and the phase angle. Models were developed to fit the master curves. The magnitude of the complex modulus had an S-shape master curve; the phase angle had a master curve whose shape was similar to that of the probability density function of a normal distribution. These findings agree with the viscoelasticity theory.

The viscoelastic Poisson's ratio is another input required for the self-consistent micromechanics model. The newly developed test protocol provided sufficient information for determining the viscoelastic Poisson's ratio as a function of frequency. The axial strain and radial strain were fit

into functions of time. The Laplace transform was applied to the axial strain function and the radial strain function. The Grasley's method (Grasley 2007) was then used to determine the viscoelastic Poisson's ratio as a function of frequency.

Compared to the traditional relaxation modulus test protocol and the dynamic modulus protocol, the newly developed test protocol was more feasible and efficient to characterize the viscoelastic properties of the asphalt mixtures. In addition, the newly developed test did not introduce any damage to the specimen so the same specimen could be re-tested using the repeated direction tension test protocol to obtain the fatigue properties of the same specimen.

### Significant Results

The theoretical derivation, computer programming and data analysis were presented and documented for the inverse and forward self-consistent micromechanics models of an asphalt mixture.

A new test protocol was developed that was able to provide sufficient information to characterize the viscoelastic properties of asphalt mixtures. These viscoelastic properties are required inputs of the inverse and forward self-consistent micromechanics models.

### Significant Problems, Issues and Potential Impact on Progress

The aggregate test equipment at the Petroleum Engineering Department at Texas A&M University was not in a working condition so test could not be conducted to determine the frequency-dependent modulus of aggregate specimens cored from the large aggregates including Limestone, River Gravel and Sandstone. The test has to be delayed until the equipment is fixed if other equipment is not identified that is capable of testing the mechanical properties of the aggregate.

### Work Planned Next Quarter

The viscoelastic anisotropic properties of the asphalt mixtures under compressive loading will be tested using the Universal Testing Machine (UTM) and the Rapid Triaxial Test (RaTT) Cell. The RaTT cell will be mounted in the UTM and triaxial stress will be applied to the specimen. The axial and radial displacement of the specimen will be recorded and used to determine the viscoelastic properties of the material in the compaction direction and in the direction which is perpendicular to the compaction direction. These viscoelastic anisotropic properties will be taken as inputs to the self-consistent micromechanics models.

The progress in repairing the aggregate test equipment at the Petroleum Engineering Department will be followed so machine time can be scheduled as soon as the equipment is repaired. A search will be conducted for other equipment that might be available to independently determine the frequency-dependent properties of aggregate specimens.

## Cited References

Findley, W. N., J. S. Lai, and K. Onaran, 1989, *Creep and Relaxation of Nonlinear Viscoelastic Materials with an Introduction to Linear Viscoelasticity*. Dover Publication, Inc., Mineola, New York.

Grasley, Z. C., 2007, "Analysis of the Viscoelastic Poisson's Ratio as Applied to Portland Cement Paste." Unpublished work.

## **Work element E1b: Binder Damage Resistance Characterization (DRC) (UWM)**

### ***Subtask E1b-1: Rutting of Asphalt Binders***

#### Work Done This Quarter

In the previous quarter, the study on the effect of changing geometry and film thickness was completed. It was found that the cone-and-plate geometry delays the start of tertiary flow seen in the parallel-plate geometry, particularly at high stresses (up to 20 KPa) and high temperatures (70 °C). It was also found that using the parallel plates with film thickness of 275 μm can have the same effect as using the cone-and-plate geometry, and the response measured for a number of asphalt binders matches very well with the results of the cone-and-plate geometry.

In this quarter, the focus was placed on studying effects of temperatures and loading pattern (loading versus unloading time) on the creep behavior of selected modified and unmodified binders. Based on statistical analysis, temperature was identified as the second most important factor (following stress) that controls binder behavior. A phenomenological model was developed to predict the effects of stress and temperature on the permanent strain measured in the Dynamic Shear Rheometer (DSR) after different numbers of cycles or loading times.

The research team used the results collected in the past year to write two technical papers that were completed and submitted to two conferences. Both papers were accepted and critical review comments from the peer review process were incorporated into the final papers.

#### Significant Results

Table E1b-1.1 lists the full factorial design for the parameters of loading pattern, temperature, stress level and modification that were varied in the experiment. The first part of the table, runs 1 through 16, represent the first replicate, and the second half, runs 17 through 32, represent the second replicate. The tests were not run in the order of the test number, but rather in the randomized order that the Minitab software suggested.

Table E1b-1.1. Experimental design for studying effect of loading pattern and temperature on creep behavior.

Test No.	A Loading Pattern (-1=1-9, 1=3-27)	B Temperature (°C) (-1=46C, 1=58C)	C Stress Level (Pa) (-1=1000, 1=20000)	D Modification (-1=No, and 1=Yes)
1	-1 (1C9R)	-1 (46C)	-1 (1000)	-1 (FH 64)
2	1 (3C27R)	-1 (46C)	-1 (1000)	-1 (FH 64)
3	-1 (1C9R)	1 (58C)	-1 (1000)	-1 (FH 64)
4	1 (3C27R)	1 (58C)	-1 (1000)	-1 (FH 64)
5	-1 (1C9R)	-1 (46C)	1 (20000)	-1 (FH 64)
6	1 (3C27R)	-1 (46C)	1 (20000)	-1 (FH 64)
7	-1 (1C9R)	1 (58C)	1 (20000)	-1 (FH 64)
8	1 (3C27R)	1 (58C)	1 (20000)	-1 (FH 64)
9	-1 (1C9R)	-1 (46C)	-1 (1000)	1 (LSBS 5% 76)
10	1 (3C27R)	-1 (46C)	-1 (1000)	1 (LSBS 5% 76)
11	-1 (1C9R)	1 (58C)	-1 (1000)	1 (LSBS 5% 76)
12	1 (3C27R)	1 (58C)	-1 (1000)	1 (LSBS 5% 76)
13	-1 (1C9R)	-1 (46C)	1 (20000)	1 (LSBS 5% 76)
14	1 (3C27R)	-1 (46C)	1 (20000)	1 (LSBS 5% 76)
15	-1 (1C9R)	1 (58C)	1 (20000)	1 (LSBS 5% 76)
16	1 (3C27R)	1 (58C)	1 (20000)	1 (LSBS 5% 76)
17	-1 (1C9R)	-1 (46C)	-1 (1000)	-1 (FH 64)
18	1 (3C27R)	-1 (46C)	-1 (1000)	-1 (FH 64)
19	-1 (1C9R)	1 (58C)	-1 (1000)	-1 (FH 64)
20	1 (3C27R)	1 (58C)	-1 (1000)	-1 (FH 64)
21	-1 (1C9R)	-1 (46C)	1 (20000)	-1 (FH 64)
22	1 (3C27R)	-1 (46C)	1 (20000)	-1 (FH 64)
23	-1 (1C9R)	1 (58C)	1 (20000)	-1 (FH 64)
24	1 (3C27R)	1 (58C)	1 (20000)	-1 (FH 64)
25	-1 (1C9R)	-1 (46C)	-1 (1000)	1 (LSBS 5% 76)
26	1 (3C27R)	-1 (46C)	-1 (1000)	1 (LSBS 5% 76)
27	-1 (1C9R)	1 (58C)	-1 (1000)	1 (LSBS 5% 76)
28	1 (3C27R)	1 (58C)	-1 (1000)	1 (LSBS 5% 76)
29	-1 (1C9R)	-1 (46C)	1 (20000)	1 (LSBS 5% 76)
30	1 (3C27R)	-1 (46C)	1 (20000)	1 (LSBS 5% 76)
31	-1 (1C9R)	1 (58C)	1 (20000)	1 (LSBS 5% 76)
32	1 (3C27R)	1 (58C)	1 (20000)	1 (LSBS 5% 76)

The statistical analysis results for the response of permanent strain at the end of 10 cycles are shown in figure E1b-1.1. The main effects plots show that temperature, stress level and modification are the most important factors for this response.

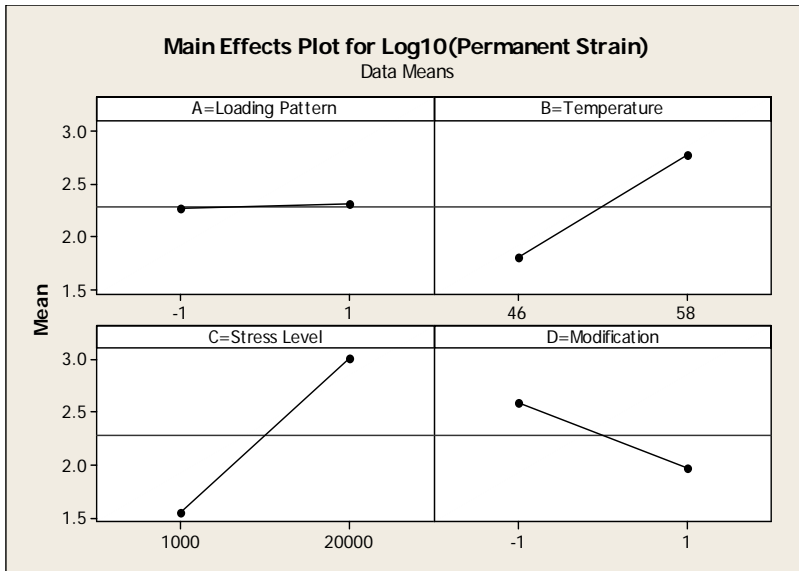


Figure E1b-1.1. Graphs. Main effects plots for log of response.

The analysis also showed that the effects of these factors have limited interaction and can be included in modeling as additive factors. The two-way interaction plots are shown in figure E1b-1.2. The results show that even at stress levels of 20,000 Pa, there are not any interactions with other factors.

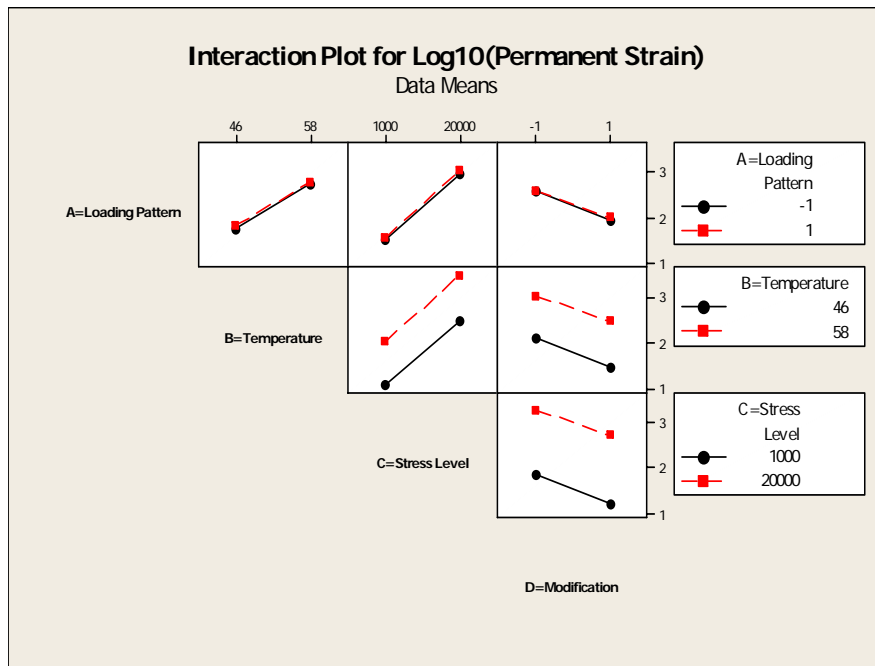


Figure E1b-1.2. Graphs. Two-way interactions plots for log transform of response.

The efforts on modeling continued this quarter. A model already exists that predicts permanent strain in specific temperature. The model, which was based on the power law with two arguments, could give the total deformations for different stress levels and loading time at a given temperature:

$$\gamma_{Binder}(t, \tau) = k_1 \cdot t^{m_1} \cdot \tau + k_2 \cdot t^{m_2} \cdot \tau^{p_2}$$

where

$\gamma$  is shear strain (dimensionless),

$t$  is time (s),

$\tau$  is shear stress (kPa), and

$k_i$ ,  $m_i$  and  $p_i$  are model parameters. These parameters vary from binder to binder.

To include the temperature effects, it was found that the log of the permanent strain is a linear function of temperature. Therefore, the relation between permanent strain and temperature can be obtained as:

$$\text{Log}_{10} \gamma = C (T - T_{\text{Ref}})$$

where

$C$  is a temperature shift factor,

$T$  is the temperature at which strain is predicted, and

$T_{\text{Ref}}$  is the temperature at which the test was conducted.

An example of temperature versus log strain is shown in figure E1b-1.3.

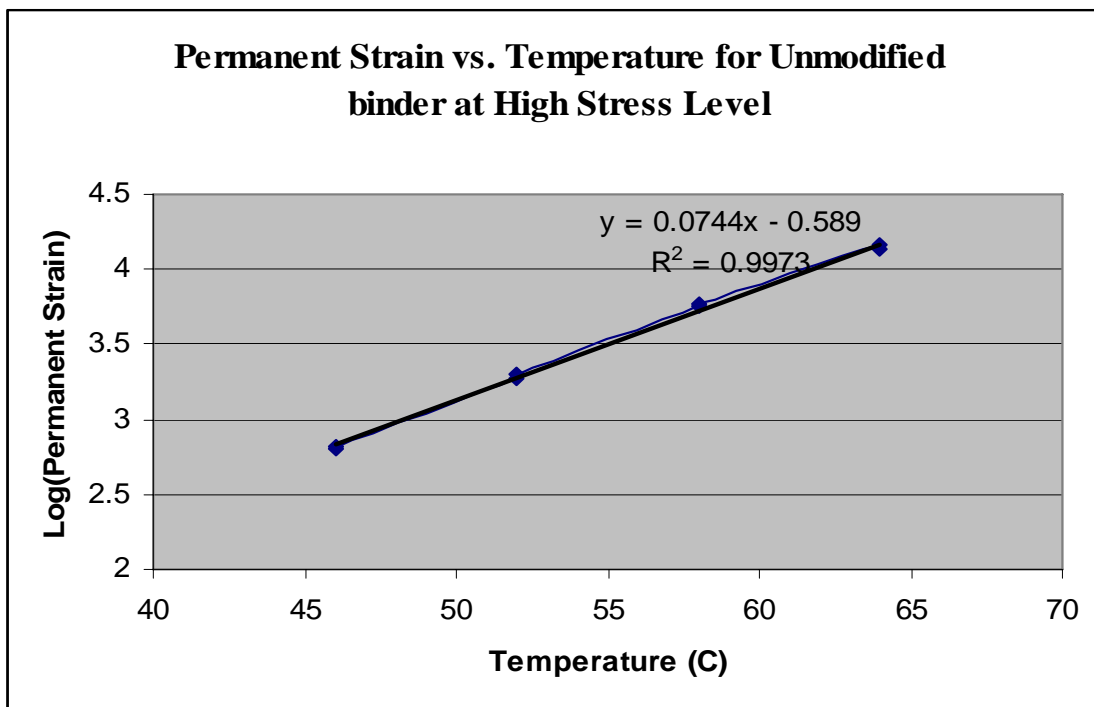


Figure E1b-1.3. Graph. Example of change in strain as a function of temperature.



The model was verified by testing three asphalts and by using it to predict the Multiple Stress Creep and Recovery (MSCR) test results at different temperatures. Figure E1b-1.4 depicts the results of the MSCR test and shows the fit. Table E1b-1.2 lists the measured and predicted values and the margin of error.

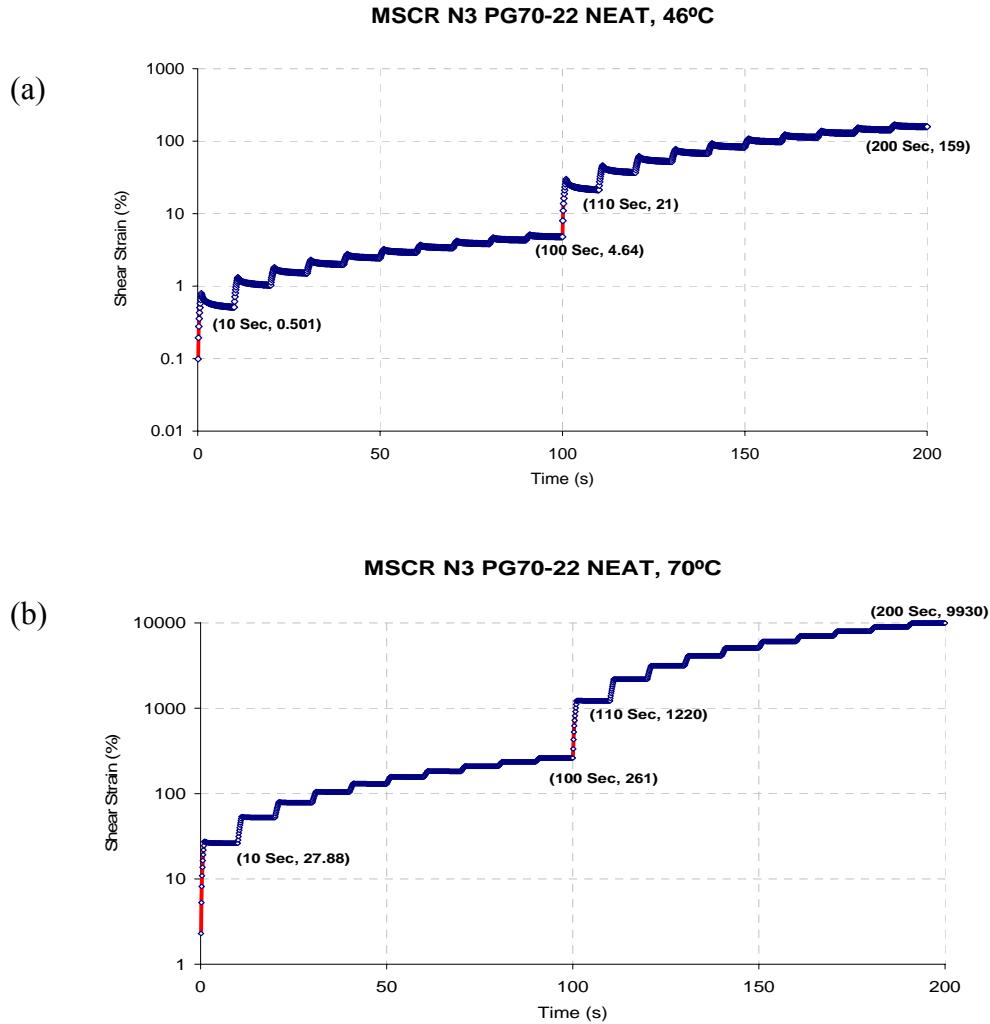


Figure E1b-1.4. Graphs. MSCR test result for neat PG 70-22 grade binder at two different temperatures, (a) 46 °C and (b) 70 °C.

Table E1b-1.2. Measured and predicted strain at different cycles in the MSCR test.

Time (s)	Strain (%) at Reference Temperature (46 °C)	Strain at Target Temperature 70 °C		
		Measured	Predicted Value (from Model)	Error %
10	0.501	27.88	30.74947646	9.33
100	4.64	261	284.7855704	8.35
110	21	1220	1288.900211	5.34
200	159	9930	9758.815882	1.75

As seen in table E1b-1.2, the error is within the acceptable range for different cycles. The results confirm that the linear temperature shift factor can be used for any loading pattern history and for any cycle.

#### Significant Problems, Issues and Potential Impact on Progress

None.

#### Work Planned Next Quarter

Testing next quarter will continue for other binders. Testing of mastics will also begin.

#### ***Subtask E1b-2: Feasibility of Determining Rheological and Fracture Properties of Thin Films of Asphalt Binders and Mastics using Nano-indentation (Year 2 start)***

#### Work Done This Quarter

The literature search continued this quarter. A list of studies (shown below) represents those studies that will be reviewed in detail to develop a literature review report and used to design the experiment details.

Beake, B., 2006, Modelling indentation creep of polymers: a phenomenological approach. *Journal of Physics, D. Applied Physics*, 39(20): 4478-4485.

Cook, R. F., and M. L. Oyen, 2007, Nanoindentation behavior and mechanical properties measurement of polymeric materials. *International Journal of Materials Research*, 98(5): 370-378.

Ingolf Schiffmann, K., 2006, Nanoindentation creep and stress relaxation tests of polycarbonate: Analysis of viscoelastic properties by different rheological models. *International Journal of Materials Research*, 97(9): 1199-1211.

Li, X., and B. Bhushan, 2002, A review of nanoindentation continuous stiffness measurement technique and its applications. *Materials Characterization*, 48(1): 11-36.

Lin, D. C., E. K. Dimitriadis, and F. Horkay, 2006, Advances in the mechanical characterization of soft materials by nanoindentation. *Recent Res. Devel. Biophys.*, 5.

Oyen, M. L., 2006, Nanoindentation hardness of mineralized tissues. *Journal of Biomechanics*, 39(14): 2699-2702.

Oyen, M. L., and C. C. Ko, 2007, Examination of local variations in viscous, elastic, and plastic indentation responses in healing bone. *Journal of Materials Science: Materials in Medicine*, 18(4): 623-628.

Partl, M. N., K. Scrivener, and P. J. M. Bartos, 2006, From Nanocem to Nanobit– Perspective on Nanotechnology in Construction Materials with a Focus on Asphaltic Materials. NSF Workshop on Nanomodifications of Cementitious Materials, August 8-11, 2006.

Pichler, C., A. Jäger, R. Lackner, and J. Eberhardsteiner, 2005, Identification of Material Properties from Nanoindentation: Application to Bitumen and Cement Paste. 22nd DANUBIA-ADRIA Symposium on Experimental Methods in Solid Mechanics, 198-199.

Yeh, S.-K., 2003, Alkaline Durability Tests for E-Glass/Vinyl Ester Reinforced Polymer with Nanoclay. Master of Science Thesis, Department of Chemical Engineering, West Virginia University.

### Significant Results

The literature search was completed, and a set of important studies for detailed review was prepared.

### Significant Problems, Issues and Potential Impact on Progress

Work was significantly delayed in waiting for approval of the Year 2 work plan. This work element includes collaboration with the University of Minnesota, but work was not started due to uncertainty about approvals.

### Work Planned Next Quarter

Next quarter, the research team will:

- Continue the literature review and the identification of equipment.
- Explore the use of nanoindentation devices.
- Begin exploratory tests on binder specimens in collaboration with the University of Minnesota.
- Draft an analysis methodology.

## **Work Element E1c: Warm and Cold Mixes**

### ***Subtask E1c-1: Warm Mixtures***

#### Work Done This Quarter

##### *Investigation of Effects of Warm Mix Additives on the Rheological Properties of Binders*

Binder testing focused on the effects of the addition of 2% Sasobit on predicted mixing and compaction temperatures and change in PG grading of two binders. The concentration of

Sasobit was determined based on industry recommendations. The binders used were a neat PG 64-22 and a polymer-modified PG 76-22 from the same source. Mixing and compaction temperatures were estimated using zero-shear viscosity (ZSV) as predicted by the Cross-Williamson model. Changes in grade were measured using the Superpave parameters of  $G^*/\sin\delta$  and  $G^*\cdot\sin\delta$ . Testing for high temperature grade was conducted on original binders and rolling thin film oven (RTFO)-aged binders. Fatigue binder parameter testing was conducted on pressure aging vessel (PAV)-aged binders. Aging procedures used were consistent with current Superpave specifications. Data are presented in tables E1c-1.1 and E1c-1.2.

#### *Evaluation of the Effects of Warm Mix Additives on Workability and Stability of Mixes*

The testing matrix to quantify the effects of Advera on mixture workability and stability presented in the ARC Q2 2008 report was completed. Data were collected and the initial analysis is 75% complete; further work is required to finalize the analysis and summarize the results. Analysis of both the volumetric and energy indices was performed on the compaction data. Volumetrics are analyzed in terms of change in air voids and Voids in Mineral Aggregate (VMA) as a function of temperature and warm mix asphalt (WMA) additive type. The level of gyrations to achieve 92% Gmm (maximum specific gravity) for the HMA compacted at 135 °C was defined as the baseline for the analysis of air voids. More direct measurements of the effects of Advera on mixture workability have been implemented through analysis of the Construction Densification Index (CDI) and the Construction Energy Index (CEI). Results are presented in figures E1c-1.1 and E1c-1.2 later in this report.

Analysis of mixture stability data was delayed due to the inability of the mixes compacted at lower pressures (300 kPa) to reach 98% Gmm after 600 gyrations. By definition, the traffic indices are based on the energy required to densify a mix from 92% Gmm to 98% Gmm. Therefore, mixes that did not reach the 98% Gmm threshold could not be analyzed directly. The research team has implemented the use of linear and exponential models to estimate the number of gyrations necessary to reach the 98% Gmm threshold. This allows for estimation of mixture stability. Results of this analysis will be presented next quarter.

#### *Project Coordination with University of Nevada, Reno*

The research team from the University of Wisconsin–Madison met with University of Nevada, Reno during the Mixtures ETG meeting September 17 to develop a plan for collaboration. It was decided that four warm mix technologies would be investigated: mineral additive (Advera), wax additive (Sasobit), surfactants and foaming. The effects of each on binder rheological properties and mixture workability will be evaluated by UW–Madison. A report will be generated and reviewed by both universities to determine pertinent mixture performance tests for a given warm mix technology. Performance testing will be conducted at the University of Nevada, Reno. Sharing of materials was also discussed to ensure that common materials are tested at both sites.

### *Field Project Selection and Coordination*

University of Nevada, Reno is working with Granite Construction to identify and collect materials from field projects in the region. The sites listed in the previous quarterly reports are still candidates, but project selection has yet to be finalized.

The UW–Madison research team and Dr. Robert Schmitt of UW–Platteville attended a field demonstration September 12 involving the use of a surfactant-based technology developed and marketed by a local contractor. The project had three different test sections:

- E1 mix design including 20% recycled asphalt pavement (RAP), HMA.
- E1 mix design including 30% RAP, WMA.
- E1 mix design including 40% RAP, WMA.

Temperatures behind the screed were around 135 °C for the HMA and 105 °C for the WMA. The quantity placed for each WMA section was approximately 700 tons. In-place densities were collected after each roller pass using a nuclear density gage, and materials were collected to perform laboratory evaluations of mixture workability. Extra material was collected to possibly conduct dynamic modulus ( $E^*$ ) and flow number (FN) performance testing as well. Laboratory and field data are currently being analyzed to investigate relationships between laboratory and field compaction. UW–Madison and UW–Platteville are involved in a similar study for HMA with the Wisconsin Department of Transportation. Data generated through both these efforts provide an opportunity for initial comparisons between HMA and WMA, and will be included in the next quarterly report. A second field project is being planned for early November, and it is expected that the research team will conduct similar testing.

### *Laboratory Testing to Evaluate WMA Foaming Technologies*

Wirtgen has supplied the research team at UW–Madison with a WLB10 laboratory foaming device for use in both tasks E1c-1 and E1c-2. An experimental plan is under development to quantify the impacts of foaming on binder rheological properties and mixture workability and performance. An initial set of mixes was prepared with binder foamed at 165 °C and 2% water. The aggregates were heated to a temperature of 125 °C and mixed with the foamed asphalt. Mixes were short-term aged and compacted at 110 °C. The effects of the foamed asphalt on compaction densification and energy indices were compared to conventional HMA and WMA prepared with Advera. Results are presented in figure E1c-1.3.

### *Assessing the Environmental/Economic Benefits of Warm Mix*

Through work with John Patrick of OPUS Consulting, a report and spreadsheet tool were identified as a potential analysis method to quantify the reduced energy consumption and emissions associated with use of WMA technologies and the associated economic implications (Patrick and Arampamoorthy 2007). A graduate student has been assigned to review this and other analysis methods.

## Significant Results

### *Investigation of Effects of Warm Mix Additives on the Rheological Properties of Binders*

Using the ZSV concept, the mixing and compaction temperatures were estimated by finding the temperature at which the ZSV was 3.0 Pa-s and 8.0 Pa-s respectively. A summary of the effect of 2% Sasobit on mixing and compaction temperatures is provided in table E1c-1.1.

Table E1c-1.1. Reduction in mixing and compaction temperatures due to the addition of 2% Sasobit.

Binder	Average Compaction Temp (°C)	Average Mixing Temp (°C)
PG 64-22	-7.05	-11.35
PG 76-22	3.05	4.25

Initial testing showed that the addition of Sasobit reduced mixing and compaction temperatures for the unmodified binder by 11 °C and 7 °C, respectively. However, test results for the modified binder showed a slight increase in both mixing and compaction temperatures. Two replicates of each sample were tested, and standard deviations for both binders were approximately 2.5 °C. The data presented will be compared to results of mixture workability testing next quarter.

Results of Superpave binder grading show that the addition of 2% Sasobit increases the high temperature grade of the unmodified binder to PG 70. However, the high temperature grade of the modified binder remains unchanged as it fails to pass the Superpave criteria at a testing temperature of 82 °C. All samples met the Superpave fatigue specification;  $G^* \cdot \sin \delta$  was conducted at the intermediate temperature associated with the binder grades determined in table E1c-1.2.

Table E1c-1.2. Effect of 2% Sasobit on the Superpave binder rutting parameter  $G^*/\sin\delta$ .

Base Grade	Additive	Aged	$G^*/\sin(\delta)$ kPa		Standard Deviation	$G^*/\sin(\delta)$ kPa @ HT + 6C		Standard Deviation	Grade
			@ HT	Average		Average	Average		
PG 64-22	Neat	OB	1.42	1.42	0.00	0.68	0.69	0.00	PG 64-22
			1.42			0.69			
		RIFO	4.01	3.85	0.22	1.88	1.82	0.09	
			3.69			1.75			
	Sasobit 2%	OB	2.33	2.50	0.24	1.13	1.27	0.20	
			2.67			1.41			
RIFO		-	-	-	2.67	2.46	0.31		
		-	-	-	2.24				
PG 76-22	Neat	OB	1.14	1.17	0.04	0.63	0.64	0.02	PG 76-22
			1.21			0.66			
		RIFO	2.57	2.57	0.00	1.40	1.42	0.02	
			2.57			1.43			
	Sasobit 2%	OB	1.49	1.48	0.01	0.90	0.88	0.02	
			1.48			0.87			
		RIFO	2.84	2.79	0.07	1.56	1.55	0.01	
			2.74			1.54			

*Evaluation of the Effects of Warm Mix Additives on Workability and Stability of Mixes*

The effects of Advera on mixture workability for the compaction temperatures of 135 °C, 110 °C and 90 °C as measured by the CEI are represented in figure E1c-1.1. This figure shows percent reduction in CEI due to the addition of Advera. A negative result indicates an increase in the CEI value.

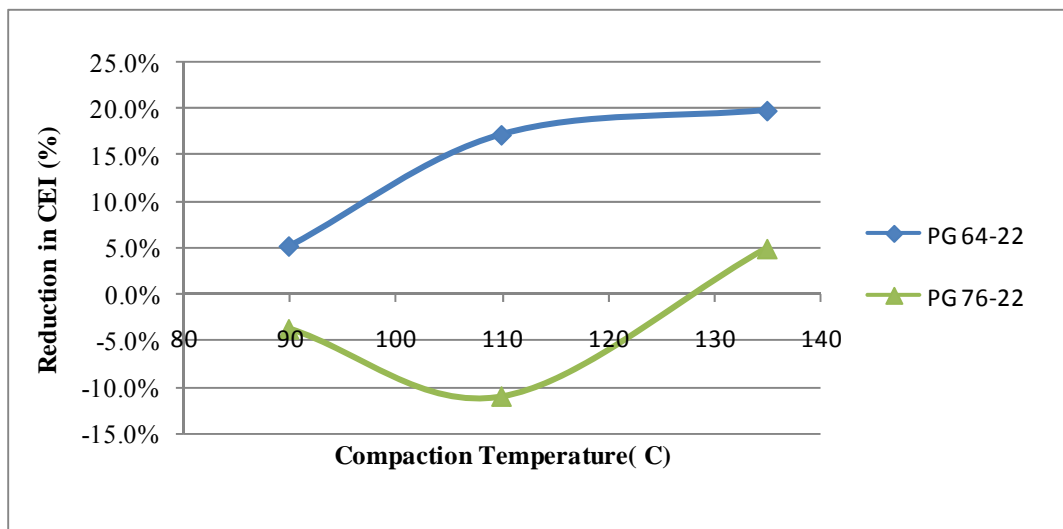


Figure E1c-1.1. Graph. Percent reduction in Construction Energy Index due to Advera for compaction at 300 kPa.

Results presented in figure E1c-1.1 show drastically different effects on workability (as measured by CEI) based on binder type. For the unmodified PG 64-22 binder, the addition of Advera enhances workability for all compaction temperatures ranging from 5% reduction in CEI at the lowest compaction temperature up to an approximately 20% decrease for compaction at 110 °C and 135 °C. The definition of CEI is the energy required to compact the mix from the density behind the screed to 92% Gmm. Therefore, a 20% reduction in CEI indicates that the addition of Advera produces a considerably more workable mix. Conversely, there is no effect of Advera on mixture workability for the modified binder until 135 °C. Two replicates were run for each mix. Mixes prepared with the unmodified binder had coefficients of variation under 3%, and mixes prepared with the modified binder had coefficients of variation of approximately 10%.

*Laboratory Testing to Evaluate WMA Foaming Technologies*

The ability of the Wirtgen WLB10 foaming machine to produce adequate mix for this subtask was evaluated through a trial in which two samples were mixed at 125 °C and compacted at 110°C. The PG 64-22 unmodified asphalt was foamed and sprayed directly on the aggregate and immediately mixed using a bucket mixer. Samples were compacted to 495 gyrations at 300 kPa and 600 kPa. The CDI and Traffic Densification Index (TDI) were obtained and compared to results of the HMA and WMA using Advera. These results are presented in figures E1c-1.2 and E1c-1.3.

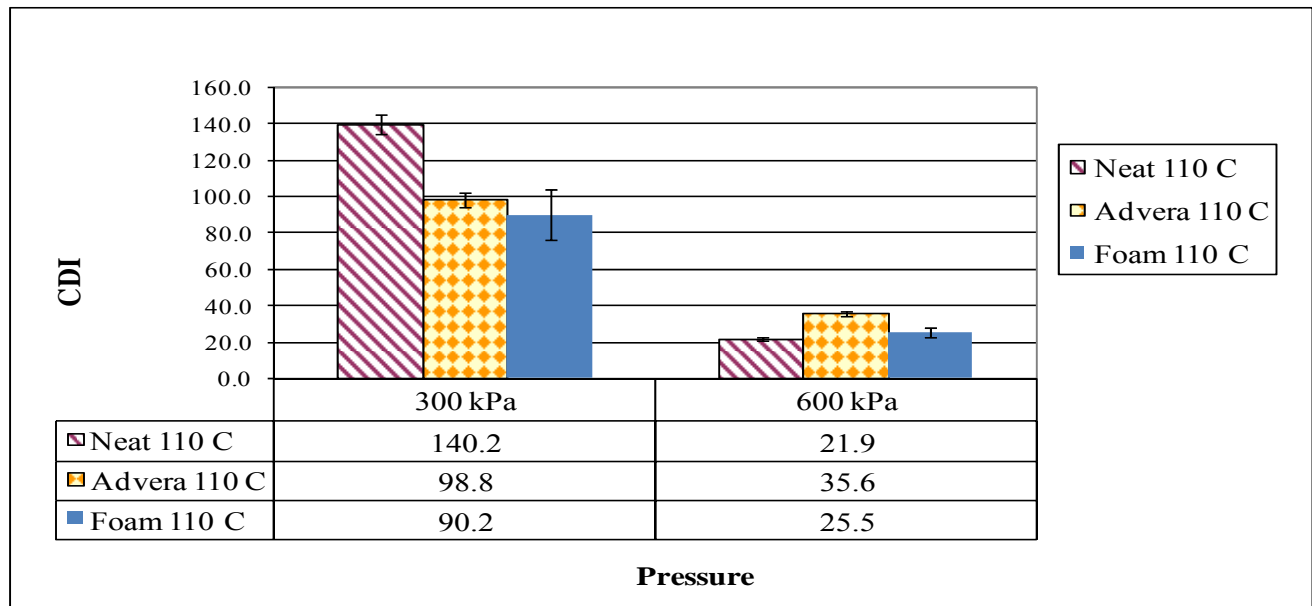


Figure E1c-1.2. Graph. Comparison of the effects of Advera and foaming on Construction Densification Index at 110 °C.

Results in figure E1c-1.2 indicate that the effects of foaming using the sample preparation procedures provided in this report are similar to those of Advera. At 300 kPa, both WMA technologies show a significant reduction in CDI, indicating enhanced workability. However, at a compaction pressure of 600 kPa, there is no significant difference between the CDI values for



the warm mix technologies relative to conventional HMA. It is hypothesized that resistance to densification at the higher compaction pressure is so small that the CDI is insensitive to the addition of WMA additives.

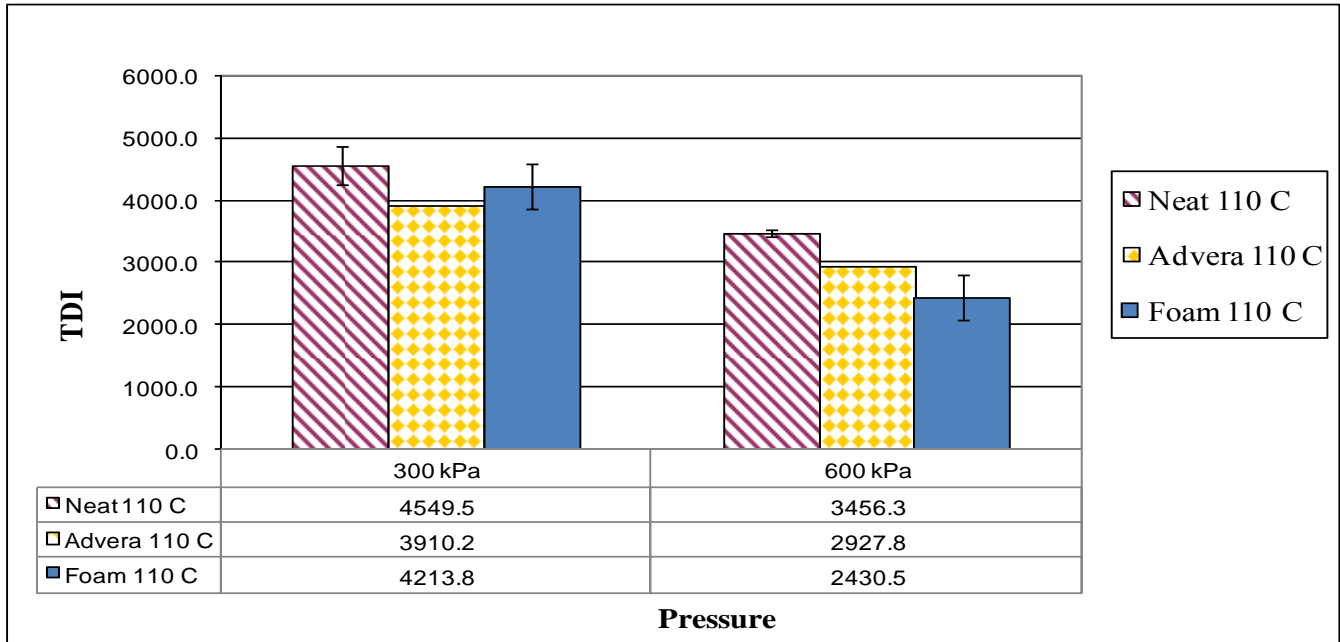


Figure E1c-1.3. Graph. Comparison of the effects of Advera and foaming on Construction Densification Index at 110 °C.

TDI is an indicator of the ability of a mix to resist permanent deformation. Work at UW–Madison has shown this index correlates well with mixture resistance to permanent deformation as measured by the FN (Mahmoud and Bahia 2004). Comparison of the TDI for the foamed mix to results of the HMA and WMA produced with Advera was conducted to ensure the laboratory foaming procedure was creating WMA consistent with the process in the field. Use of foaming in WMA technologies produces a mix that can be immediately compacted and opened to traffic, similar to HMA and other warm mix technologies. The similarity between all three mix types indicates that the laboratory foaming procedure produces a suitable mix for further evaluation. However, this assumption should be verified through mechanical testing.

Significant Problems, Issues and Potential Impact on Progress

Delays were encountered in measurement of the effect of WMA additives on binder rheological properties due to development of blending procedures to properly quantify the impact of Advera on mixture workability. As reported in the previous quarterly reports, attempts to use normal force measurements to indicate lubrication effects and measurements of reduction in viscosity were unsuccessful. Review of other potential mechanisms and test methods to quantify the enhanced workability seen in mixture testing has delayed binder characterization for Advera by two months. Moving forward, parallel efforts will be conducted to measure the effect of Advera

on binder performance properties as the mechanisms for enhanced workability are being investigated.

To fulfill the mixture workability and stability task, the research team must also obtain a device capable of measuring mix workability before compaction. The Nynas workability tester and the torque tester developed by University of Massachusetts Dartmouth have been identified as potential devices. The research team must select and obtain this equipment. At this time, the issue has not caused significant delays.

The Gantt chart for this subtask indicates that a journal paper was to be submitted to TRB in August. This milestone was not met due to the research team having sufficient binder and mixture data for only one additive. The research team decided to delay publication of journal papers until it had a more comprehensive data set, including different WMA technologies and mixture performance testing results.

The Wirtgen WLB10 is not capable of foaming asphalt with similar water concentrations to the Astec system currently being used in double-barrel drum plants. The Astec system uses 1% water, but the WLB10 is capable of a minimum of 2% water. The research team will investigate the feasibility of reducing the water content to 1%.

To date, the research team has collected field data from only one project, but continues to coordinate with industry in both the Midwest and western regions of the United States to identify field projects. The research team continues to work with industry partners and provide data and support to assist in organizing field projects. The activity has been delayed two months.

#### Work Planned Next Quarter

The research team will complete the following tasks related to binder properties next quarter:

##### *Investigation of Effects of Warm Mix Additives on the Rheological Properties of Binders*

- Complete the evaluation of Sasobit, including testing of low temperature properties and more advanced methods for evaluation of binder rutting (Multiple Stress Creep and Recovery [MSCR] test) and fatigue (Binder Yield Energy Test [BYET]).
- Complete the performance evaluation of Advera and continue to review potential test methods to measure the effects of Advera on workability.
- Develop an experimental plan for rheological evaluation of foamed asphalts.

##### *Evaluation of the Effects of Warm Mix Additives on Workability and Stability of Mixes*

- Finish the analysis of compaction data collected for Advera and recompact samples as needed.
- Complete the test matrix presented in the ARC Q2 2008 report for Sasobit.

- Select either the Nynas workability tester or University of Massachusetts Dartmouth torque tester to measure mixture workability and begin testing.

#### *Mixture Performance Testing*

- Review binder and mixture testing results with University of Nevada, Reno to define appropriate performance tests for a given additive. UW–Madison will submit reports for Advera and Sasobit for review.
- Develop an experimental plan with University of Nevada, Reno to coordinate binder, mixture workability and mixture performance testing on a common set of materials.

#### *Field Project Selection and Coordination*

- Work with industry contacts in Wisconsin for field testing and materials sampling projects, tentatively scheduled for early November, and complete materials testing and data analysis for these projects.
- Continue to work with industry for future field project opportunities.

#### *Assessing the Environmental/Economic Benefits of Warm Mix*

- Continue the review of current analysis methods available to quantify the environmental and economic benefits of WMA, including review of emission and energy consumption values used in analysis to ensure they are consistent with practices in the United States.

#### Cited References

Mahmoud, A. F., and H. Bahia, 2004, Using the Gyrotory Compactor to Measure Mechanical Stability of Asphalt Mixtures. Report WHRP 05-02. Wisconsin Highway Research Program.

Patrick, J., and H. Arampamoorthy, 2007, Quantifying the Benefits of Waste Minimisation. Report prepared by OPUS Engineering Consultants, Land Transport New Zealand.

#### ***Subtask E1c-2: Development and Evaluation of a Volumetric Mix Design Process for Cold Mix Asphalt***

##### Work Done This Quarter

Efforts this quarter were related to laboratory evaluation of emulsions and quantifying energy consumption used in the application of emulsion technologies relative to conventional HMA.

##### *Evaluation of emulsions*

In evaluating emulsions, the research team focused on testing, data analysis and publishing two papers related to this subtask.

- Hanz, A., Z. Arega, and H. Bahia, 2008, Rheological Characterization of Emulsion Residues Recovered Using Newly Developed Evaporative Techniques. Submitted to TRB Committee AFK 50 for review. Comments have not yet been received.
- Hanz, A., Z. Arega, and H. Bahia, 2008, Advanced Methods for Quantifying Emulsion Setting and Adhesion to Aggregates. Submitted to the International Symposium on Asphalt Emulsion Technology (ISAET). Work was presented at the ISAET conference in Arlington, Virginia, September 25, 2008.

Both papers were highlighted in a meeting of the Project Advisory Group held after the ISAET conference in Arlington. Minutes of the meeting are in a draft format and will be made available next quarter.

The submittal of these papers facilitates the execution of the experiment as described in the work plan. Evaluation of the draft ASTM evaporative recovery method has allowed the research team to work with the Project Advisory Group to reach a decision point in selection of the draft ASTM residue recovery procedure that will be used in the research project. Definition of the residue recovery procedure, in conjunction with coordinating with the FHWA Emulsion Task Force and the Federal Lands study through Dr. Gayle King, allows for rheological characterization of the emulsion residue for comparison with laboratory performance testing.

In addition, a paper titled “Performance Grading of Bitumen Emulsions,” was submitted to the Australian Road Research Board (ARRB) and was presented by Hussain Bahia in July. The paper was co-authored by Andrew Hanz of the University of Wisconsin–Madison and Dr. Kim Jenkins of the University of Stellenbosch in South Africa.

Development of tests to quantify the setting behavior and development of adhesion in surface treatments is a key step in defining construction properties of emulsions. The ability of an emulsion to set and develop an adhesive bond with the aggregate will dictate early performance of the surface treatment. An HL-120 Hobart mixer was purchased to conduct laboratory performance tests on the entire chip seal system for correlation with emulsion setting measurements captured by the Dynamic Shear Rheometer (DSR). The equipment arrived in late September, and data will be generated next quarter.

An agreement was established for University of Stellenbosch to be a cost share partner in this work. This quarter, cost share activities included a project meeting held in Madison, Wisconsin, August 25-26, attended by Dr. Jenkins. In addition, Andre Greyling of University of Stellenbosch spent two weeks in Madison to become familiar with proposed testing procedures. The University of Stellenbosch will be involved in the development of adhesion testing procedures for emulsions. A conference call was held September 30 to design the experiment and establish testing procedures. Biweekly conference calls with the research team have been scheduled. The research team also received comments on testing procedures from the Project Advisory Group; its comments will be addressed in the next quarter.

## *Energy Analysis*

Mr. John Patrick of OPUS Consulting, New Zealand, and ARRB staff, led by R. John Oliver, were consulted for input into development of methodologies to compute energy consumption, user delays and emissions associated with application of surface treatments. OPUS Consulting developed a spreadsheet to perform these computations (Patrick and Arampamoorthy 2007), which is currently under review by the research team. This methodology and others are currently being investigated through literature review to select an analysis tool and modify inputs, default values and outputs to better reflect practice in the United States. The Project Advisory Group identified similar efforts by COLAS in France and the Asphalt Emulsion Manufacturers Association. These will be reviewed and considered as development moves forward. The research team is also developing a technical memo to define opportunities for collaboration with ARRB.

## Significant Results

### *Residue Recovery*

Residue recovery at lower temperatures was investigated due to concerns that the conditions of current distillation and evaporative methods specified by ASTM degrade the polymer network, creating a disconnect between materials tested in the laboratory and in-place materials in the field. Results of the evaporative residue recovery procedure currently under review by ASTM indicate that the temperatures used in the recovery method allow for measurement of the effect of both latex and polymer modification on emulsion performance. The development and integrity of the polymer network were monitored through use of percent recovery as measured by the Multiple Stress Creep and Recovery (MSCR) test conducted at different recovery times. Results are presented in figure E1c-2.1.

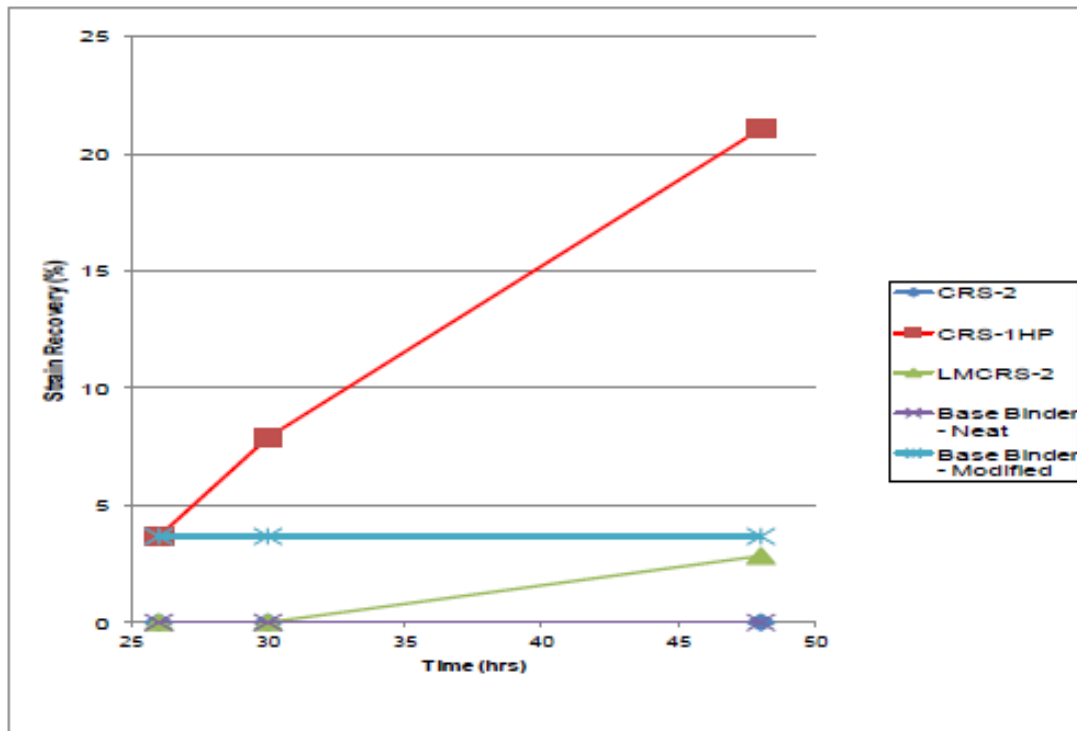


Figure E1c-2.1. Graph. Percent strain recovery for different emulsions as a function of residue recovery time. (Note: base binders were not aged; data for these are shown only for reference.)

Elastic recovery indicates the ability of a material to recover from strain during rest periods in the MSCR testing protocol. In general, unmodified materials will not exhibit elastic recovery. Figure E1c-2.1 shows residues for the latex-modified emulsion (CRS-1HP) and polymer-modified emulsion (LMCRS-2) exhibit approximately 3% and 20% strain recovery, respectively, whereas the unmodified emulsion shows 0% recovery.

Rheological evaluation of the proposed recovery method also indicated the potential for aging of the residual binder during the second day of the procedure, which involves residue recovery at 60 °C. Results of strain sweep testing show values of  $G^*/\sin\delta$  at 12% strain that are 100% to 150% higher for the recovered emulsion residues compared to un-aged base binder. The data are provided in figure E1c-2.2. Further work is needed to determine if differences in performance are due to aging of the residue or whether other factors, such as the effects of the emulsifier, need to be considered.

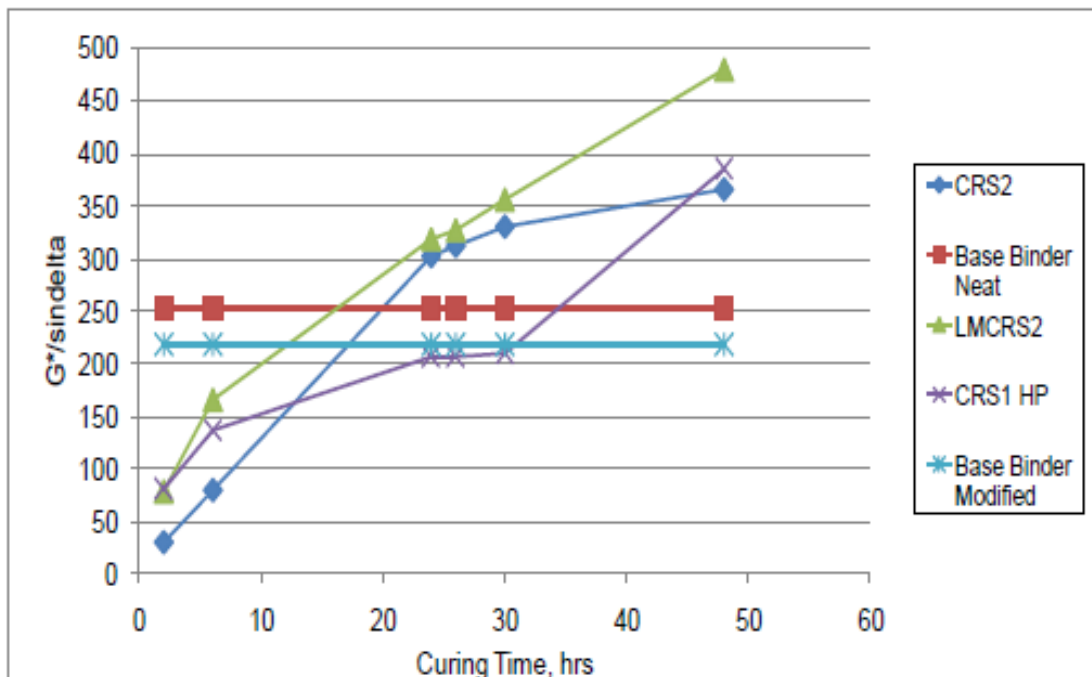


Figure E1c-2.2. Graph.  $G^*/\sin\delta$  of the emulsion residue as a function of recovery time. (Note: base binders were not aged; data for these are shown only for reference.)

### Adhesion Testing

Existing equipment used in both the paint and asphalt industries was selected for measuring the development of adhesion while an emulsion sets. Specifically, the Pneumatic Adhesion Tensile Testing Instrument (PATTI) and the PosiTest by DeFelsko were selected for further evaluation. Both instruments are referenced in ASTM D4541, “Pull-off Strength of Coatings Using Portable Adhesion Testers.” Although the University of Wisconsin–Madison and FHWA have established procedures for measuring the bond strength of asphalt to aggregate and the effects of moisture damage, there have not been procedures for use with emulsion. A tentative test procedure was developed and used to evaluate the feasibility of applying the PATTI and PosiTest to emulsion set on aggregate surfaces of different chemistries. Initial results showed that the PosiTest required significant equipment modifications before use in emulsions. Reasonable results were obtained from the PATTI test. In development of the testing, a CRS-2 emulsion was cured on granite and limestone substrates with adhesive strength measured after 2 and 24 hours. Results of the testing are provided in figure E1c-2.3.

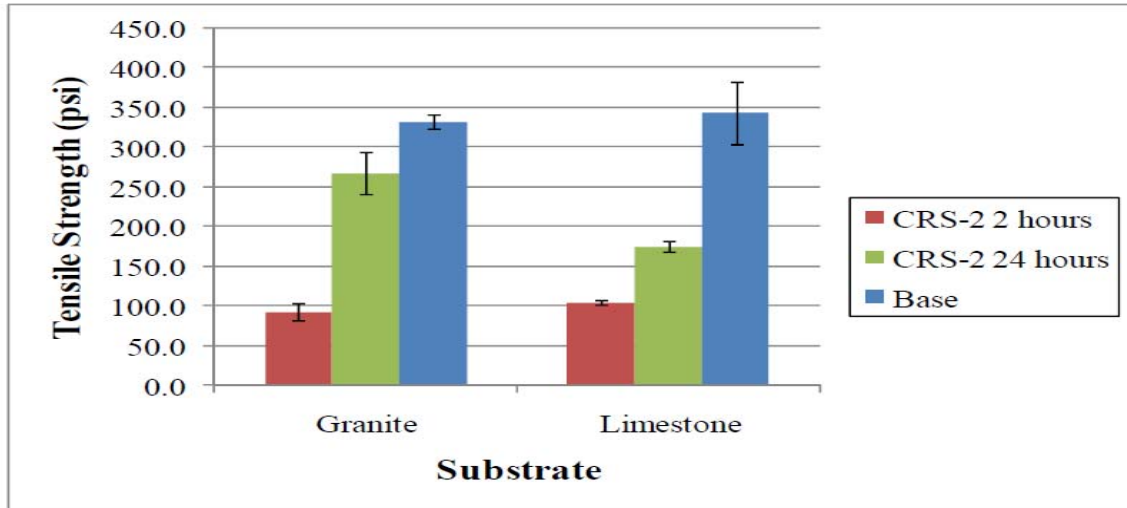


Figure E1c-2.3. Graph. Adhesion testing results for CRS-2 emulsion after 2 hour and 24 hour curing times.

As shown in figure E1c-2.3, initial testing demonstrated that the test was able to show the effects of curing time and substrate mineralogy on development of adhesion. Testing and sample preparation protocols will be developed next quarter. The research team has partnered with the University of Stellenbosch for these efforts.

#### Significant Problems, Issues and Potential Impact on Progress

The level of aging shown by the residue was unexpected and should be investigated further. To quantify the contribution of binder aging to increased residue stiffness, the base binders will be subjected to the same recovery conditions as the emulsion residues and tested at the time intervals specified in the draft TRB paper. Furthermore, per the suggestion of the Project Advisory Group, the Karl Fischer titration method will be conducted on the emulsion residues to determine the amount of water remaining in the material after the recovery procedure. These activities will allow the research team to decide if further investigation into the recovery method is needed. This work has not caused significant delays, as the Project Advisory Group approved the proposal to move forward using the draft ASTM recovery method.

The PosiTest as delivered by the manufacturer was inadequate for use in the research project due to inadequate control of film thickness and an inability to control loading rate. Modifications to the equipment are currently under way to address these issues. It is expected that the additional development work will result in a delay of one month until results using the PosiTest are available.

The literature review report has been delayed an additional three months due to the added scope related to the energy and waste minimization efforts previously referenced. An interim literature review report, including background information published in the TRB and ISAET papers, will be submitted before the end of 2008.



## Work Planned Next Quarter

Work next quarter will focus on the following tasks.

- *Emulsion Residue Recovery.* The research team will address the Project Advisory Group's comments, including analysis of the effects of aging on the base binders and measurement of the water loss in the emulsion at specified times using the Karl Fischer titration method as specified by ASTM. New findings will be incorporated into the draft TRB paper and reviewed with the Project Advisory Group.
- *Emulsion Setting.* The research team will develop an experimental plan to relate strain sweep and MSCR results as measured by the DSR with chip seal performance as measured by the ASTM D7000 sweep test. The relationship will be verified through testing of emulsion residue from the sweep test and comparing the results to the rheological properties of the residue for an emulsion cured for a set time and mineral substrate.
- *Adhesion Testing.* The research team will:
  - Continue development of adhesion testing procedures for both the PATTI and PosiTest.
  - Finalize and execute the experimental plan developed with the University of Stellenbosch for measurement of the development of emulsion bond strength over time.
  - Hold biweekly conference calls with the University of Stellenbosch.
- *Energy Analysis.* The research team will:
  - Complete the literature review, including recommendations for an analysis methodology, and submit to the Project Advisory Group for review.
  - Continue collaborative efforts with OPUS Consulting and ARRB.

## Cited References

Patrick, J., and H. Arampamoorthy, 2007, Quantifying the Benefits of Waste Minimisation. Report prepared by OPUS Engineering Consultants, Land Transport New Zealand.

## **CATEGORY E2: DESIGN GUIDANCE**

### **Work element E2a: Comparison of Modification Techniques (UWM Year 2 start)**

#### Work Done This Quarter

This work element was restructured after multiple discussions among consortium partners and experts. The work plan, budget and new schedule were approved.

### Significant Results

The work plan for this element has been restructured to include manufacturer-prepared modified binders. Modifiers will be sought to provide both low and high levels of modification (one and two PG grade bumps). A minimum of three manufacturers will be solicited to provide materials so that three different modifiers at a minimum are included in this work plan.

The research team will recommend a base binder, but the ultimate binder selection will be at the manufacturer's discretion. In the event that a manufacturer decides to use a different base binder than the one recommended, the manufacturer will be asked to provide a sample of its selected base binder along with the modified materials.

### Significant Problems, Issues and Potential Impact on Progress

None.

### Work Planned Next Quarter

Next quarter, the research team plans to collect all of the materials and begin testing.

## **Work element E2b: Design System for HMA Containing a High Percentage of RAP Material (UNR)**

### Work Done This Quarter

The UNR team evaluated the impact of the extraction method on the physical properties of the Nevada-andesite aggregates by comparing their measured properties before and after extraction. Additionally, the UNR team evaluated the impact of reflux and centrifuge on the properties of the recovered binder from the Nevada-andesite mix according to the process shown in figure E2b.1.

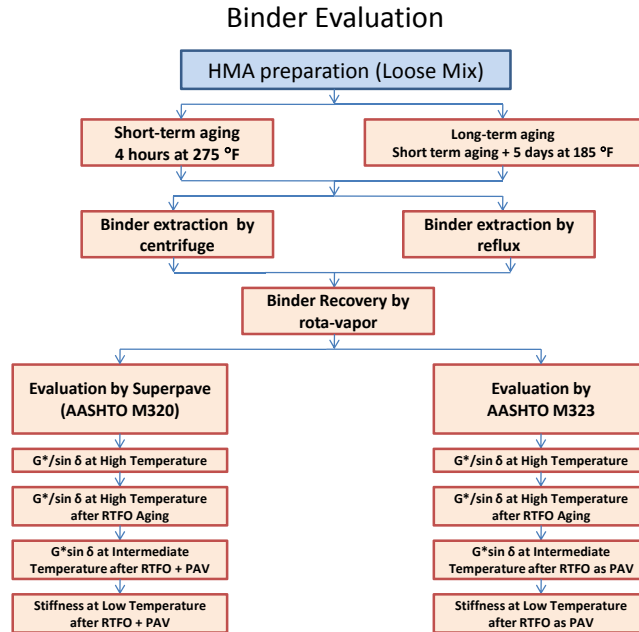


Figure E2b.1. Binder evaluation sketch.

A Superpave mix design was conducted for the Handley Ranch, CA aggregates using the same PG64-22 asphalt binder. Additionally, the physical properties of the original blend aggregates from Handley Ranch were measured. The UNR team started the extraction of the aggregates from the long-term oven aged mixtures using the reflux, centrifuge, and ignition oven. The following physical properties of the extracted aggregates are going to be measured:

- Gradation, LA abrasion, soundness, absorption, specific gravity, fine aggregate angularity (FAA), coarse aggregate angularity (CAA), fractured faces, sand equivalent, and durability index.

NCAT conducted the mix designs for the two selected sources for evaluation and are in the progress of testing the physical properties of the extracted aggregates using the three extraction methods.

UWM completed the protocol for testing of mortars made with RAP (-#8). The team moved to using Teflon-coated raw steel molds for a smoother testing surface. In order to use the stiffness results measured with the Bending Beam Rheometer (BBR) for these mortars, the team developed a spreadsheet to back-calculate the stiffness of the RAP binder. Simple correlation equations were used to convert mortar stiffness to binder stiffness; blending equations were also used.

A step-by-step procedure was proposed to test RAP mortars and to use BBR data on fresh binder to determine if a binder grade change is required and what the grade of the new binder should be. A step-by-step procedure to prepare the mortar, molds and samples was also developed.

A graduate student from the UNR team visited UWM for three days and collaborated with UWM in the development of the BBR procedure for testing RAP mortars.

### Significant Results

Below are selected results for the Nevada-andesite aggregates (figure E2b.2) and the recovered PG64-22 asphalt binder from the Nevada mixes (figure E2b.3).

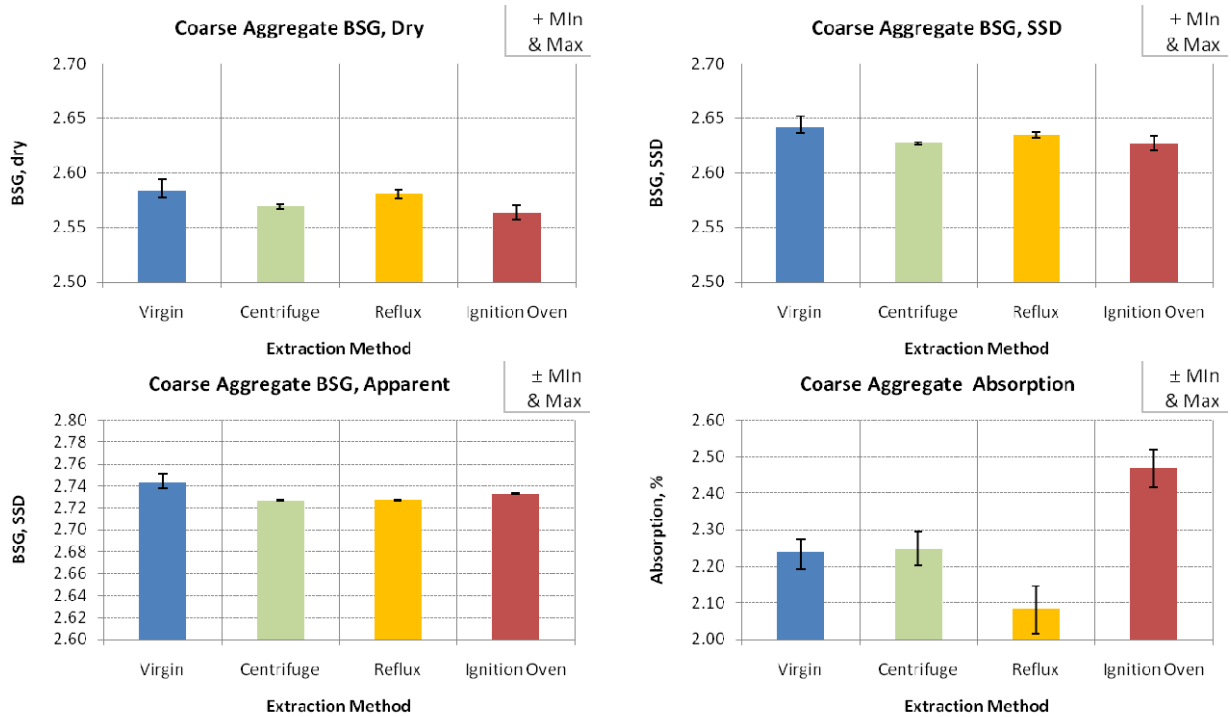


Figure E2b.2. Specific gravity & absorption of coarse aggregates (AASHTO T85).

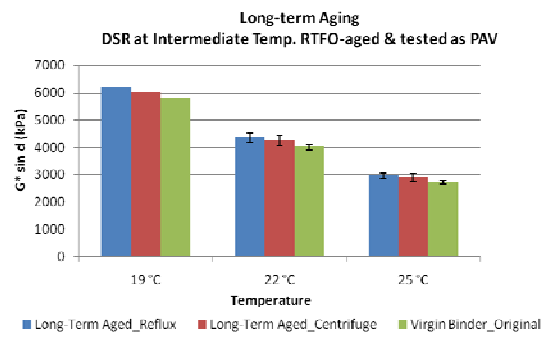
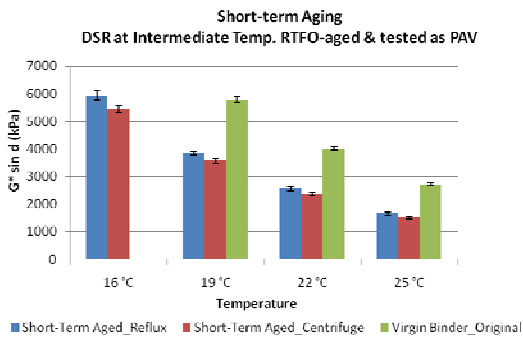
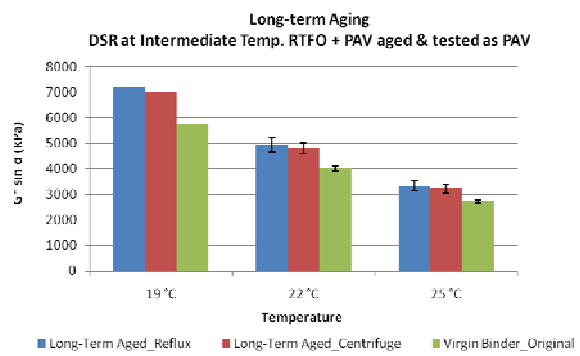
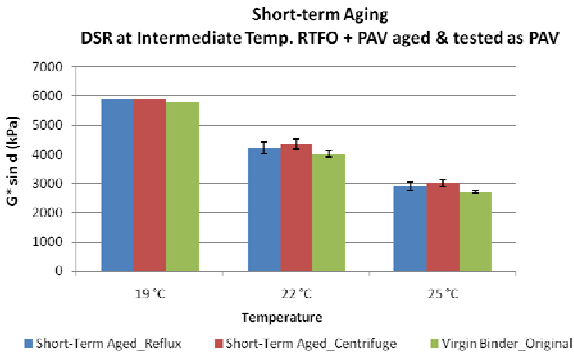
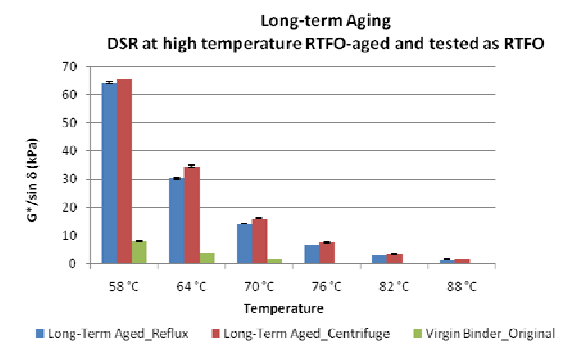
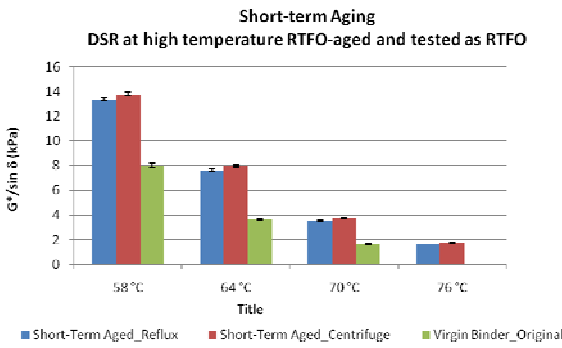
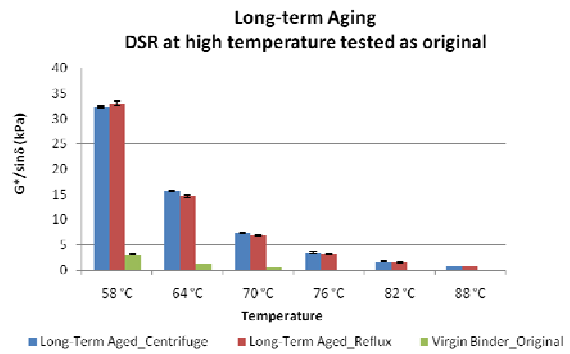
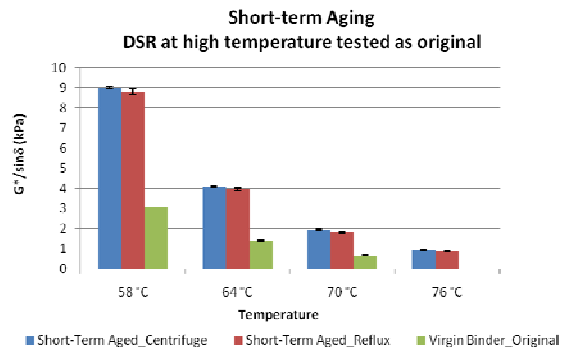


Figure E2b.3. Recovered PG64-22 asphalt binder properties from the Nevada mixes.

A literature review on the evaluation of rheological properties of binders in RAP without extraction and recovery was completed by UWM and summarized in a paper submitted to TRB (Bautista et al. 2009). The aim of this review was to develop a protocol to estimate the low-temperature rheological properties of binders in RAP without the damaging effects of extraction with solvents. The results of the study paper were encouraging. The findings indicated that the new procedure can capture the effect of aged properties of bitumen in RAP and can be used to estimate the low temperature PG grade of the blended binder.

### Significant Problems, Issues and Potential Impact on Progress

UNR still did not receive the third source of aggregate from South Dakota for laboratory evaluation.

The limited amount of data collected so far for RAP mortars testing has resulted in a data set that is highly variable and sometimes inconsistent. It is not clear whether the RAP sampling and mixing are the problem, or whether the problem is in the preparation of the samples. This will be addressed as more data are collected.

The team also faced challenges with the BBR procedures. The trimming process for the samples in this study is more time-consuming compared with standard BBR samples because the material is stiffer. In addition, the demolding process is more difficult than a conventional BBR demolding process; this is possibly due to the use of Teflon-coated molds and Teflon tape.

### Work Planned Next Quarter

UNR will continue evaluating the impact of extraction method on the physical properties of the Handley Ranch aggregates.

Write a report summarizing the findings of both UNR and NCAT test results for extraction methods.

Run additional tests on the mortar to obtain more data and achieve greater consistency and lower variability. The team will also finalize the protocol to decide when a PG grade change is required and to determine the effect of RAP content on the PG grade in the recycled mixture. Possible changes in aggregate gradation will also be addressed.

### Cited References

Bautista, E.G., S. Mangiafico, and H.U. Bahia, 2009, Evaluation of Rheological Properties of Binders in RAP Without Extraction and Recovery. Paper submitted for presentation and publication at the Transportation Research Board 88th Annual Meeting, January 11-15, 2009, Washington, D.C.

## Work element E2c: Critically Designed HMA Mixtures (UNR)

### Work Done This Quarter

The UNR team analyzed the calculated deviator stress from the 3D-Move responses of the PG64-22 mix under the moving 18-wheel truck.

Additionally, the following 3D-Move runs for the Lockwood (andesite) + PG52-22 mix using the mixture specific dynamic modulus were completed:

- Pavement structures:
  - 4” HMA over 6” base
  - 6” HMA over 8” base
  - 8” HMA over 10” base
- Geometries:
  - Level road
- Speeds:
  - 60 mph without braking
  - 40 mph without braking
  - 20 mph without braking
- Tire-Pavement Pressure Distribution
  - Uniform
- HMA layer temperature
  - 40°C
  - 50°C
  - 60°C
  - 70°C

### Significant Results

The maximum deviator stress and the time of loading in the HMA layer at 2 inches below the pavement surface were calculated for the PG64-22 mix (figures E2b.4 and E2b.5). The time of loading was determined by best fitting a sinusoidal wave shape for the deviator stress pulse that was calculated from the octahedral shear stress ( $\tau_{oct}$ ) under a moving 18-wheel truck at different speeds and temperatures (equations 1-2).

$$\begin{aligned}\tau_{oct}^2 &= \frac{1}{9}[(\sigma_{xx} - \sigma_{yy})^2 + (\sigma_{yy} - \sigma_{zz})^2 + (\sigma_{zz} - \sigma_{xx})^2] + \frac{2}{3}\tau_{xy}^2 + \tau_{yz}^2 + \tau_{xz}^2 \\ &= \frac{1}{9}[(\sigma_1 - \sigma_2)^2 + (\sigma_2 - \sigma_3)^2 + (\sigma_3 - \sigma_1)^2]\end{aligned}\quad (1)$$

$$\sigma_d = \frac{3}{\sqrt{2}} \tau_{oct} \quad (2)$$

Additionally, all the data for the pulse time was combined and a general relationship between the loading time at 2 inches below the pavement surface and vehicle speed and temperature was found. The pavement thickness did not have a statistically significant impact on the pulse time at 2 inches below the pavement surface. A fitting parameter  $R^2$  of 0.974 was found.

$$\log(t) = -0.76969 - 0.00504 * Temp - 0.01133 * Speed \quad (3)$$

where,

$t$  = deviator stress pulse time at 2 inches below pavement surface in seconds

$Temp$  = pavement temperature in °C

$Speed$  = vehicle speed in mph



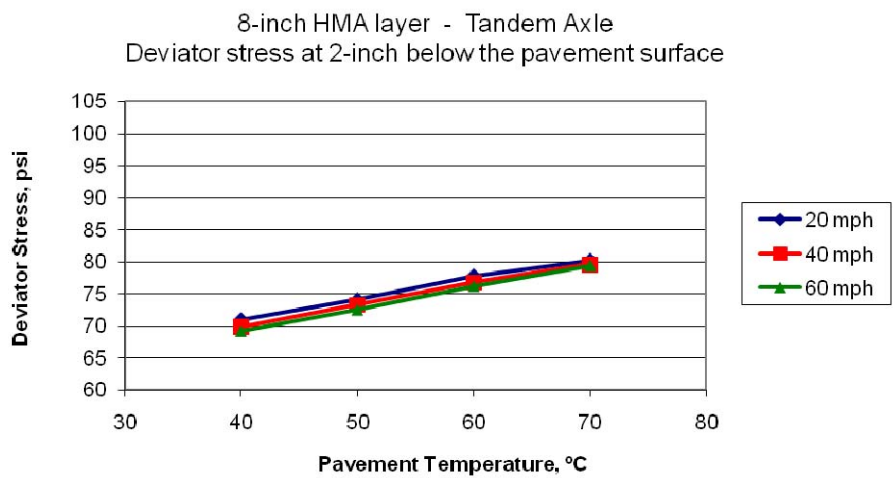
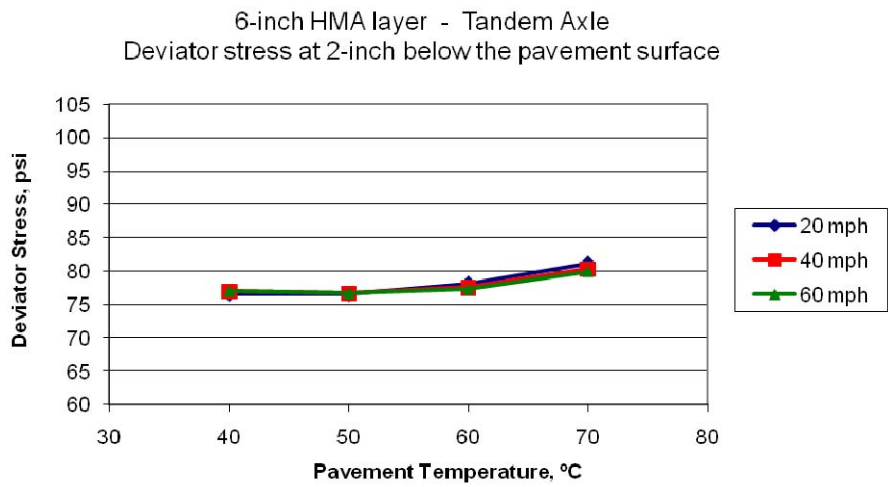
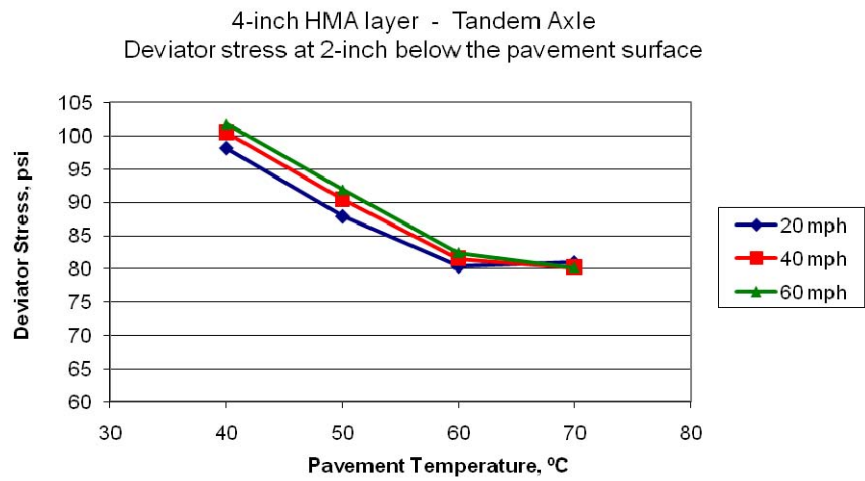
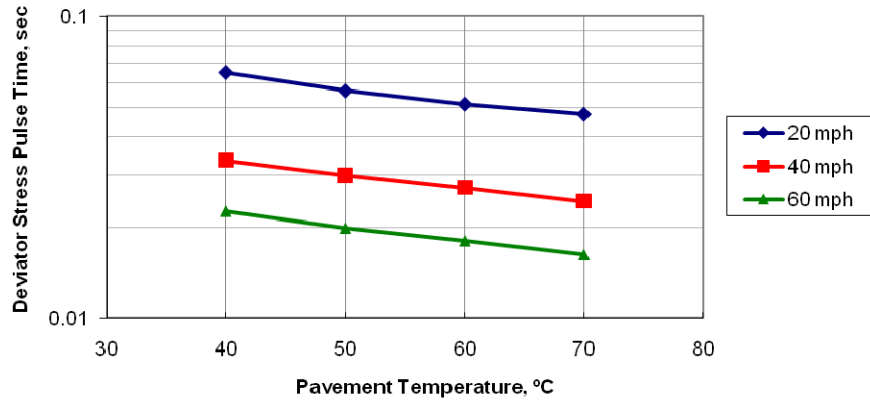
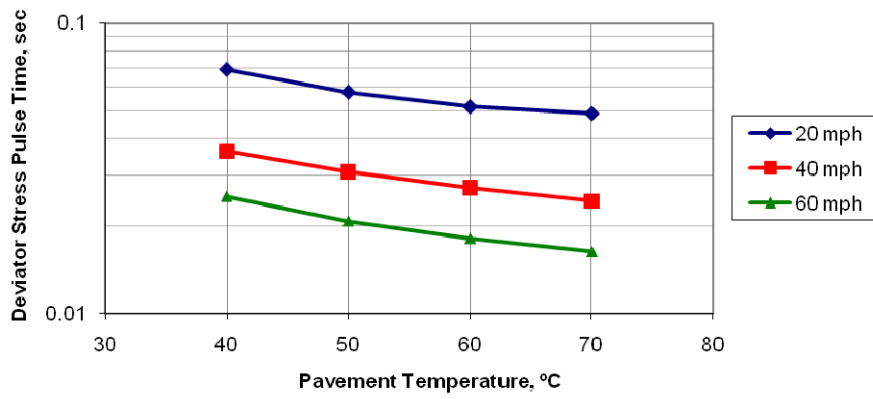


Figure E2b.4. Maximum deviator stress at 2-inch from the pavement surface – PG64-22 mix.

4-inch HMA layer - Tandem Axle  
Pulse time at 2-inch below the pavement surface



6-inch HMA layer - Tandem Axle  
Pulse time at 2-inch below the pavement surface



8-inch HMA layer - Tandem Axle  
Pulse time at 2-inch below the pavement surface

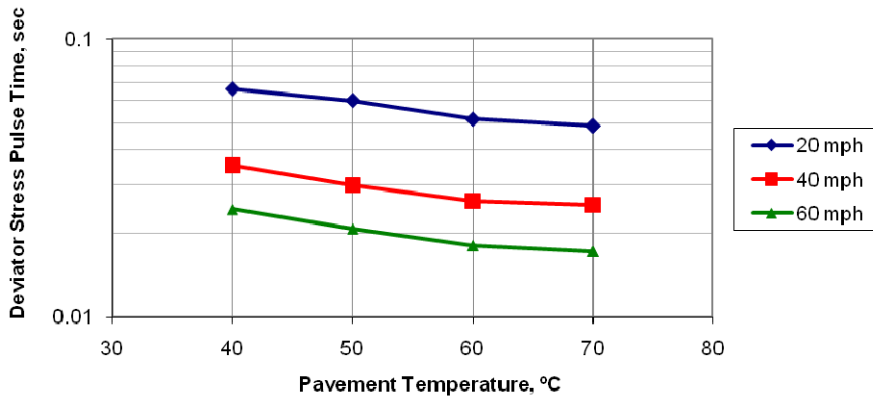


Figure E2b.5. Deviator stress pulse time at 2-inch below the pavement surface – PG64-22 mix.

## Significant Problems, Issues and Potential Impact on Progress

None.

## Work Planned Next Quarter

Analyze the data for the PG52-22 mixture and identify the following:

- Time of loading at 2 inches below pavement surface
- Magnitude of the confining and deviator stresses throughout the HMA layer

The calculations of the 3D-Move model will continue to cover all the loading conditions that were described in the experimental plan for this work element.

Complete the mix design for the Lockwood aggregate source with PG58-22 binder and measure its dynamic modulus master curve and damping ratio.

## **Work element E2d: Thermal Cracking Resistant Mixes for Intermountain States (UNR & UWM)**

### Work Done This Quarter

The UNR team continued the long-term oven aging process for the following binders as described in the experimental plan for this work element:

- Neat PG64-22
- Polymer modified PG64-28 (using the same PG64-22 crude source) that meets the specs of UT, NV, and CA.

Additionally, the aged binders are under testing for rheological properties.

The UNR team continued working on the analyses of the pavement temperature profiles data from the LTPP and Westrack pavement sections.

On the other hand, the UNR team continued the TSRST experiment on investigating the impact of specimen size and shape.

Efforts at UW this quarter included parts of Subtask E2d-2, “Identify the Causes of the Thermal Cracking,” and Subtask E2d-3, “Identify an Evaluation and Testing System.” These are described below.

The new all-in-one testing device has been completed. It will allow the research team to conduct multiple types of testing:

- Binder thermal dilatometric testing.

- Mixture thermal linear expansion and contraction testing.
- Mixture Thermal Stress Restrained Specimen Test (TSRST).

Different configurations of the equipment were evaluated in order to determine the easiest and most efficient testing procedures.

Redesign of the dilatometric cells continued; the new design resulted in difficulties with obtaining and maintaining a perfect seal of the binder sample cell throughout the test.

The modification of the Bending Beam Rheometer (BBR) for Single-Edge Notched Bending (SENB) testing was nearly completed, with latest work focused on the pneumatic and electronic connections.

### Significant Results

Figure E2d.1a shows the results for the measured mass loss and gain of the PG64-22 asphalt binder when aged at different temperatures and periods in the forced convection (horizontal airflow) ovens. Figure E2d.1b shows the measured  $G^* \sin \delta$  for the aged PG64-22 asphalt binder at 100°C and at the various curing times.

Figure E2d.2 shows typical plots for the pavement maximum and minimum temperatures along with the calculated temperature rates for the LTPP section 040113, Kingman, Arizona between March 1, 2002 and February 29, 2004.

Single components of the glass transition temperature testing device and the TSRST device were checked for proper functioning. Simulated binder tests showed satisfactory results. New calibration samples were manufactured using Invar in order to improve the calibration procedure.

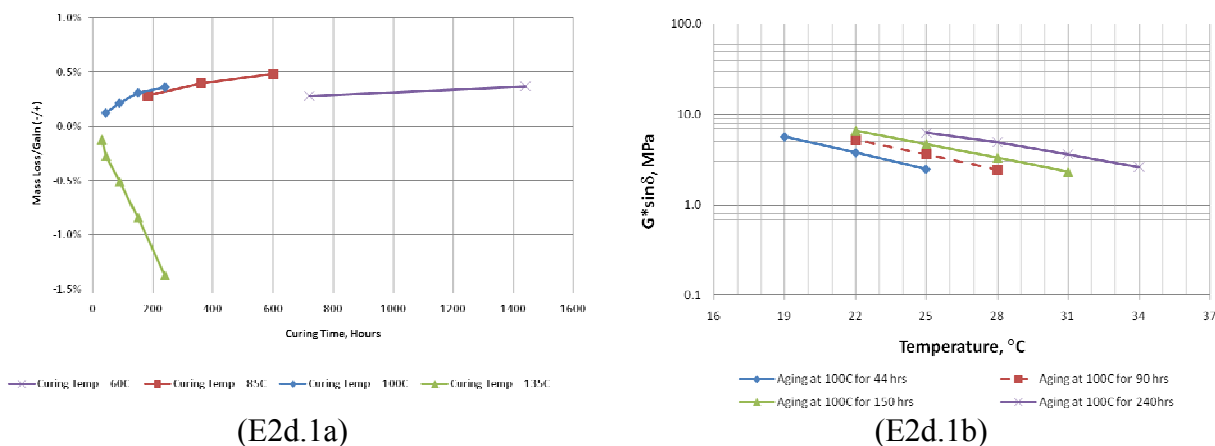
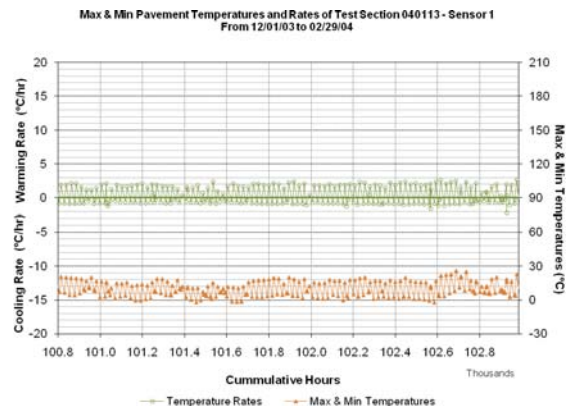
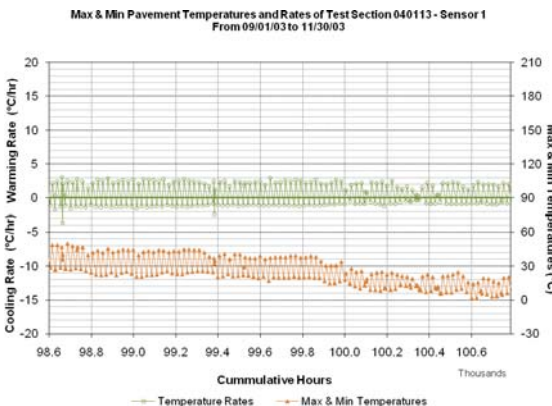
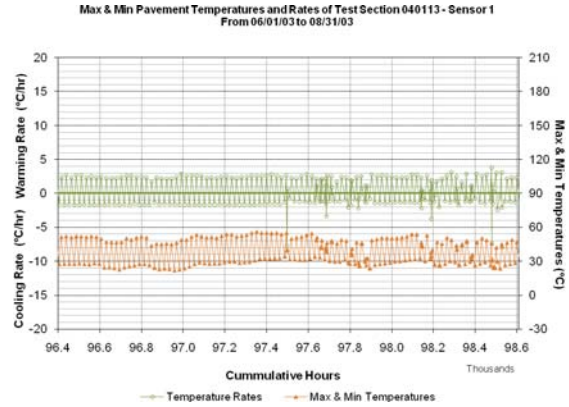
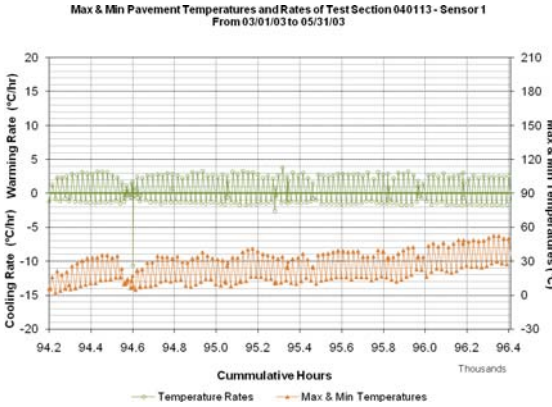
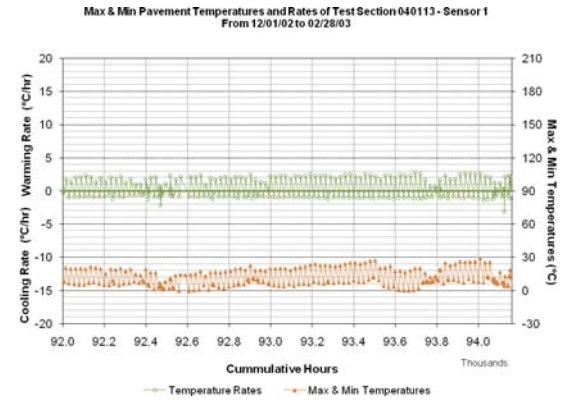
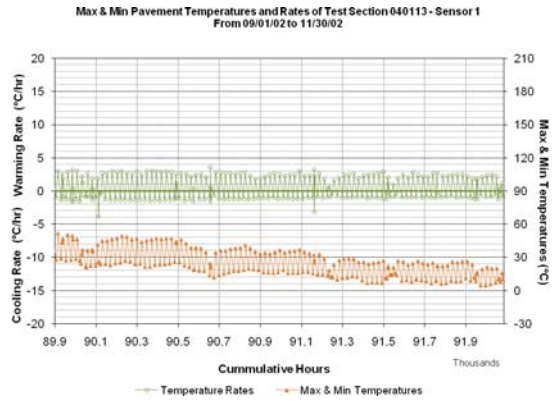
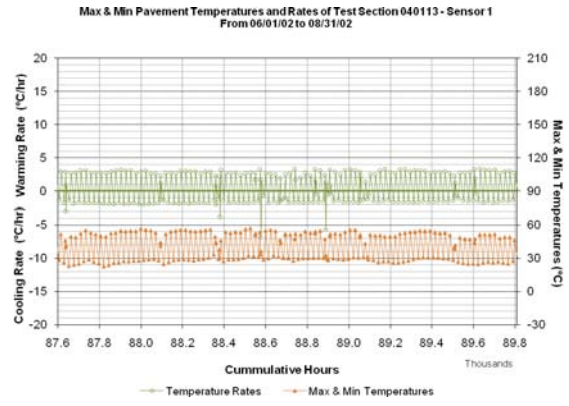
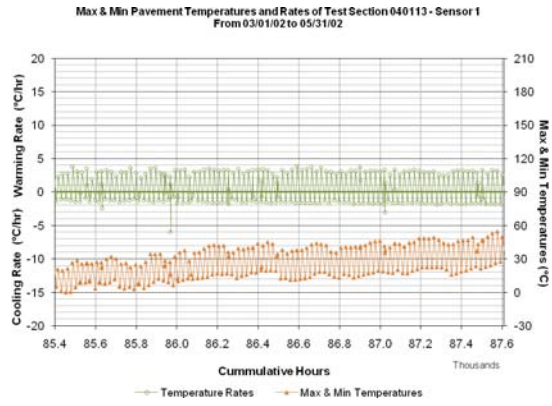


Figure E2d.1a. PG64-22 Mass loss/gain at various curing temperatures and times;  
E2d.1b.  $G^* \sin \delta$  for the PG64-22 at 100°C and various curing times.



E2d.2. Minimum and maximum temperatures along with temperature rates at sensor 1 of the LTPP 040113 pavement section.

To improve the reliability of the measurements, it was decided to run all tests using a dummy sample inside one of the dilatometric cells. A third cell, identical to those currently in use, was built to make it possible to test two samples at a time. New pressure sensors were ordered and their proper functioning was verified by comparing their output with parallel manual readings.

The device was nearly ready to carry out the experimental plan; the new improvements will be implemented on one cell at a time.

The modified BBR load frame was assembled, as shown in figure E2d.3.



Figure E2d.3. Photograph. Assembled frame of the new BBR and SENB equipment.

#### Significant Problems, Issues and Potential Impact on Progress

The new position of the holes for the capillary tubes in the all-in-one device necessitated work on the tubes. Initially, connections were made by using metallic plumbing connections (figure

E2d.4). This was not a viable solution because the connection inside the environmental chamber caused excessive height variation in the large volume of alcohol in the tubes. For this reason, it was decided to use glass tubes bent at 90° to eliminate the problem. However, plugging the bent tube to the dilatometric cell proved to be difficult. As a solution, holes will be drilled through the lid of the device to allow using straight capillary tubes.

Another problem was that the new BBR and SENB device exhibited problems with the air bearing system. New pressure gages were ordered.

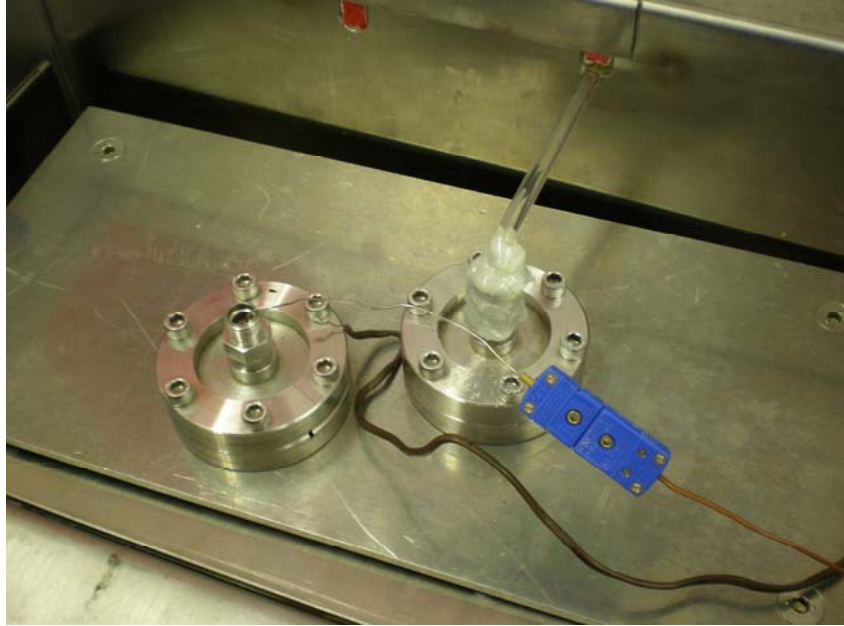


Figure E2d.4. Photograph. The latest temporary setup of the all-in-one device for glass transition temperature measurements.

#### Work Planned Next Quarter

Continue the aging process of binders and continue measuring the properties of the aged binders. Continue the analysis of the temperature profiles data from the LTPP sections and the Westrack. Continue the investigation on the impact of specimen size and shape and start the investigation on the impact of cooling rate.

Next quarter the team plans to begin and complete the experimental plan for measuring glass transition temperature. The team will run tests on both binders and mixtures. In addition, the new BBR and SENB equipment will be completed and its proper functioning will be checked.

## **Work element E2e: Design Guidance for Fatigue and Rut Resistance Mixtures (AAT)**

### Work Done This Quarter

No effort was expended this Quarter on this work element pending.

### Significant Results

Improvements have been identified for the following models developed in NCHRP Project 9-25:

- (1) Hirsch Model for dynamic modulus,
- (2) Resistivity Model for rutting resistance,
- (3) Continuum Damage Fatigue Model
- (4) Permeability Model

Preliminary experimental plans have been developed to address the needed model improvements.

### Significant Problems, Issues and Potential Impact on Progress

None.

### Work Planned Next Quarter

Final experimental designs will be prepared using the specific materials selected by the Asphalt Research Consortium.



Engineered Materials Year 2	Year 2 (4/2008-3/2009)												Team
	4	5	6	7	8	9	10	11	12	1	2	3	
<b>(1) High Performance Asphalt Materials</b>													
E1a: Analytical and Micro-mechanics Models for Mechanical behavior of mixtures													TAMU
E1a-1: Analytical Micromechanical Models of Binder Properties										P	JP	P	
E1a-2: Analytical Micromechanical Models of Modified Mastic Systems										P	JP	P	
E1a-3: Analytical Models of Mechanical Properties of Asphalt Mixtures			P	P	JP					P	JP	P	
E1a-4: Analytical Model of Asphalt Mixture Response and Damage										P	JP	P	
E1b: Binder Damage Resistance Characterization													UWM
E1b-1: Rutting of Asphalt Binders													
E1b-1-1: Literature review													
E1b-1-2: Select Materials & Develop Work Plan		DP, P					P						
E1b-1-3: Conduct Testing							P						
E1b-1-4: Analysis & Interpretation						JP			P			JP	
E1b-1-5: Standard Testing Procedure and Recommendation for Specifications													
E1b-2: Feasibility of Determining rheological and fracture properties of thin films of asphalt binders and mastics using nano-indentation													UWM
E1b-2i: Literature Review and Identification of Equipment													
E1b-2ii: Exploratory Use of Nanoindentation Devices							M&A					JP	
E1b-2iii: Conduct of Exploratory Tests on Binder Specimens										P		P	
E1b-2iv: Compare the Binders Responses with DSR													
E1b-2v: Develop & Design Testing Setup													
E2a: Comparison of Modification Techniques													UWM
E2a-1: Literature Review Report													
E2a-2: Develop a new system for classification of additives								P					P
E2a-3: Conduct testing and propose models										DP			P
E2a-4: Write an asphalt modification manual													
E2a-5: Develop database for effect of additives													
E2c: Critically Designed HMA Mixtures													UNR
E2c-1: Identify the Critical Conditions													
E2c-2: Conduct Mixtures Evaluations										JP	D		F
E2c-3: Develop a Simple Test													
E2c-4: Develop Standard Test Procedure													
E2c-5: Evaluate the Impact of Mix Characteristics													
E2d: Thermal Cracking Resistant Mixes for Intermountain States													UWM/UNR
E2d-1: Identify Field Sections													
E2d-2: Identify the Causes of the Thermal Cracking										D		F	
E2d-3: Identify an Evaluation and Testing System													
E2d-4: Modeling and Validation of the Developed System													
E2d-5: Develop a Standard													
E2e: Design Guidance for Fatigue and Rut Resistance Mixtures													AAT
E2e-1: Identify Model Improvements													
E2e-2: Design and Execute Laboratory Testing Program					JP						P		
E2e-3: Perform Engineering and Statistical Analysis to Refine Models													
E2e-4: Validate Refined Models													
E2e-5: Prepare Design Guidance													
<b>(2) Green Asphalt Materials</b>													
E2b: Design System for HMA Containing a High Percentage of RAP Material													UNR
E2b-1: Develop a System to Evaluate the Properties of RAP Materials													
E2b-1.b: Develop a System to Evaluate the Properties of the RAP Binder		P		JP								P	
E2b-2: Compatibility of RAP and Virgin Binders													
E2b-3: Develop a Mix Design Procedure													
E2b-4: Impact of RAP Materials on Performance of Mixtures													
E2b-5: Field Trials													
E1c: Warm and Cold Mixes													UWM
E1c-1: Warm Mixes													
E1c-1i: Effects of Warm Mix Additives on Rheological Properties of Binders													
E1c-1ii: Effects of Warm Mix Additives on Mixture Workability and Stability				JP	P					D		DP	F
E1c-1iii: Mixture Performance Testing													
E1c-1iv: Develop Revised Mix Design Procedures													
E1c-1v: Field Evaluation of Mix Design Procedures and Performance Recommendations													
E1c-2: Improvement of Emulsions' Characterization and Mixture Design for Cold Bitumen Applications													
E1c-2i: Review of Literature and Standards				JP,P		D				F			
E1c-2ii: Creation of Advisory Group													
E1c-2iii: Identify Tests and Develop Experimental Plan													P, DP
E1c-2iv: Develop Material Library and Collect Materials													
E1c-2v: Conduct Testing Plan													

**Deliverable codes**  
D: Draft Report  
F: Final Report  
M&A: Model and algorithm  
SW: Software  
JP: Journal paper  
P: Presentation  
DP: Decision Point

**Deliverable Description**  
Report delivered to FHWA for 3 week review period.  
Final report delivered in compliance with FHWA publication standards  
Mathematical model and sample code  
Executable software, code and user manual  
Paper submitted to conference or journal  
Presentation for symposium, conference or other  
Time to make a decision on two parallel paths as to which is most promising to follow through

Work planned  
Work completed  
Parallel topic

Engineered Materials Year 2 - 5	Year 2 (4/08-3/09)				Year 3 (4/09-3/10)				Year 4 (04/10-03/11)				Year 5 (04/11-03/12)				Team
	Q1	Q2	Q3	Q4	Q1	Q2	Q3	Q4	Q1	Q2	Q3	Q4	Q1	Q2	Q3	Q4	
<b>(1) High Performance Asphalt Materials</b>																	
E1a: Analytical and Micro-mechanics Models for Mechanical behavior of mixtures																	TAMU
E1a-1: Analytical Micromechanical Models of Binder Properties				P, JP	JP	P	P	JP	M&A	D	F, SW						
E1a-2: Analytical Micromechanical Models of Modified Mastic Systems				P, JP	JP	P	P		M&A	JP	D	F, SW					
E1a-3: Analytical Models of Mechanical Properties of Asphalt Mixtures	P	P, JP		P, JP	JP	P	P	M&A		D	SW, JP	F					
E1a-4: Analytical Model of Asphalt Mixture Response and Damage				P, JP	JP	P	P		M&A	D	F, JP	SW					
E1b: Binder Damage Resistance Characterization																	UWM
E1b-1: Rutting of Asphalt Binders																	
E1b-1-1: Literature review																	
E1b-1-2: Select Materials & Develop Work Plan	DP, P		P														
E1b-1-3: Conduct Testings								JP	D	F							
E1b-1-4: Analysis & Interpretation		JP	P	JP	P			M&A			JP						
E1b-1-5: Standard Testing Procedure and Recommendation for Specifications										P		DP	P	D	JP	F	
E1b-2: Feasibility of Determining rheological and fracture properties of thin films of asphalt binders and mastics using nano-indentation																	
E1b-2i. Literature Review and Identification of Equipment			M&A	JP	M&A, SW	JP	D	F									
E1b-2ii. Exploratory Use of Nanoindentation Devices																	
E1b-2iii. Conduct of Exploratory Tests on Binder Specimens				P						JP		P					
E1b-2iv. Compare the Binders Responses with DSR														JP			
E1b-2v. Develop & Design Testing Setup															D	P, F	
E2a: Comparison of Modification Techniques																	UWM
E2a-1: Literature Review Report		P		P		P	D	F									
E2a-2: Develop a new system for classification of additives																	
E2a-3: Conduct testing and propose models			DP	P			JP	P			JP						
E2a-4: Write an asphalt modification manual									P		P			D	P, F		
E2a-5: Develop database for effect of additives									P		P			D	P, F		
E2c: Critically Designed HMA Mixtures																	UNR
E2c-1: Identify the Critical Conditions			JP	D, F													
E2c-2: Conduct Mixtures Evaluations									D, F	JP							
E2c-3: Develop a Simple Test													D, F	JP			
E2c-4: Develop Standard Test Procedure													D, F				
E2c-5: Evaluate the Impact of Mix Characteristics																D, F	
E2d: Thermal Cracking Resistant Mixes for Intermountain States																	UWM/UNR
E2d-1: Identify Field Sections			D, F														
E2d-2: Identify the Causes of the Thermal Cracking									D, F	JP							
E2d-3: Identify an Evaluation and Testing System													D, F	JP			
E2d-4: Modeling and Validation of the Developed System																D, F	
E2d-5: Develop a Standard																D, F	
E2e: Design Guidance for Fatigue and Rut Resistance Mixtures																	AAT
E2e-1: Identify Model Improvements																	
E2e-2: Design and Execute Laboratory Testing Program		JP		P				D, F									
E2e-3: Perform Engineering and Statistical Analysis to Refine Models						JP		P				D, F					
E2e-4: Validate Refined Models										JP		P					
E2e-5: Prepare Design Guidance															M&A	D, F	
<b>(2) Green Asphalt Materials</b>																	
E2b: Design System for HMA Containing a High Percentage of RAP Material																	UNR
E2b-1: Develop a System to Evaluate the Properties of RAP Materials		JP		P	D, F	JP											
E2b-1.b: Develop a System to Evaluate the Properties of the RAP Binder	P			JP	P		GP										
E2b-2: Compatibility of RAP and Virgin Binders					D, F	JP											
E2b-3: Develop a Mix Design Procedure									D, F	JP							
E2b-4: Impact of RAP Materials on Performance of Mixtures																D, F	
E2b-5: Field Trials										JP						D, F	
E1c: Warm and Cold Mixes																	
E1c-1: Warm Mixes																	
E1c-1i: Effects of Warm Mix Additives on Rheological Properties of Binders.																	
E1c-1ii: Effects of Warm Mix Additives on Mixture Workability and Stability		JP, P	D	F, DP													UWM
E1c-1iii: Mixture Performance Testing								JP	P, DP								UWM
E1c-1iv: Develop Revised Mix Design Procedures										JP	P						UWM/UNR
E1c-1v: Field Evaluation of Mix Design Procedures and Performance Recommendations														JP	D	P, F	UWM/UNR
E1c-2: Improvement of Emulsions' Characterization and Mixture Design for Cold Bitumen Applications																	UWM
E1c-2i: Review of Literature and Standards		JP, P, D	F														
E1c-2ii: Creation of Advisory Group																	
E1c-2iii: Identify Tests and Develop Experimental Plan					P, DP			P, DP									
E1c-2iv: Develop Material Library and Collect Materials.																	
E1c-2v: Conduct Testing Plan						JP											
E1c-2vi: Develop Performance Selection Guidelines										JP	D	P, F					
E1c-2vii: Validate Guidelines														JP	P		
E1c-2viii: Develop CMA Mix Design Procedure												P					
E1c-2ix: Develop CMA Performance Guidelines														JP	D	F	

**Deliverable codes**  
D: Draft Report  
F: Final Report  
M&A: Model and algorithm  
SW: Software  
JP: Journal paper  
P: Presentation  
DP: Decision Point

**Deliverable Description**  
Report delivered to FHWA for 3 week review period.  
Final report delivered in compliance with FHWA publication standards  
Mathematical model and sample code  
Executable software, code and user manual  
Paper submitted to conference or journal  
Presentation for symposium, conference or other  
Time to make a decision on two parallel paths as to which is most promising to follow through

Work planned  
Work completed  
Parallel topic

## **PROGRAM AREA: VEHICLE-PAVEMENT INTERACTION**

### **CATEGORY VP1: WORKSHOP**

#### **Work element VP1a: Workshop on Super-Single Tires**

The Workshop on Wide-Base Tires was held at FHWA TFHRC on October 25-26, 2007. FHWA has prepared draft minutes of the Workshop. All attendees have been reimbursed for their travel expenses.

The Workshop minutes are posted on the ARC website. The minutes can be found at the following link: <http://www.arc.unr.edu/Workshops.html>

This work element is complete.

### **CATEGORY VP2: DESIGN GUIDANCE**

#### **Work element VP2a: Mixture Design to Enhance Safety and Reduce Noise of HMA (UWM)**

##### Work Done This Quarter

The research team at the University of Wisconsin–Madison completed the development of the waveguide sound absorption device and continued work on measuring the effect of surface abrasion on the macrotexture of HMA slab specimens.

Details of the waveguide device were finalized, and the current design and methodology of the equipment are described below.

##### *Geometric*

The geometric design of the waveguide device follows the recommendations by Chung and Blaser (1980) and the ASTM E1050 standard (ASTM 2008). The final waveguide geometry is presented in figure VP2a.1. The design parameters include the separation of the specimen to the closer microphone, the separation between microphones and the distance of the second microphone to the speaker. These parameters are related to the waveguide diameter, the speed of sound, and the maximum and lower testing frequencies.

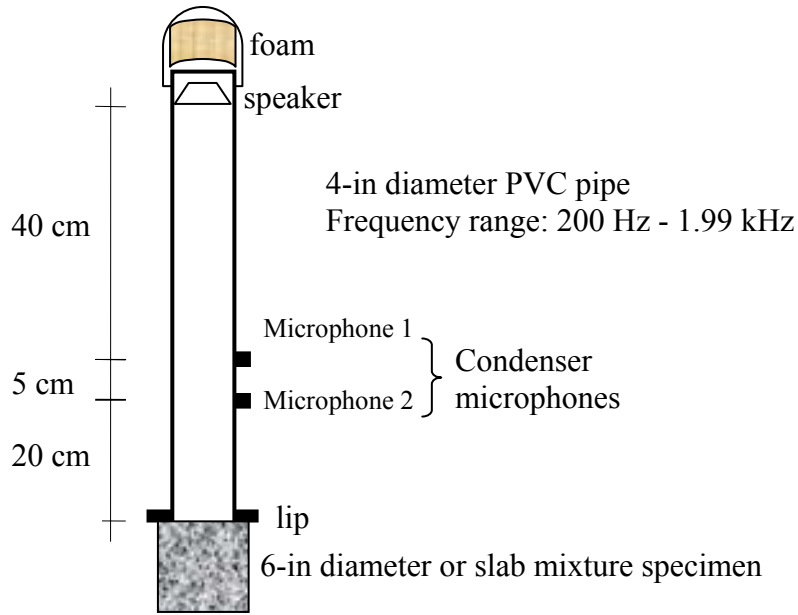


Figure VP2a.1. Illustration. Sketch of the waveguide device.

### *Maximum Testing Frequency*

The upper testing frequency ( $f_u$ ) is defined as:

$$f_u < K \frac{c}{D} = 0.586 \frac{340 \frac{\text{m}}{\text{s}}}{0.1 \text{m}} = 1992 \text{ Hz}$$

where

$c$  is the speed of sound (meters per second),  
 $D$  is the tube diameter (meters), and  
 $K$  is a constant.

### *Separation Between Microphones*

The maximum separation between microphones ( $s$ ) is:

$$s \ll \frac{c}{2 \cdot f_u} = \frac{340 \frac{\text{m}}{\text{s}}}{2 \cdot 1992 \text{ Hz}} = 0.085 \text{ m}$$

It is recommended that the maximum distances  $s$  should be less than  $0.80 \cdot c / (2 \cdot f_u)$ , or

$$s < 0.8 \frac{c}{2 \cdot f_u} = 0.8 \frac{340 \frac{\text{m}}{\text{s}}}{2 \cdot 1992 \text{ Hz}} = 0.069 \text{ m}$$

It was selected  $s = 0.05$  m.

### *Separation Between Specimen and Microphone 2*

The separation ( $l$ ) between the specimen and microphone 2 is controlled by the surface roughness of the specimen and the attenuation of the sound wave. For flat surfaces, a minimum distance of one tube diameter is recommended; for nonhomogeneous surfaces, the distance should be at least one tube diameter; and for asymmetrical surfaces, the distance should be at least two tube diameters. For distances more than three tube diameters, the data analysis should consider the attenuation within the tube. For this device,  $l$  was set at two tube diameters.

### *Separation Between Speaker and Microphone 1*

It is recommended that a minimum of three tube diameters should be used to allow a proper distance to generate plane waves. For this device, this distance was set at four tube diameters.

### *Sensors*

- Microphone: Radio Shack condenser microphone element (omnidirectional; diameter 9.83 mm; flat response in the 50 Hz to 3 kHz range).
- Speaker: Projects Unlimited 230 Hz to 12 kHz, 8 ohm, 4 W acoustic speaker (length 66.3 mm, width 66.3 mm, height 29 mm).
- Data acquisition card: National Instrument multifunction data acquisition card to collect the microphone data and to drive the speaker.

### *Data Reduction*

The steps for data reduction are as follows:

1. Calibrate the system and correction for differences in microphone response.
  - a. Place microphone 1 in position 1 and microphone 2 in position 2, and determine the frequency response  $H_I$  when a highly absorbing material is placed as the testing surface. Details in the calculation of the frequency response between input and output accelerometers are given by Santamarina and Fratta (2005).
  - b. Place microphone 1 in position 2 and microphone 2 in position 1, and determine the frequency response  $H_{II}$  when a highly absorbing material is placed as the testing surface.
  - c. Calculate the calibration factor  $H_c$  as:
$$H_c = \sqrt{H_I \cdot H_{II}}$$
2. Determine the frequency response  $H$  for the desired test material when microphone 1 is in position 1 and microphone 2 is in position 2.
3. Calculate the complex reflection  $R$  coefficient as:

$$R = \frac{\frac{H}{H_c} - e^{-j k \cdot s}}{e^{j k \cdot s} - \frac{H}{H_c}} e^{-j 2 k \cdot (l+s)}$$

where

$k = 2\pi f/c$  is the wave number, and  
 $j$  is the imaginary operator.

- Calculate the sound absorption coefficient  $\alpha$  as:

$$\alpha = 1 - |R|^2$$

A LabView algorithm was developed to operate the device and perform the data analysis, as shown in figure VP2a.2. This algorithm drives the speaker using a random signal excitation, calculates the system frequency response using 64 averaged signals, and plots the calculated results including the coherence (a measurement of the data quality). Figure VP2a.3 is a picture of the waveguide device, peripheral electronics and tested specimens.

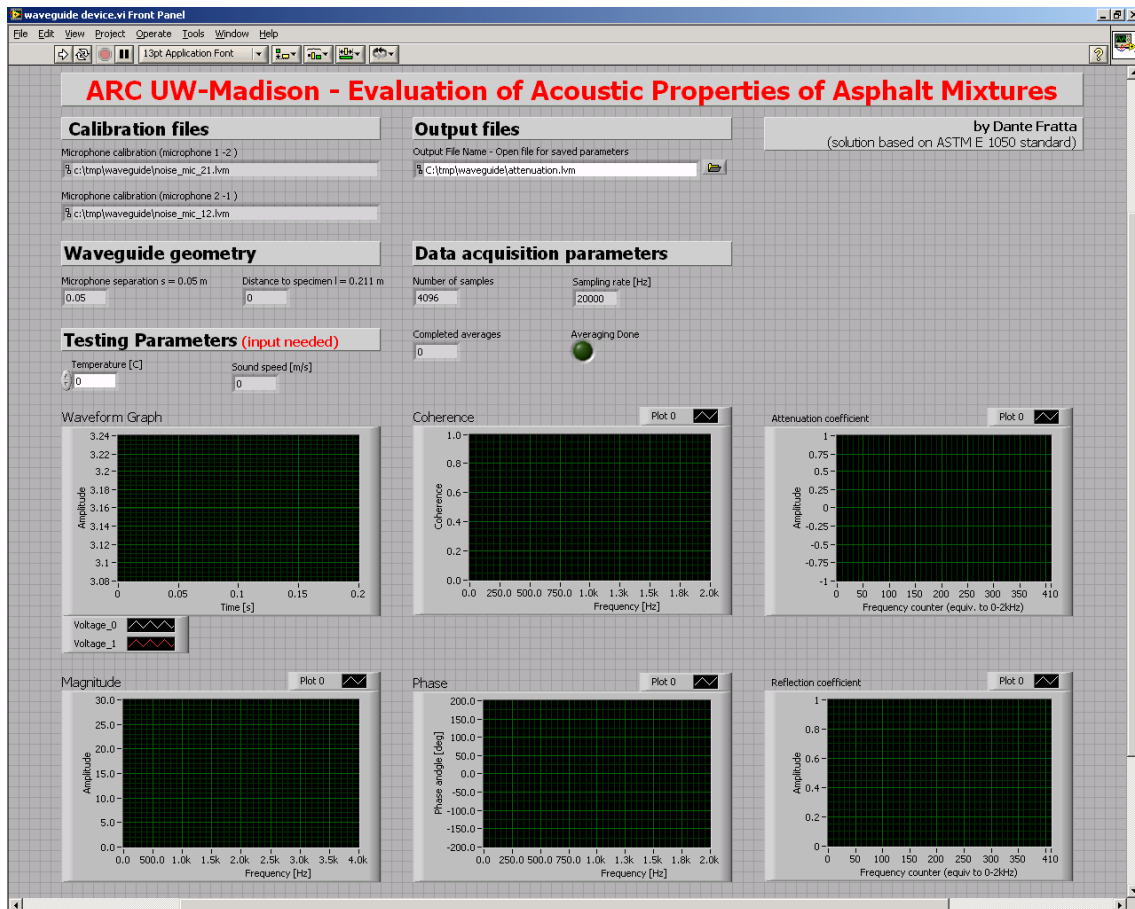


Figure VP2a.2. Screen shot. The LabView front panel.

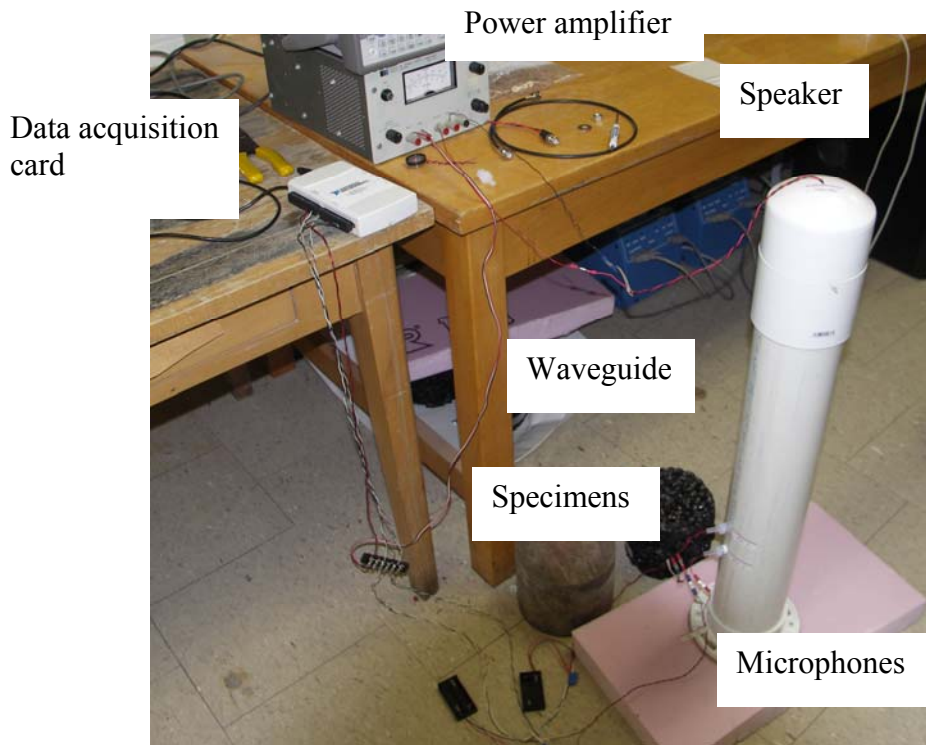


Figure VP2a.3. Photograph. The complete waveguide device and peripheral electronics.

### Significant Results

After it was calibrated, the system was tested using four different surfaces to rank the system response: foam, construction insulation foam, open grade HMA specimen and steel. The averaged absorption coefficient responses are presented in figure VP2a.4. Note that the open course data has two series. The second series (“open course - pushed in”) was performed to evaluate the effect of the seal at the waveguide lip. As expected, the calculated absorption coefficient changed with improved sealing.

Macrottexture measurements were also investigated for lab-compacted slab specimens from a previous study. Four specimens were selected: two with a “smooth” initial roughness (defined as Mean Texture Depth (MTD)  $< 0.2$  mm) and two with a “rough” initial surface (MTD  $> 0.2$  mm). Initial MTD was measured using the sand-patch method, and then the surfaces were abraded using a drill-operated abrasive pad for 1 minute intervals. Initial results are shown in figure VP2a.5, and testing and analysis of additional specimens are ongoing. Preliminary data show that the application of the abrasive pad onto the smooth specimens increases MTD, whereas the MTD appears to decrease after application of the abrasive pad onto the rough specimens.

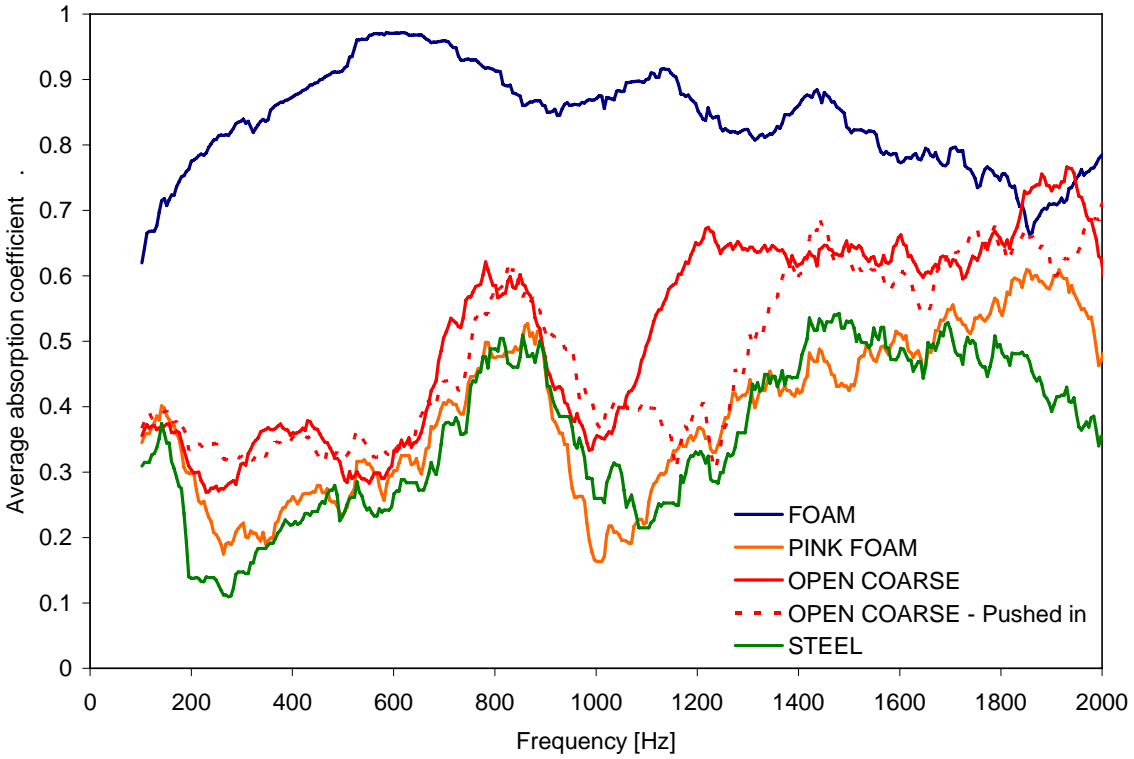


Figure VP2a.4. Graph. Summary of preliminary testing of the waveguide absorption device.

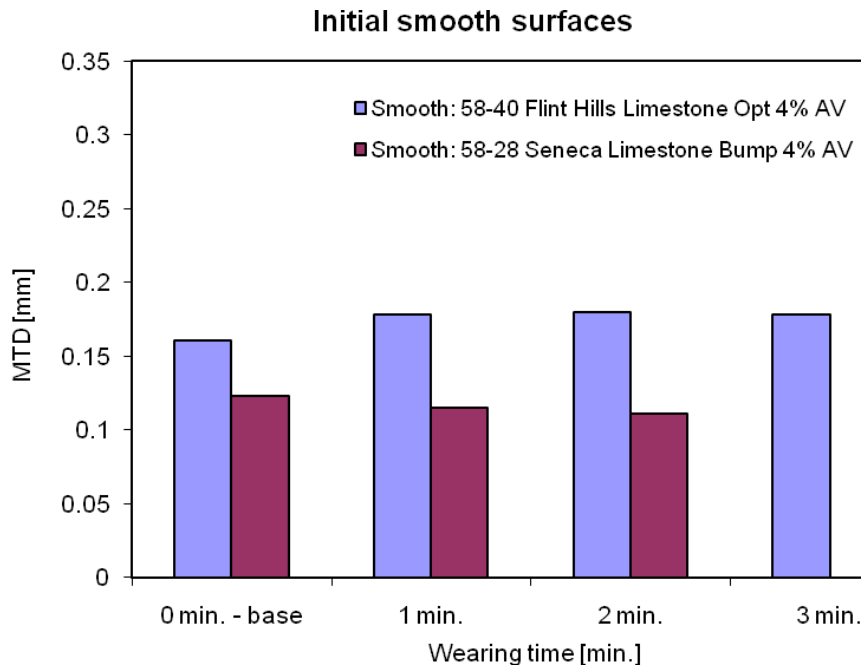


Figure VP2a.5. Graph. MTD results before and after abrasion for the smooth lab-compacted slab specimens.



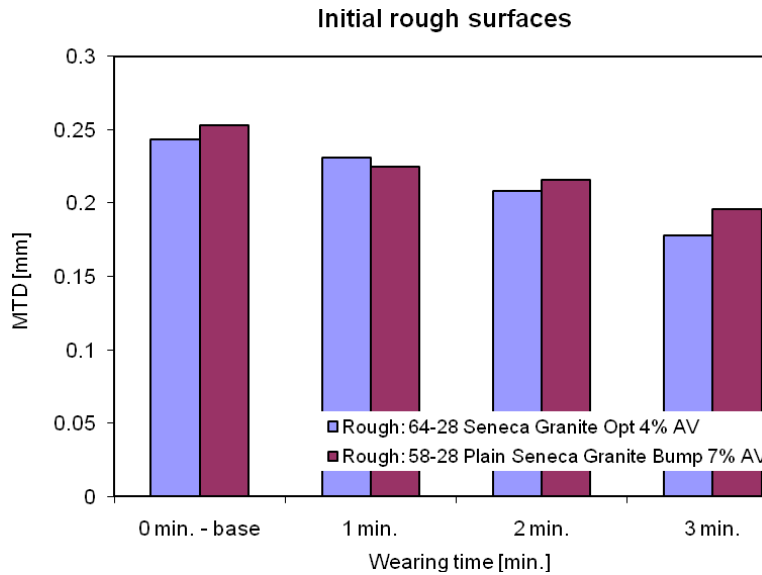


Figure VP2a.6. Graph. MTD results before and after abrasion for the rough lab-compacted slab specimens.

### Significant Problems, Issues and Potential Impact on Progress

None.

### Work Planned Next Quarter

During Q4 2008, the research team will:

- Evaluate the use of the sweep test or alternative techniques to simulate polishing by traffic.
- Continue collecting data using the waveguide device on HMA specimens.
- Run parametric studies as described in the Year 2 work plan to investigate the effect of mixture design properties on the surface characteristics of HMA.

### Cited References

ASTM, 2008, E 1050–07 Standard test method for impedance and absorption of acoustical materials using a tube, two microphones and a digital frequency analysis system. American Society of Testing and Materials. West Conshohocken, PA.

Chung, J. Y., and D. A. Blaser, 1980, Transfer function method of measuring acoustic intensity in a duct system with flow. *Journal of Acoustic Society of America*, 68(6): 1570-1577.

Santamarina, J. C., and D. Fratta, 2005, *Discrete Signals and Inverse Problems: An Introduction for Engineers and Scientists*. John Wiley and Sons, Chichester, UK.

## CATEGORY VP3: MODELING

### *Work element VP3a: Pavement Response Model to Dynamic Loads (UNR Year 2 start)*

#### Work Done This Quarter

Working on the 3D-Move model to make it a menu-driven software.

#### Significant Results

The following figures show selected snapshots from the newly developed 3D-Move user friendly interface. Whenever possible, a structure similar to that of the MEPDG software is followed.

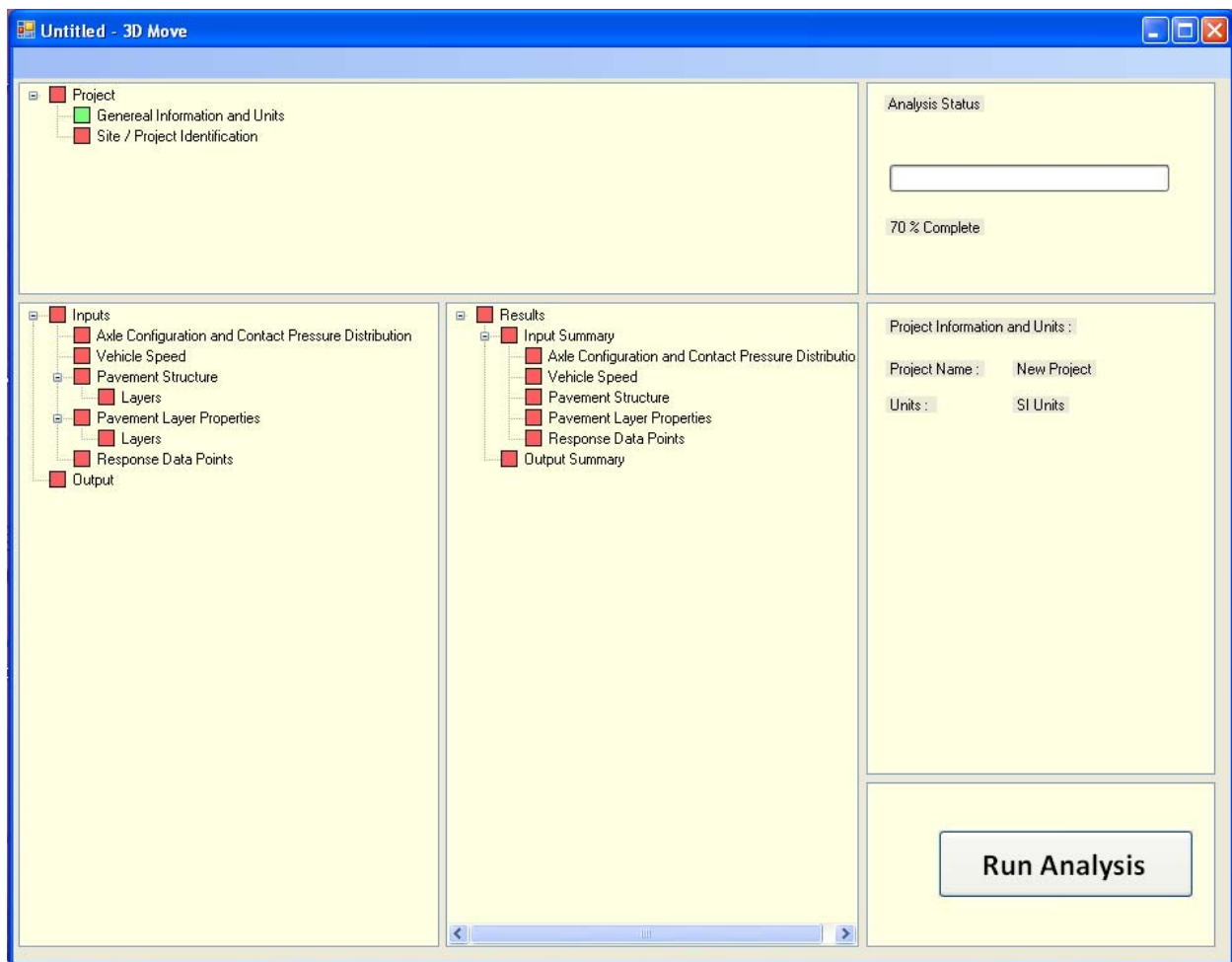


Figure VP3a.1. 3D-Move program.

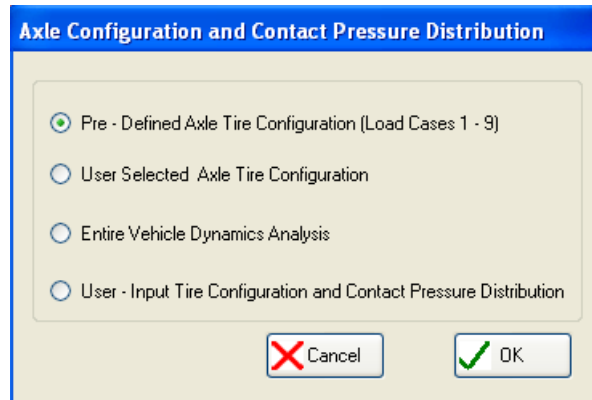


Figure VP3a.2. 3D-Move axle configuration and contact pressure distribution selection options.

**Pre - defined Load Cases**

Load Case 1-4   Load Case 5-8   Load Case 9

**Load Case 5 : Rectangular Shaped Dual Tire Tandem Axle Load with Non-Uniform Pressure**

\* Not to scale

This is a dual tire tandem axle load represented with four rectangular contact areas. The contact pressure is assumed to be non-uniform over the contact area (Sebbaly et al., 1992). Here it is assumed that uniform stresses exist within each rib and there is non zero contact stresses in the gap between the ribs. The half axle load is 90 kN (22.5 kN/tire).

**Load Case 6 : Rectangular Shaped Dual Tire Single Axle Load with Non-Uniform Pressure**

\* Not to scale

This is a dual tire single axle load represented with two rectangular contact areas. The contact pressure is assumed to be non-uniform over the contact area (Sebbaly et al., 1992). Here it is assumed that uniform stresses exist within each rib and there are no contact stresses in the gap between the ribs. The half axle load is 45 kN (22.5 kN/tire).

**Load Case 7 : Circular Shaped Super Single Tire Tandem Axle Load Uniform Pressure**

\* Not to scale

This is a super single tire tandem axle load represented by two circular contact areas. The contact pressure is assumed to be uniform over the contact area with magnitude of 862 kPa. The half axle load is 90 kN (45 kN/tire).

**Load Case 8 : Elliptical Shaped Super Single Tire Tandem Axle Load Uniform Pressure**

\* Not to scale

This is a super single tire tandem axle load represented by two elliptical contact areas (as per de Beer et al., 1996). The contact pressure is assumed to be non-uniform over the contact area. The half axle load is 90.0 kN (45.0 kN/tire).

Click on the Image to select Load case

**User Input Tire Configuration and Contact Pressure Distribution**

Unit Converter - All

Unit Converter : Length

Mesh Details for Loaded Area

Element size in X direction (DX)  m

Element size in Y direction (DY)  m

Unit Converter : Pressure

Contact Pressure (Specify only Non Zero Values)

Location Number - N (X - Direction)	Location Number - M (Y - Direction)	Normal Vertical Stress in Z Direction (kPa)	Contact Shear Stress in XZ Direction (kPa)	Contact Shear Stress in YZ Direction (kPa)

Figure VP3a.3. 3D-Move pre-defined and user input axle/tire configuration.

Significant Problems, Issues and Potential Impact on Progress

None.

Work Planned Next Quarter

Continue working on the 3D-Move model to make it a menu-driven software.

Start collecting and developing the database for non-uniform tire/pavement contact pressure distribution.

Vehicle-Pavement Interaction Year 2	Year 2 (4/2008-3/2009)											Team	
	4	5	6	7	8	9	10	11	12	1	2		3
<b>(1) Workshop</b>													
VP1a: Workshop on Super-Single Tires													UNR
<b>(2) Design Guidance</b>													
VP2a: Mixture Design to Enhance Safety and Reduce Noise of HMA													UWM
VP2a-1: Evaluate common physical and mechanical properties of asphalt mixtures with enhanced frictional skid characteristics													DP
VP2a-2: Evaluate pavement macro- and micro-textures and their relation to tire and pavement noise-generation mechanisms													DP
VP2a-3: Develop a laboratory testing protocol for the rapid evaluation of the macro and micro-texture of pavements					M&A								P
VP2a-4: Run parametric studies on tire-pavement noise and skid response							JP						
VP2a-5: Establish collaboration with established national laboratories specialized in transportation noise measurements. Gather expertise on measurements and analysis													
VP2a-6: Model and correlate acoustic response of tested tire-pavement systems													
VP2a-7: Proposed optimal guideline for design to include noise reduction, durability, safety and costs													
<b>(3) Pavement Response Model Based on Dynamic Analyses</b>													
VP3a: Pavement Response Model to Dynamic Loads													UNR
VP3a-1: Dynamic Loads										JP			
VP3a-2: Stress Distribution at the Tire-Pavement Interface													
VP3a-3: Pavement Response Model													
VP3a-4: Overall Model													

**Deliverable codes**

- D: Draft Report
- F: Final Report
- M&A: Model and algorithm
- SW: Software
- JP: Journal paper
- P: Presentation
- DP: Decision Point

**Deliverable Description**

- Report delivered to FHWA for 3 week review period.
- Final report delivered in compliance with FHWA publication standards
- Mathematical model and sample code
- Executable software, code and user manual
- Paper submitted to conference or journal
- Presentation for symposium, conference or other
- Time to make a decision on two parallel paths as to which is most promising to follow through

	Work planned
	Work completed
	Parallel topic

**Vehicle-Pavement Interaction Years 2 - 5**

	Year 2 (4/08-3/09)				Year 3 (4/09-3/10)				Year 4 (04/10-03/11)				Year 5 (04/11-03/12)				Team
	Q1	Q2	Q3	Q4	Q1	Q2	Q3	Q4	Q1	Q2	Q3	Q4	Q1	Q2	Q3	Q4	
<b>(1) Workshop</b>																	
VP1a: Workshop on Super-Single Tires																	UNR
<b>(2) Design Guidance</b>																	
VP2a: Mixture Design to Enhance Safety and Reduce Noise of HMA																	UWM
VP2a-1: Evaluate common physical and mechanical properties of asphalt mixtures with enhanced frictional skid characteristics				DP													
VP2a-2: Evaluate pavement macro- and micro-textures and their relation to tire and pavement noise-generation mechanisms				DP													
VP2a-3: Develop a laboratory testing protocol for the rapid evaluation of the macroand micro-texture of pavements		M&A		P													
VP2a-4: Run parametric studies on tire-pavement noise and skid response			JP			JP	D	P, F									
VP2a-5: Establish collaboration with established national laboratories specialized in transportation noise measurements. Gather expertise on measurements and analysis																	
VP2a-6: Model and correlate acoustic response of tested tire-pavement systems										JP	D	F					
VP2a-7: Proposed optimal guideline for design to include noise reduction, durability, safety and costs											D	P, F					
<b>(3) Pavement Response Model Based on Dynamic Analyses</b>																	
VP3a: Pavement Response Model to Dynamic Loads																	UNR
VP3a-1: Dynamic Loads			JP						D, F	JP							
VP3a- 2: Stress Distribution at the Tire-Pavement Interface									D, F	JP							
VP3a-3: Pavement Response Model					SW - b version							SW, JP					
VP3a-4: Overall Model												D	F				

**Deliverable codes**

- D: Draft Report
- F: Final Report
- M&A: Model and algorithm
- SW: Software
- JP: Journal paper
- P: Presentation
- DP: Decision Point

**Deliverable Description**

- Report delivered to FHWA for 3 week review period.
- Final report delivered in compliance with FHWA publication standards
- Mathematical model and sample code
- Executable software, code and user manual
- Paper submitted to conference or journal
- Presentation for symposium, conference or other
- Time to make a decision on two parallel paths as to which is most promising to follow through

	Work planned
	Work completed
	Parallel topic





## **PROGRAM AREA: VALIDATION**

### **CATEGORY V1: FIELD VALIDATION**

#### **Work element V1a: Use and Monitoring of Warm Mix Asphalt Sections (Year 1 start)**

##### Work Done This Quarter

The Yellowstone National Park warm-mix and control hot-mix sections were monitored in early September. The Park Service allowed the acquisition of small samples of pavement that were obtained by using a ½ inch masonry drill bit and a 1 inch nominal lapidary core bit. The pavement samples were obtained from the shoulder of the pavement near the beginning of each of the nine monitoring sections. The nine monitoring sections are comprised of three from each of the three materials, control hot-mix, Advera additive, and Sasobit additive. The small samples obtained are for assessment of the aging that has occurred in the pavement. These samples are unconventional in the sense that they are not typical 4 or 6-inch pavement cores, however, the research team at WRI is investigating if accurate aging data can be obtained from small samples. If this is successful, it will be a very rapid and inexpensive method to obtain samples from in service pavements for assessing aging, both near the surface and with depth.

There was no distress noted in any of the monitoring sections which is what was expected of pavement sections that have been in service for only one year.

##### Significant Results

None.

##### Significant Problems, Issues and Potential Impact on Progress

None.

##### Work Planned Next Quarter

It is planned to continue processing the small pavement samples obtained from the Yellowstone sections to determine if aging data can be obtained.

#### **Work element V1b: Construction and Monitoring of additional Comparative Pavement Validation sites (Year 1 start)**

##### Work Done This Quarter

No activity this quarter.

### Significant Results

None.

### Significant Problems, Issues and Potential Impact on Progress

None.

### Work Planned Next Quarter

Short synopses of the material variables that the ARC desires for validation sections will be prepared and sent to Eric Weaver for the LTPP Regional Contractors meeting in mid-November 2008. More detailed descriptions of the desired validation sections will be prepared following the short synopses to use for discussions with state DOT representatives in states where LTPP sections are going out of service and there is a possibility of constructing new sections for ARC research.

## **CATEGORY V2: ACCELERATED PAVEMENT TESTING**

### **Work element V2a: Accelerated Pavement Testing including Scale Model Load Simulation on Small Test Track (Later start)**

#### Work Done This Quarter

No accelerated testing has been planned.

#### Significant Results

None.

#### Significant Problems, Issues and Potential Impact on Progress

None.

#### Work Planned Next Quarter

The Consortium is interested in acquiring accelerated pavement testing and is open to collaboration with others.

### **Work element V2b: Construction of Validation Sections at the Pecos Research & Testing Center (Later start)**

This work element is included to indicate that this may be a possibility for accelerated pavement testing for ARC research because it is a facility in the TAMU system.

## **CATEGORY V3: R&D VALIDATION**

### **Work element V3a: Continual Assessment of Specifications (UWM)**

#### Work Done This Quarter

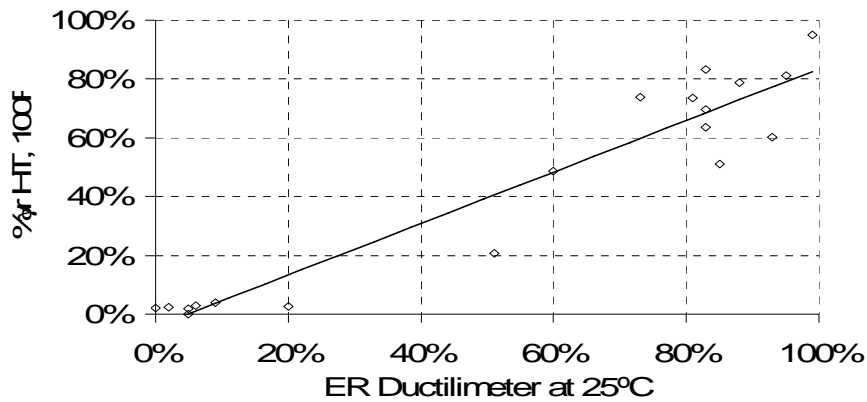
Work last quarter focused on the relationship between elastic recovery, percent recovery and the nonrecoverable compliance (measured Jnr values) using the Multiple Stress Creep Recovery (MSCR) test. The analysis included a consideration of data from previous projects and data published in the literature. A number of correlations were plotted to examine the benefits of replacing the elastic recovery with the percent recovery from the MSCR test at various stress levels. The analysis also included repeated mixture creep data that were collected for selected unmodified and modified binders. These were tested at various stress levels. A presentation on the correlations was made at the Binder ETG meeting in September.

Work on the new binder fatigue parameter continued. A technical paper was completed and submitted to AAPT regarding the monotonic binder test: the Binder Yield Energy Test (BYET). In addition, the research team completed both an analysis of the modeling to represent the effects of pavement structure on binder fatigue criteria and an analysis of developing a framework to include this in future binder specifications. The results of these analyses were presented at the binder ETG meeting in September.

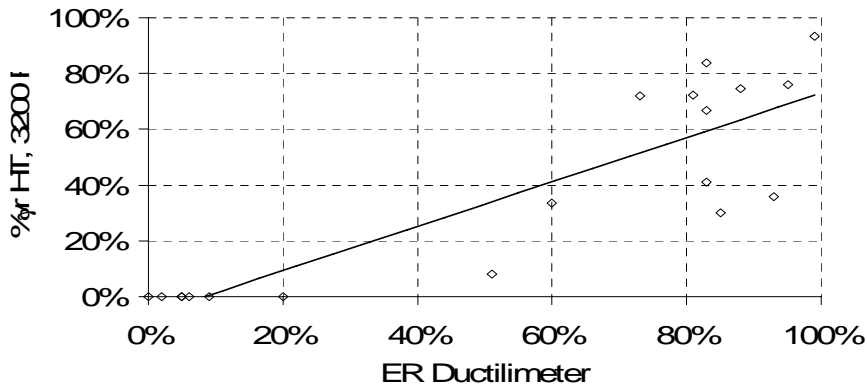
Work on the development of the single-edge notched beam test to measure fracture properties was also completed. A prototype of the device was tested and is ready for use in this task and other tasks related to this project. In addition, a prototype of the Asphalt Binder Cracking Device (ABCD) was received from Professor S. Kim of Ohio University as part of the round robin testing program for the device. The ABCD will be used to test selected asphalt binders, and a report about the practicality and repeatability of the test as compared to other options will be prepared.

#### Significant Results

Figure V3a.1 depicts an example of the correlations between elastic recovery and percent recovery from the MSCR test measured using 100 Pa and 3200 Pa stress levels. The results indicate that the percent recovery at the high temperature of grade can easily differentiate between unmodified and modified binders. Using the percent recovery from the 3200 Pa test appears to give a better delineation between unmodified and modified binders.



a) (% at HT) from MSCR at 100 Pa versus ER.



b) (% at HT) from MSCR at 3200 Pa versus ER.

Figure V3a.1. Graphs. Percent recovery at high grade temperature (% at HT) from MSCR at (a) 100 Pa and (b) 3200 Pa versus elastic recovery (ER).

The nonrecoverable creep compliance ( $J_{nr}$ ) was also used in the analysis (table V3a.1). It can be seen that for this set of binders, the  $J_{nr}$  can differentiate between modified and unmodified asphalts and can replace elastic recovery. While the data sample size was small, it is noteworthy that testing at 3200 Pa can capture significant differences among the modified binders that cannot be captured by the elastic recovery. It is also apparent that there are limited differences between the 100 Pa results and the 3200 Pa results, which could indicate there is a need to include testing at higher stress levels. This issue of the appropriate high stress level is under investigation in task E1b-1.

Table V3a.1. Values of nonrecoverable compliance (Jnr) for various binders.

PG Grade	Modification	Jnr 100Pa	Jnr 3200Pa
58-28	Neat	0.24	0.28
70-22	Neat	0.26	0.30
76-16	Air Blown	0.36	0.41
70-28	Elvaloy	0.034	0.032
64-34	Elvaloy	0.044	0.044
70-28	SBS	0.006	0.009
82-22	SBS	0.072	0.12
64-34	SB	0.027	0.031
70-34	SB	0.019	0.025

For the binder fatigue testing results, the Accelerated Load Facility (ALF) data were used to back-calculate a target value for acceptance of the Yield Energy (YE). Figure V3a.2 shows typical results for a selection of binders. It clearly shows that the YE measure can differentiate between binders of the same PG grade. The results were used to select a threshold value of 1.0 MPa as the base minimum value for YE for conditions of average pavement structure and average traffic. Like the framework used for the MSCR test results, traffic needs to be included in determining the threshold limits. Because this is a fatigue test, the pavement structure, which defines the strain level, should be included as well. Table V3a.2 shows how the binder fatigue criteria vary from the value of 1.0 MPa under different traffic and strain conditions. It is noted that the test temperature recommended is 8 °C lower than the current intermediate temperature in the PG grading system.

### Binder Yield Energy at ~ (IT - 8°C)

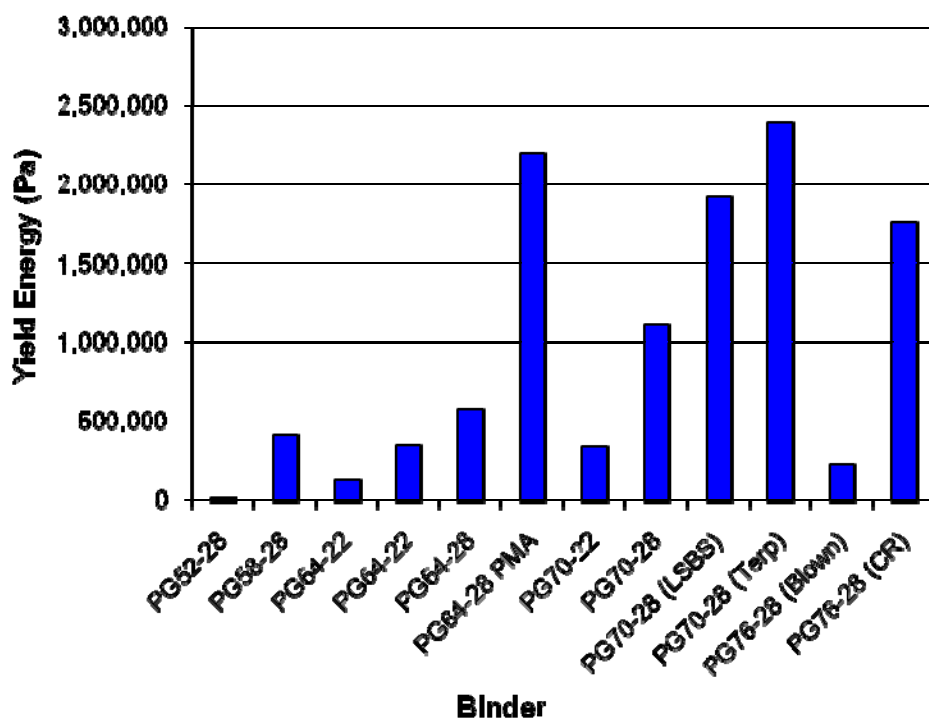


Figure V3a.2. Graph. Typical results of the Yield Energy test.

Table V3a.2. Proposed limits for Yield Energy to control binder fatigue resistance.

(Adjusted to 1.0 MPa, at <b>IT-8C</b> )				
Pavement Micro-strain		1000	600	200
	Binder Strain	5%	3%	1%
Traffic ESALs	1000000	<b>1.20</b>	<b>0.90</b>	<b>0.25</b>
	3000000	<b>1.35</b>	<b>1.00</b>	<b>0.30</b>
	10000000	<b>1.50</b>	<b>1.10</b>	<b>0.35</b>

### Significant Problems, Issues and Potential Impact on Progress

None.

### Work Planned Next Quarter

Work will continue on the analysis of the MSCR results at various stress levels and on determining the importance of percent recovery. The analysis of the YE values and the modeling to derive a binder fatigue parameter and fatigue limits will also continue.

Work will also start on collecting data for the binder fracture test results and the analysis of a parameter to be used as part of the binder specification for low temperature cracking.

### **Work element V3b: Validation of the MEPDG Asphalt Materials Models Using New MEPDG Sites and Selected LTPP Sites (UNR, UWM)**

#### ***Subtask V3b-1: Design and Build Sections (Start Year 1, Year 2, and Year 3)***

### Work Done This Quarter

Conducted a mechanistic-empirical pavement design for Wisconsin DOT for a new flexible pavement to be placed at USH 151 in Fond du Lac County using the MEPDG software, version 1.0. This project consists of the reconstruction of approximately 2.3 miles of USH 151 located approximately 0.25 mile south of the village of Pipe and extends northerly through the villages of Pipe and Calumetville to the north Fond du Lac County line. This section of the USH 151 is classified as a minor arterial with a posted speed limit of 55 mph in the rural stretches and 35 mph through the villages of Pipe and Calumetville.

### Significant Results

Submitted an MEPDG design report for Wisconsin DOT for the USH 151 reconstruction project. The project is anticipated to be constructed in summer of 2009.

### Significant Problems, Issues and Potential Impact on Progress

Only three agencies have committed to the construction of MEPDG sites: the Washoe RTC in northern Nevada in 2008, The South Dakota DOT in 2009/2010, and the Wisconsin DOT in 2009. The researchers are facing significant hesitation from the DOTs to use the MEPDG to design and construct HMA pavements. The level of this work element may have to be reduced.

### Work Planned Next Quarter

Continue discussions with the states to select field sections for the MEPDG validations sites. Complete the MEPDG design and construct the Washoe RTC project.

***Subtask V3b-2: Additional Testing (Start Year 2, Year 3, and Year 4)***

Work Done This Quarter

No activity this quarter.

Significant Results

None.

Significant Problems, Issues and Potential Impact on Progress

None.

Work Planned Next Quarter

No work planned.

***Subtask V3b-3: Select LTPP Sections (Start Year 1 thru Year 5)***

Work Done This Quarter

The research team's discussions with Binder ETG members indicated that care needs to be taken in breaking down the binders received from the LTPP materials library. In order to take 1 gallon samples of the binders currently contained in 5 gallon pails, a sampling protocol was drafted and submitted for review by FHWA officials. Binders must be heated to sufficient fluidity, but it is important not to overheat them because this simulates oxidative aging. The new sampling protocol minimizes the required heating, as described here:

1. The lid will be detached from the pail but will remain in place in order to cover the sample while in the oven. This should reduce the amount of oxygen entering the container while still allowing for the safe thermal expansion of the air inside the container.
2. The pail will be placed in an oven set to 130 °C for 4 hours. After each hour, the material will be stirred by hand using a heated large spatula, and a temperature reading will be taken and recorded. If, after 4 hours, the material is sufficiently fluid (this is currently a subjective judgment), the mixing will continue for 10 to 15 minutes. Following the mixing, 1 gallon of the material will be poured directly from the 5 gallon pail to fill a 1 gallon can.
3. If the material is not sufficiently fluid after 4 hours, the lid will be placed back on the pail, and the material will be placed back in the oven at 130 °C for 30 minutes. Afterward, the binder will be stirred again and the temperature recorded. Step 3 will be repeated until the material is sufficiently fluid. Once sufficiently fluid, 1 gallon of material will be sampled as described in step 2.



4. The total time in the oven will not exceed 5.5 hours at 130 °C. If the material is not sufficiently fluid after this time has elapsed, the binder will be scooped from the pail into the can, and this will be documented for reference.

#### Significant Results

The proposed sampling protocol was sent out for review so that binder testing can begin shortly.

#### Significant Problems, Issues and Potential Impact on Progress

None.

#### Work Planned Next Quarter

Samples will be taken from each container and set aside for testing. Short- and long-term aging will be performed so that testing can be carried out on the traditional three oxidative aging states of asphalt binder: original, rolling thin film oven (RTFO) and pressure aging vessel (PAV). Tests will begin in accordance with the matrix described in the Year 2 Asphalt Research Consortium (ARC) work plan.

#### ***Subtask V3b-4: Testing of Extracted Binders from LTPP Sections (Start Year 1)***

#### Work Done This Quarter

No activity this quarter.

#### Significant Results

None.

#### Significant Problems, Issues and Potential Impact on Progress

The 20 percent cost share to perform testing on LTPP samples to augment the LTPP database has not been identified. If a cost share is not obtained, this work will not be completed.

#### Work Planned Next Quarter

No work planned.

#### ***Subtask V3b-5: Review and Revisions of Materials Models (Start Year 2, Year 3, Year 4, and Year 5)***

#### Work Done This Quarter

No activity this quarter.

Significant Results

None.

Significant Problems, Issues and Potential Impact on Progress

None.

Work Planned Next Quarter

No work planned.

**Subtask V3b-6: Evaluate the Impact of Moisture and Aging (Start Year 3, Year 4, and Year 5)**

This is a Year 3 start.

Validation Year 2	Year 2 (4/2008-3/2009)												Team	
	4	5	6	7	8	9	10	11	12	1	2	3		
<b>(1) Field Validation</b>														
V1a: Use and Monitoring of Warm Mix Asphalt Sections														WRI
V1b: Construction and Monitoring of additional Comparative Pavement Validation sites														WRI
<b>(2) Accelerated Pavement Testing</b>														
V2a: Accelerated Pavement Testing including Scale Model Load Simulation on small test track (This work element will include all accelerated pavement testing)														WRI
V2b: Construction of validation sections at the Pecos Research & Testing Center														WRI
<b>(3) R&amp;D Validation</b>														
V3a: Continual Assessment of Specification														UWM
V3a-1: Evaluation of the PG-Plus practices and the motivations for selecting the "plus" tests.								P		D	F			
V3a-2: Detailed analysis of all PG-Plus tests being proposed or in use today, documentation of benefits and costs of these tests, and comparison with new											P			
V3a-3: Development of protocols for new binder tests and database for properties measured														
V3a-4: Development of specification criteria for new tests based on field evaluation of construction and performance														
V3a-5: Interviews and surveys for soliciting feedback on binder tests and specifications													JP	
V3b: Validation of the MEPDG Asphalt Materials Models and Early Verification of Technologies Developed by ARC using new MEPDG Sites and Selected LTPP sites														UNR/UWM/WRI
V3b-1: Design and Build Sections														UNR
V3b-2: Additional Testing														UWM
V3b-3: Select LTPP Sites to Validate New Binder Testing Procedures												P		
V3b-4: Testing of Extracted Binders from LTPP Sections														
V3b-5: Review and Revisions of Materials Models														
V3b-6: Evaluate the Impact of Moisture and Aging														

**Deliverable codes**

- D: Draft Report
- F: Final Report
- M&A: Model and algorithm
- SW: Software
- JP: Journal paper
- P: Presentation
- DP: Decision Point

**Deliverable Description**

- Report delivered to FHWA for 3 week review period.
- Final report delivered in compliance with FHWA publication standards
- Mathematical model and sample code
- Executable software, code and user manual
- Paper submitted to conference or journal
- Presentation for symposium, conference or other
- Time to make a decision on two parallel paths as to which is most promising to follow through

Work planned  
 Work completed  
 Parallel topic

Validation Years 2 - 5	Year 2 (4/08-3/09)				Year 3 (4/09-3/10)				Year 4 (04/10-03/11)				Year 5 (04/11-03/12)				Team
	Q1	Q2	Q3	Q4	Q1	Q2	Q3	Q4	Q1	Q2	Q3	Q4	Q1	Q2	Q3	Q4	
<b>(1) Field Validation</b>																	
V1a: Use and Monitoring of Warm Mix Asphalt Sections																	WRI
V1b: Construction and Monitoring of additional Comparative Pavement Validation sites																	WRI
<b>(2) Accelerated Pavement Testing</b>																	
V2a: Accelerated Pavement Testing including Scale Model Load Simulation on small test track																	WRI
V2b: Construction of validation sections at the Pecos Research & Testing Center																	WRI
<b>(3) R&amp;D Validation</b>																	
V3a: Continual Assessment of Specification																	
V3a-1: Evaluation of the PG-Plus practices and the motivations for selecting the "plus" tests.		P	D,F														UWM
V3a-2: Detailed analysis of all PG-Plus tests being proposed or in use today, documentation of benefits and costs of these tests, and comparison with new tests			P														
V3a-3: Development of protocols for new binder tests and database for properties measured					P		JP		P								
V3a-4: Development of specification criteria for new tests based on field evaluation of construction and performance								JP	P			JP	P		JP		
V3a-5: Interviews and surveys for soliciting feedback on binder tests and specifications				JP	P			JP	P		JP		P		D	F	
V3b: Validation of the MEPDG Asphalt Materials Models and Early Verification of Technologies Developed by ARC using new MEPDG Sites and Selected LTPP sites																	
V3b-1: Design and Build Sections										D, F							UNR/UWM
V3b-2: Additional Testing													D, F				
V3b-3: Select LTPP Sites to Validate New Binder Testing Procedures				P						JP		P			D	F	
V3b-4: Testing of Extracted Binders from LTPP Sections																	
V3b-5: Review and Revisions of Materials Models																D, F	
V3b-6: Evaluate the Impact of Moisture and Aging																D, F	

**Deliverable codes**  
D: Draft Report  
F: Final Report  
M&A: Model and algorithm  
SW: Software  
JP: Journal paper  
P: Presentation  
DP: Decision Point

**Deliverable Description**  
Report delivered to FHWA for 3 week review period.  
Final report delivered in compliance with FHWA publication standards  
Mathematical model and sample code  
Executable software, code and user manual  
Paper submitted to conference or journal  
Presentation for symposium, conference or other  
Time to make a decision on two parallel paths as to which is most promising to follow through

 Work planned  
 Work completed  
 Parallel topic

## **PROGRAM AREA: TECHNOLOGY DEVELOPMENT**

### **Work element TD1: Prioritize and Select Products for Early Development (Year 1)**

#### Work Done This Quarter

None. This work element was completed last Quarter.

#### Significant Results

Six early technology development projects have been identified and all have received favorable ratings from the ETGs.

#### Significant Problems, Issues and Potential Impact on Progress

None.

#### Work Planned Next Quarter

No work planned.

### **Work element TD2: Develop Early Products (Year 2)**

#### Work Done This Quarter

Work continued on the Simplified Continuum Damage Fatigue project. The research team began preparing a draft standard test method for Simplified Continuum Damage Fatigue Testing. This method is in the format of an AASHTO standard test method. It describes the testing and analysis that are required to generate fatigue curves for asphalt concrete mixtures. An accompanying spreadsheet has been developed to perform the analysis. The draft standard method is approximately 50 percent complete.

#### Significant Results

An improved method was developed for analysis of continuum damage fatigue data. Two new and very useful concepts were included in the improved method. The first is the concept of reduced loading cycles. Reduced loading cycles can be used as a much simpler alternative to the continuum damage parameter,  $S$ , in developing damage functions for asphalt concrete mixtures. The second concept introduced in the improved analysis approach is that of effective strain, which is the applied strain minus the endurance limit. This innovation in continuum damage analysis allows for the calculation of endurance limits from relatively limited fatigue data, and is a much quicker and more elegant approach to this problem than performing flexural fatigue tests over a range of strains for weeks or even months.

### Significant Problems, Issues and Potential Impact on Progress

None.

### Work Planned Next Quarter

The draft standard test method for the continuum damage fatigue test will be completed and the practice will be applied to fatigue data from several mixtures. A ruggedness test plan will be developed for the continuum damage fatigue test.

### **Work element TD3: Identify Products for Mid-Term and Long-Term Development (Years 2, 3, and 4)**

#### Work Done This Quarter

The research team continued to review interim research products to identify potential mid-term and long-term development projects.

#### Significant Results

None.

### Significant Problems, Issues and Potential Impact on Progress

None.

### Work Planned Next Quarter

The research team will continue to review interim research products to identify potential mid-term and long-term development projects.

### **Work Element TD4: Develop Mid-Term and Long-Term Products (Years 3, 4, and 5)**

This activity is planned for later in the project.

## **PROGRAM AREA: TECHNOLOGY TRANSFER**

### **CATEGORY TT1: OUTREACH AND DATABASES**

#### **Work element TT1a: Development and Maintenance of Consortium Website (Duration: Year 1 through Year 5)**

##### Work Done This Quarter

The ARC website was maintained and updated. Newsletter uploaded to the ARC website.

##### Significant Results

None.

##### Significant Problems, Issues and Potential Impact on Progress

None.

##### Work Planned Next Quarter

Continue maintaining and updating the ARC website.

#### **Work element TT1b: Communications (Duration: Year 1 through Year 5)**

##### Work Done This Quarter

The third ARC Newsletter published by October 2008.

##### Significant Results

None.

##### Significant Problems, Issues and Potential Impact on Progress

None.

##### Work Planned Next Quarter

None.

## **Work element TT1c: Prepare Presentations and Publications**

### Work Done This Quarter

Consortium members made presentations on the progress of the research at the Binder, and Mix & Construction ETG meetings in Reno, Nevada during the week of September 15, 2008.

The following publications were prepared, submitted, and accepted (as noted) by the Texas A&M team.

Bommavaram, R., A. Bhasin, and D. N. Little, "Use of Dynamic Shear Rheometer to Determine the Intrinsic Healing Properties of Asphalt Binders", *Transportation Research Record*, TRB, National Research Council, 2009 – Accepted for presentation and provisional for publication.

Bhasin, A., D. N. Little, R. Bommavaram, and M. L. Greenfield, "Intrinsic Healing in Asphalt Binders – Measurement and Impact of Molecular Morphology", Sixth International Conference on Maintenance and Rehabilitation of Pavements and Technological Control, Torino, Italy, 2009 – Abstract accepted .

Y. Kim, J. S. Lutfi, and D. H. Allen. "Determination of Representative Volume Elements of Asphalt Concrete Mixtures and Their Numerical Validation through Finite Element Method." *Transportation Research Record*, TRB, accepted for publication.

Y. Kim, D. H. Allen, and D. N. Little, "Damage Modeling of Asphalt Concrete Mixtures through Computational Micromechanics and Cohesive Zone Fracture." *Journal of the Association of Asphalt Paving Technologists*, AAPT, under review.

### Work Planned Next Quarter

Consortium members Harnsberger, Sebaaly, and Bahia will make presentations on Asphalt Compatibility, and RAP research at the RAP ETG meeting in Phoenix, Arizona on October 28 and 29, 2008.

## **Work element TT1d: Development of Materials Database (Duration: Year 2 through Year 5)**

### Work Done This Quarter

Worked on developing the Microsoft Access database tables according to the ERD diagram. Started the work on converting the ARC website from a static to a dynamic web site using the Microsoft Active Server Pages (ASP.NET) web application.

### Significant Results

None.



Significant Problems, Issues and Potential Impact on Progress

None.

Work Planned Next Quarter

Continue the work on the database and the dynamic web site.

**Work element TT1e: Development of Research Database (Duration: Year 2 through Year 5)**

Work Done This Quarter

No activity this quarter.

Significant Results

None.

Significant Problems, Issues and Potential Impact on Progress

None.

Work Planned Next Quarter

Prepare a framework for the research database.

**Work Element TT1f: Workshops and Training**

Work Done This Quarter

No activity this quarter.

Significant Results

None.

Significant Problems, Issues and Potential Impact on Progress

None.

Work Planned Next Quarter

No activities are planned for the next quarter.

Technology Transfer	Year 2 (4/2008-3/2009)												Team
	4	5	6	7	8	9	10	11	12	1	2	3	
<b>(1) Outreach and Databases</b>													
TT1a: Development and Maintenance of Consortium Website													
TT1b: Communications													
TT1c: Prepare presentations and publications													
TT1d: Development of Materials Database													
TT1d-1: Identify the overall Features of the Web Application													
TT1d-2: Identify Materials Properties to Include in the Materials Database													
TT1d-3: Define the Structure of the Database													
TT1d-4: Create and Populate the Database													
TT1e: Development of Research Database													
TT1e-1: Identify the Information to Include in the Research Database													
TT1e-2: Define the Structure of the Database													
TT1e-3: Create and Populate the Database													
TT1f: Workshops and Training													

**Deliverable codes**

- D: Draft Report
- F: Final Report
- M&A: Model and algorithm
- SW: Software
- JP: Journal paper
- P: Presentation
- DP: Decision Point

**Deliverable Description**

- Report delivered to FHWA for 3 week review period.
- Final report delivered in compliance with FHWA publication standards
- Mathematical model and sample code
- Executable software, code and user manual
- Paper submitted to conference or journal
- Presentation for symposium, conference or other
- Time to make a decision on two parallel paths as to which is most promising to follow through

Work planned  
 Work completed  
 Parallel topic

Technology Transfer	Year 2 (4/08-3/09)				Year 3 (4/09-3/10)				Year 4 (04/10-03/11)				Year 5 (04/11-03/12)				Team
	Q1	Q2	Q3	Q4	Q1	Q2	Q3	Q4	Q1	Q2	Q3	Q4	Q1	Q2	Q3	Q4	
<b>(1) Outreach and Databases</b>																	
TT1a: Development and Maintenance of Consortium Website																	
TT1b: Communications																	
TT1c: Prepare presentations and publications																	
TT1d: Development of Materials Database																	
TT1d-1: Identify the overall Features of the Web Application																	
TT1d-2: Identify Materials Properties to Include in the Materials Database																	
TT1d-3: Define the Structure of the Database																	
TT1d-4: Create and Populate the Database																	
TT1e: Development of Research Database																	
TT1e-1: Identify the Information to Include in the Research Database																	
TT1e-2: Define the Structure of the Database																	
TT1e-3: Create and Populate the Database																	
TT1f: Workshops and Training																	

**Deliverable codes**

- D: Draft Report
- F: Final Report
- M&A: Model and algorithm
- SW: Software
- JP: Journal paper
- P: Presentation
- DP: Decision Point

**Deliverable Description**

- Report delivered to FHWA for 3 week review period.
- Final report delivered in compliance with FHWA publication standards
- Mathematical model and sample code
- Executable software, code and user manual
- Paper submitted to conference or journal
- Presentation for symposium, conference or other
- Time to make a decision on two parallel paths as to which is most promising to follow through

Work planned  
 Work completed  
 Parallel topic